IEC TR 61869-100

Edition 1.0 2017-01

TECHNICAL REPORT

colour inside

Instrument transformers –
Part 100: Guidance for application of current transformers in power system protection

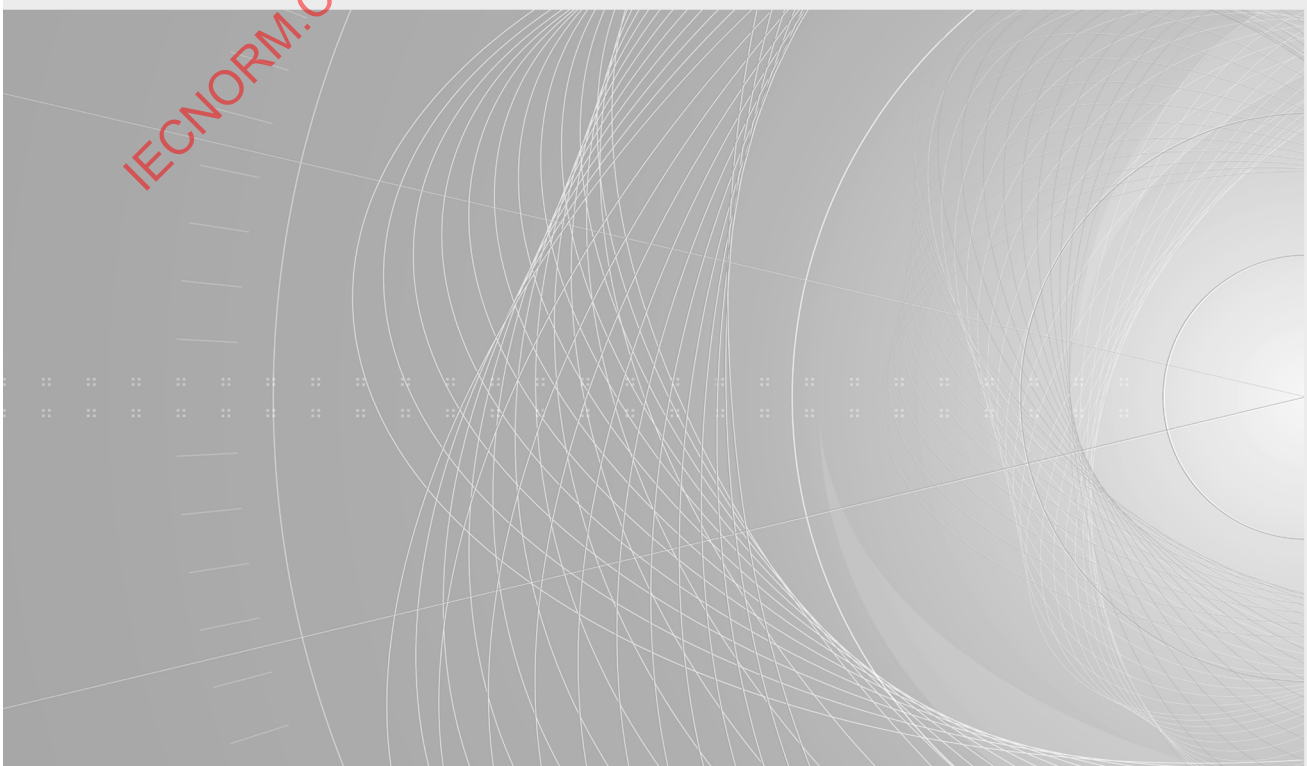

IEC TR 61869-100:2017-01(en)

IEC Central Office
3, rue de Varembé
CH-1211 Geneva 20
Switzerland

Tel.: +41 22 919 02 11
Fax: +41 22 919 03 00
info@iec.ch
www.iec.ch

About the IEC
The International Electrotechnical Commission (IEC) is the leading global organization that prepares and publishes International Standards for all electrical, electronic and related technologies.

About IEC publications
The technical content of IEC publications is kept under constant review by the IEC. Please make sure that you have the latest edition, a corrigenda or an amendment might have been published.

IEC Catalogue - webstore.iec.ch/catalogue
The stand-alone application for consulting the entire bibliographical information on IEC International Standards, Technical Specifications, Technical Reports and other documents. Available for PC, Mac OS, Android Tablets and iPad.

IEC publications search - www.iec.ch/searchpub
The advanced search enables to find IEC publications by a variety of criteria (reference number, text, technical committee,…). It also gives information on projects, replaced and withdrawn publications.

IEC Just Published - webstore.iec.ch/justpublished
Stay up to date on all new IEC publications. Just Published details all new publications released. Available online and also once a month by email.

Electropedia - www.electropedia.org
The world's leading online dictionary of electronic and electrical terms containing 20 000 terms and definitions in English and French, with equivalent terms in 16 additional languages. Also known as the International Electrotechnical Vocabulary (IEV) online.

IEC Glossary - std.iec.ch/glossary
65 000 electrotechnical terminology entries in English and French extracted from the Terms and Definitions clause of IEC publications issued since 2002. Some entries have been collected from earlier publications of IEC TC 37, 77, 86 and CISPR.

IEC Customer Service Centre - webstore.iec.ch/csc
If you wish to give us your feedback on this publication or need further assistance, please contact the Customer Service Centre: csc@iec.ch.

IEC TR 61869-100

Edition 1.0 2017-01

TECHNICAL REPORT

colour inside

Instrument transformers – Part 100: Guidance for application of current transformers in power system protection

INTERNATIONAL ELECTROTECHNICAL COMMISSION

ICS 17.220.20

ISBN 978-2-8322-3808-0

CONTENTS

FOREWORD 7
INTRODUCTION 9
1 Scope 10
2 Normative references 10
3 Terms and definitions and abbreviations 10
3.1 Terms and definitions 10
3.2 Index of abbreviations 12
4 Responsibilities in the current transformer design process 14
4.1 History 14
4.2 Subdivision of the current transformer design process 14
5 Basic theoretical equations for transient designing 15
5.1 Electrical circuit 15
5.1.1 General 15
5.1.2 Current transformer 18
5.2 Transient behaviour 20
5.2.1 General 20
5.2.2 Fault inception angle 22
5.2.3 Differential equation 23
6 Duty cycles 25
6.1 Duty cycle C – O 25
6.1.1 General 25
6.1.2 Fault inception angle 27
6.1.3 Transient factor K_{tf} and transient dimensioning factor K_{td} 28
6.1.4 Reduction of asymmetry by definition of the minimum current inception angle 50
6.2 Duty cycle C – O – C – O 53
6.2.1 General 53
6.2.2 Case A:No saturation occurs until t' 54
6.2.3 Case B:Saturation occurs between t'_{al} and t' 56
6.3 Summary 58
7 Determination of the transient dimensioning factor K_{td} by numerical calculation 61
7.1 General 61
7.2 Basic circuit 61
7.3 Algorithm 62
7.4 Calculation method 63
7.5 Reference examples 64
8 Core saturation and remanence 69
8.1 Saturation definition for common practice 69
8.1.1 General 69
8.1.2 Definition of the saturation flux in the preceding standard IEC 60044-1 69
8.1.3 Definition of the saturation flux in IEC 61869-2 71
8.1.4 Approach “5 % – Factor 5” 72
8.2 Gapped cores versus non-gapped cores 73
8.3 Possible causes of remanence 75
9 Practical recommendations 79
9.1 Accuracy hazard in case various PR class definitions for the same core 79

9.2 Limitation of the phase displacement $\Delta\varphi$ and of the secondary loop time constant T_s by the transient dimensioning factor K_{td} for TPY cores 79
10 Relations between the various types of classes 80
10.1 Overview 80
10.2 Calculation of e.m.f. at limiting conditions 80
10.3 Calculation of the exciting (or magnetizing) current at limiting conditions 81
10.4 Examples 81
10.5 Minimum requirements for class specification 82
10.6 Replacing a non-gapped core by a gapped core 82
11 Protection functions and correct CT specification 83
11.1 General 83
11.2 General application recommendations 83
11.2.1 Protection functions and appropriate classes 83
11.2.2 Correct CT designing in the past and today 85
11.3 Overcurrent protection: ANSI code: (50/51/50N/51N/67/67N); IEC symbol: I> 87
11.3.1 Exposition 87
11.3.2 Recommendation 89
11.3.3 Example 89
11.4 Distance protection: ANSI codes: 21/21N, IEC code: Z< 89
11.4.1 Exposition 89
11.4.2 Recommendations 91
11.4.3 Examples 91
11.5 Differential protection 98
11.5.1 Exposition 98
11.5.2 General recommendations 99
11.5.3 Transformer differential protection (87T) 99
11.5.4 Busbar protection: Ansi codes (87B) 104
11.5.5 Line differential protection: ANSI codes (87L) (Low impedance) 107
11.5.6 High impedance differential protection 109
Annex A (informative) Duty cycle C – O software code 128
Annex B (informative) Software code for numerical calculation of K_{td} 130
Bibliography 135

Figure 1 – Definition of the fault inception angle γ 12
Figure 2 – Components of protection circuit 16
Figure 3 – Entire electrical circuit 17
Figure 4 – Primary short circuit current 18
Figure 5 – Non-linear flux of L_{ct} 19
Figure 6 – Linearized magnetizing inductance of a current transformer 20
Figure 7 – Simulated short circuit behaviour with non-linear model 21
Figure 8 – Three-phase short circuit behaviour 23
Figure 9 – Composition of flux 24
Figure 10 – Short circuit current for two different fault inception angles 26
Figure 11 – ψ_{max} as the curve of the highest flux values 26
Figure 12 – Primary current curves for the 4 cases for 50 Hz and φ = 70° 27
Figure 13 – Four significant cases of short circuit currents with impact on magnetic saturation of current transformers 28

Figure 14 – Relevant time ranges for calculation of transient factor 31
Figure 15 – Occurrence of the first flux peak depending on T_p, at 50 Hz 32
Figure 16 – Worst-case angle $\theta_{tf,\psi max}$ as function of T_p and t'_{al} 33
Figure 17 – Worst-case fault inception angle $\gamma_{tf,\psi max}$ as function of T_p and t'_{al} 34
Figure 18 – $K_{tf,\psi max}$ calculated with worst-case fault inception angle $\theta_{\psi max}$ 34
Figure 19 – Polar diagram with $K_{tf,\psi max}$ and $\gamma_{tf,\psi max}$ 35
Figure 20 – Determination of K_{tf} in time range 1 40
Figure 21 – Primary current curves for 50Hz, T_p = 1 ms, $\gamma_{\psi max}$ = 166° for t'_{al} = 2 ms 41
Figure 22 – worst-case fault inception angles for 50Hz, T_p = 50 ms and T_s = 61 ms 42
Figure 23 – transient factor for different time ranges 43
Figure 24 – K_{tf} in all time ranges for T_s = 61 ms at 50 Hz with t'_{al} as parameter 44
Figure 25 – Zoom of Figure 24 44
Figure 26 – Primary current for a short primary time constant 45
Figure 27 – K_{tf} values for a short primary time constant 46
Figure 28 – Short circuit currents for various fault inception angles 47
Figure 29 – Transient factors for various fault inception angles (example) 48
Figure 30 – Worst-case fault inception angles for each time step (example for 50 Hz) 48
Figure 31 – Primary current for two different fault inception angles (example for 16,67 Hz) 49
Figure 32 – Transient factors for various fault inception angles (example for 16,67 Hz) 50
Figure 33 – Worst-case fault inception angles for every time step (example for 16,67 Hz) 50
Figure 34 – Fault occurrence according to Warrington 51
Figure 35 – estimated distribution of faults over several years 52
Figure 36 – Transient factor K_{tf} calculated with various fault inception angles γ 53
Figure 37 – Flux course in a C-O-C-O cycle of a non-gapped core 54
Figure 38 – Typical flux curve in a C-O-C-O cycle of a gapped core, with higher flux in the second energization 55
Figure 39 – Flux curve in a C-O-C-O cycle of a gapped core, with higher flux in the first energization 56
Figure 40 – Flux curve in a C-O-C-O cycle with saturation allowed 57
Figure 41 – Core saturation used to reduce the peak flux value 58
Figure 42 – Curves overview for transient designing 59
Figure 43 – Basic circuit diagram for numerical calculation of K_{td} 62
Figure 44 – K_{td} calculation for C-O cycle 64
Figure 45 – K_{td} calculation for C-O-C-O cycle without core saturation in the first cycle 65
Figure 46 – K_{td} calculation for C-O-C-O cycle considering core saturation in the first cycle 66
Figure 47 – K_{td} calculation for C-O-C-O cycle with reduced asymmetry 67
Figure 48 – K_{td} calculation for C-O-C-O cycle with short t'_{al} and t''_{al} 68
Figure 49 – K_{td} calculation for C-O-C-O cycle for a non-gapped core 69
Figure 50 – Comparison of the saturation definitions according to IEC 60044-1 and according to IEC 61869-2 70
Figure 51 – Remanence factor K_r according to the previous definition IEC 60044-1 71

Figure 52 – Determination of saturation and remanence flux using the DC method for a gapped core 72
Figure 53 – Determination of saturation and remanence flux using DC method for a non-gapped core 72
Figure 54 – CT secondary currents as fault records of arc furnace transformer 76
Figure 55 – 4-wire connection 77
Figure 56 – CT secondary currents as fault records in the second fault of auto reclosure 78
Figure 57 – Application of instantaneous/time-delay overcurrent relay (ANSI codes 50/51) with definite time characteristic 88
Figure 58 – Time-delay overcurrent relay, time characteristics 88
Figure 59 – CT specification example, time overcurrent 89
Figure 60 – Distance protection, principle (time distance diagram) 90
Figure 61 – Distance protection, principle (R/X diagram) 91
Figure 62 – CT Designing example, distance protection 92
Figure 63 – Primary current with C-O-C-O duty cycle 96
Figure 64 – Transient factor K_{tf} with its envelope curve K_{tfp} 96
Figure 65 – Transient factor K_{tf} for CT class TPY with saturation in the first fault 97
Figure 66 – Transient factor K_{tf} for CT class TPZ with saturation in the first fault 97
Figure 67 – Transient factor K_{tf} for CT class TPX 98
Figure 68 – Differential protection, principle 99
Figure 69 – Transformer differential protection, faults 100
Figure 70 – Transformer differential protection 101
Figure 71 – Busbar protection, external fault 104
Figure 72 – Simulated currents of a current transformer for bus bar differential protection 107
Figure 73 – CT designing for a simple line with two ends 108
Figure 74 – Differential protection realized with a simple electromechanical relay 110
Figure 75 – High impedance protection principle 111
Figure 76 – Phasor diagram for external faults 112
Figure 77 – Phasor diagram for internal faults 113
Figure 78 – Magnetizing curve of CT 114
Figure 79 – Single-line diagram of busbar and high impedance differential protection 117
Figure 80 – Currents at the fault location (primary values) 119
Figure 81 – Primary currents through CTs, scaled to CT secondary side 120
Figure 82 – CT secondary currents 120
Figure 83 – Differential voltage 121
Figure 84 – Differential current and r.m.s. filter signal 121
Figure 85 – Currents at the fault location (primary values) 122
Figure 86 – Primary currents through CTs, scaled to CT secondary side 122
Figure 87 – CT secondary currents 123
Figure 88 – Differential voltage 123
Figure 89 – Differential current and r.m.s. filtered signal 124
Figure 90 – Currents at the fault location (primary values) 124
Figure 91 – Primary currents through CTs, scaled to CT secondary side 125

Figure 92 – CT secondary currents 125
Figure 93 – Differential voltage 126
Figure 94 – Differential current and r.m.s. filtered signal 126
Figure 95 – Differential voltage without varistor limitation 127

Table 1 – Four significant cases of short circuit current inception angles 27
Table 2 – Equation overview for transient designing 60
Table 3 – Comparison of saturation point definitions 73
Table 4 – Measured remanence factors 74
Table 5 – Various PR class definitions for the same core 79
Table 6 – e.m.f. definitions 80
Table 7 – Conversion of e.m.f. values 80
Table 8 – Conversion of dimensioning factors 81
Table 9 – Definitions of limiting current 81
Table 10 – Minimum requirements for class specification 82
Table 11 – Effect of gapped and non-gapped cores 83
Table 12 – Application recommendations 84
Table 13 – Calculation results of the overdimensioning of a TPY core 103
Table 14 – Calculation results of overdimensioning as PX core 103
Table 15 – Calculation scheme for line differential protection 109
Table 16 – Busbar protection scheme with two incoming feeders 117

INTERNATIONAL ELECTROTECHNICAL COMMISSION

_____

INSTRUMENT TRANSFORMERS –

Part 100: Guidance for application of current transformers in power system protection

FOREWORD

1) The International Electrotechnical Commission (IEC) is a worldwide organization for standardization comprising all national electrotechnical committees (IEC National Committees). The object of IEC is to promote international co-operation on all questions concerning standardization in the electrical and electronic fields. To this end and in addition to other activities, IEC publishes International Standards, Technical Specifications, Technical Reports, Publicly Available Specifications (PAS) and Guides (hereafter referred to as "IEC Publication(s)"). Their preparation is entrusted to technical committees; any IEC National Committee interested in the subject dealt with may participate in this preparatory work. International, governmental and non-governmental organizations liaising with the IEC also participate in this preparation. IEC collaborates closely with the International Organization for Standardization (ISO) in accordance with conditions determined by agreement between the two organizations.
2) The formal decisions or agreements of IEC on technical matters express, as nearly as possible, an international consensus of opinion on the relevant subjects since each technical committee has representation from all interested IEC National Committees.
3) IEC Publications have the form of recommendations for international use and are accepted by IEC National Committees in that sense. While all reasonable efforts are made to ensure that the technical content of IEC Publications is accurate, IEC cannot be held responsible for the way in which they are used or for any misinterpretation by any end user.
4) In order to promote international uniformity, IEC National Committees undertake to apply IEC Publications transparently to the maximum extent possible in their national and regional publications. Any divergence between any IEC Publication and the corresponding national or regional publication shall be clearly indicated in the latter.
5) IEC itself does not provide any attestation of conformity. Independent certification bodies provide conformity assessment services and, in some areas, access to IEC marks of conformity. IEC is not responsible for any services carried out by independent certification bodies.
6) All users should ensure that they have the latest edition of this publication.
7) No liability shall attach to IEC or its directors, employees, servants or agents including individual experts and members of its technical committees and IEC National Committees for any personal injury, property damage or other damage of any nature whatsoever, whether direct or indirect, or for costs (including legal fees) and expenses arising out of the publication, use of, or reliance upon, this IEC Publication or any other IEC Publications.
8) Attention is drawn to the Normative references cited in this publication. Use of the referenced publications is indispensable for the correct application of this publication.
9) Attention is drawn to the possibility that some of the elements of this IEC Publication may be the subject of patent rights. IEC shall not be held responsible for identifying any or all such patent rights.

The main task of IEC technical committees is to prepare International Standards. However, a technical committee may propose the publication of a technical report when it has collected data of a different kind from that which is normally published as an International Standard, for example "state of the art".

IEC TR 61869-100, which is a technical report, has been prepared by IEC technical committee 38: Instrument transformers.

The text of this technical report is based on the following documents:

Enquiry draft	Report on voting
38/469/DTR	38/475A/RVC

Full information on the voting for the approval of this technical report can be found in the report on voting indicated in the above table.

This publication has been drafted in accordance with the ISO/IEC Directives, Part 2.

A list of all the parts in the IEC 61869 series, published under the general title *Instrument transformers*, can be found on the IEC website.

The committee has decided that the contents of this publication will remain unchanged until the stability date indicated on the IEC web site under "http://webstore.iec.ch" in the data related to the specific publication. At this date, the publication will be

- reconfirmed,
- withdrawn,
- replaced by a revised edition, or
- amended.

A bilingual version of this publication may be issued at a later date.

IMPORTANT – The 'colour inside' logo on the cover page of this publication indicates that it contains colours which are considered to be useful for the correct understanding of its contents. Users should therefore print this document using a colour printer.

INTRODUCTION

Since the publication of IEC 60044-6:1992[1], *Requirements for protective current transformers for transient performance*, the area of application of this kind of current transformers has been extended. As a consequence, the theoretical background for the dimensioning according to electrical requirements has become much more complex. For IEC 61869-2 to remain as user-friendly as possible, the explanation of the background information has been transferred to this part of IEC 61869.

1 Withdrawn and replaced by IEC 61869-2:2012.

INSTRUMENT TRANSFORMERS –

Part 100: Guidance for application of current transformers in power system protection

1 Scope

This part of IEC 61869 is applicable to inductive protective current transformers meeting the requirements of the IEC 61869-2 standard.

It may help relay manufacturers, CT manufacturers and project engineers to understand how a CT responds to simplified or standardized short circuit signals. Therefore, it supplies advanced information to comprehend the definition of inductive current transformers as well as their requirements.

The document aims to provide information for the casual user as well as for the specialist. Where necessary, the level of abstraction is mentioned in the document. It also discusses the question about the responsibilities in the design process for current transformers.

2 Normative references

The following documents are referred to in the text in such a way that some or all of their content constitutes requirements of this document. For dated references, only the edition cited applies. For undated references, the latest edition of the referenced document (including any amendments) applies.

IEC 60255 (all parts), *Measuring relays and protection equipment*

IEC 60909-0:2016, *Short circuit currents in three-phase a.c. systems – Calculation of currents*

IEC 61869-1:2007, *Instrument transformers – General requirements*

IEC 61869-2:2012, *Instrument transformers – Additional requirements for current transformers*

3 Terms and definitions and abbreviations

3.1 Terms and definitions

For the purposes of this document, the terms and definitions given in IEC 61869-1:2007 and IEC 61869-2:2012 and the following apply.

ISO and IEC maintain terminological databases for use in standardization at the following addresses:

- IEC Electropedia: available at http://www.electropedia.org/
- ISO Online browsing platform: available at http://www.iso.org/obp

3.1.1
rated primary short circuit current
I_{psc}
r.m.s. value of the a.c. component of a transient primary short-circuit current on which the accuracy performance of a current transformer is based

[SOURCE: IEC 61869-2:2012, 3.3.206]

3.1.2
rated short-time thermal current
I_{th}
maximum value of the primary current which a transformer will withstand for a specified short time without suffering harmful effects, the secondary winding being short-circuited

[SOURCE: IEC 60050-321:1986, 321-02-22; IEC 61869-2:2012, 3.3.203]

3.1.3
initial symmetrical short circuit current
I''_k
r.m.s. value of the a.c. symmetrical component of a prospective (available) short-circuit current, applicable at the instant of short circuit if the impedance remains at zero-time value

[SOURCE: IEC 60909-0:2001, 1.3.5]

Note 1 to entry: While I_{th} is a basic parameter of a plant and of its components, I_{psc} is an accuracy requirement, and has a determining influence on the saturation behaviour of a current transformer. The protection system will ensure tripping at a current I''_k, which is usually lower than I_{th}. Depending on the protection requirement, a current transformer may saturate much before reaching I''_k. Therefore, in certain cases, I_{psc} may be much lower than I''_k.

3.1.4
primary current
I_p
current flowing through the primary winding of a current transformer

3.1.5
secondary current
I_s
current flowing through the secondary winding of a current transformer

3.1.6
angular frequency
ω
angular frequency of the primary current

3.1.7
time
t
time

3.1.8
phase angle of the system short circuit impedance
φ
phase angle of the system short circuit impedance

3.1.9
fault inception angle
γ
inception angle of the primary short circuit, being 180° at voltage maximum (see Figure 1)

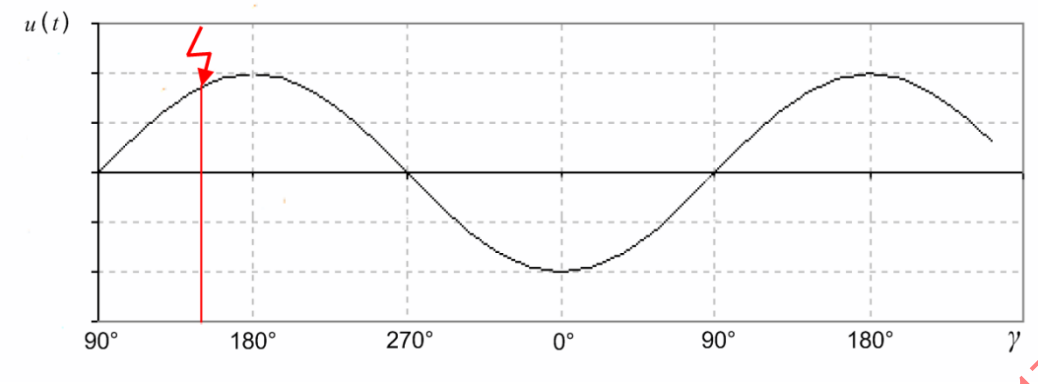

Key

u primary voltage

γ fault inception angle

Figure 1 – Definition of the fault inception angle γ

3.1.10
minimum fault inception angle
γ_m
lowest value of fault inception angle γ to be considered in the design of a current transformer

3.1.11
alternative definition of fault inception angle
θ
inception angle of the primary short circuit, defined as $\gamma - \varphi$

3.2 Index of abbreviations

This table comprises Table 3.7 of IEC 61869-2:2012, complemented with the terms and definitions given in 3.1.1 to 3.1.11.

AIS	Air-Insulated Switchgear
ALF	Accuracy limit factor
CT	Current Transformer
CVT	Capacitive Voltage Transformer
E_{al}	rated equivalent limiting secondary e.m.f.
E_{ALF}	secondary limiting e.m.f. for class P and PR protective current transformers
E_{FS}	secondary limiting e.m.f. for measuring current transformers
E_k	rated knee point e.m.f.
f	frequency
F	mechanical load
F_c	factor of construction
f_R	rated frequency
F_{rel}	relative leakage rate
FS	instrument security factor
GIS	Gas-Insulated Switchgear
I''_k	Initial symmetrical short circuit current
$\hat{I}_{al}$	peak value of the exciting secondary current at E_{al}
I_{cth}	rated continuous thermal current

I_{dyn}	rated dynamic current
I_e	exciting current
I_{PL}	rated instrument limit primary current
I_p	primary current
I_{pr}	rated primary current
I_{psc}	rated primary short circuit current
I_s	secondary current
I_{sr}	rated secondary current
IT	Instrument Transformer
I_{th}	rated short-time thermal current
i_ε	instantaneous error current
k	actual transformation ratio
k_r	rated transformation ratio
K_R	remanence factor
K_{ssc}	rated symmetrical short circuit current factor
K_{td}	transient dimensioning factor
K_{tf}	transient factor
K_x	dimensioning factor
L_{ct}	non-linear inductance of a current transformer
L_m	linearized magnetizing inductance of a current transformer
L1,L2,L3	designation of the phases in the electrical three-phase system
n_s	number of secondary turns
R_b	rated resistive burden
R_{ct}	secondary winding resistance
R_s	secondary loop resistance
S_r	rated output
t	time
t'	duration of the first fault
t''	duration of the second fault
t'_{al}	specified time to accuracy limit in the first fault
t''_{al}	specified time to accuracy limit in the second fault
t_{fr}	fault repetition time
T_p	specified primary time constant
T_s	secondary loop time constant
U_m	highest voltage for equipment
U_{sys}	highest voltage for system
VT	Voltage Transformer
$\Delta\varphi$	phase displacement
ε	ratio error
ε_c	composite error
$\hat{\varepsilon}$	peak value of instananeous error

$\hat{\varepsilon}_{ac}$	peak value of alternating error component
φ	phase angle of the system short circuit impedance
γ	fault inception angle
γ_{m}	minimum fault inception angle
θ	alternative definition of fault inception angle
ψ	secondary linked magnetic flux in the current transformer core
ψ_{r}	remanent flux
ψ_{sat}	saturation flux
ω	angular frequency

4 Responsibilities in the current transformer design process

4.1 History

The IEC 60044-6 standard “Instrument transformers – Part 6: Requirements for protective current transformers for transient performance" was introduced in 1992 (at that time as IEC 44-6). It was the first standard that considered the transient performance of protective CT.

In the well-known P-class, the usually indispensable over-dimensioning due to the primary DC component has to be “hidden” in the accuracy limit factor or in the burden.

The definition of the new classes TPX, TPY and TPZ was strongly “cycle-oriented”, defining all necessary parameters of a C-O and of a C-O-C-O cycle. These classes allowed the shifting of responsibility for the calculation of the over-dimensioning due to the primary DC component (represented by the “transient factor” K_{td}, nowadays called “transient dimensioning factor”) to the CT manufacturer.

The transient performance classes never became widely accepted by different reasons:

– Their specification by duty cycles (and time to accuracy limit if necessary) is much more complex than the conventional classes 5P and 10P, which were originally foreseen for electromechanical relays.
– The duty cycle definition does no longer reflect the actual criteria for defining the overdimensioning factors.

Nowadays, it is common practice that the relay developers stipulate the required overdimensioning of the protection current transformers, taking into account the wave form of the primary signal as well as their own protection requirements.

When IEC 60044-6 was integrated in IEC 61869-2, it was taken into account that the cycle definition plays a declining role, as the aspects explained above have to be considered. Therefore, the definition of transient performance was extended by allowing the direct definition of the transient dimensioning factor K_{td} instead of the cycle parameters. This new way of specification is easy and similar to that of the well-known P-classes. One intention of this technical report is to explain such possible alternative specifications for several critical applications.

4.2 Subdivision of the current transformer design process

In modern digital relays, the decision-making time has decreased continuously as a result of increasing sampling rates and by refining the protection algorithms. As a consequence, the required saturation-free time of the current transformers has been reduced correspondingly.

This leads to smaller CT cores, what is in line with the development of modern compact gas-insulated switchgears. Furthermore, some of the algorithms apply Fourier and r.m.s. filtering of the dynamic CT current signal. As a consequence, the relays react more 'smoothly' to high currents with possible saturation. For these reasons, the required CT performance and final core size cannot be expressed solely by the initial saturation time and one simple analytical formula.

Therefore, it is recommended that the relay developers first use analytical formulae for an initial consideration. In a second step, they may test their algorithms with a simulation model of the CT core and publish the requirements in terms of simple parameters (e.g. over-dimensioning factor, transient dimensioning factor, etc.) for significant worst case fault scenarios in the protection relay manual (or other documents). During the project engineering phase, the published requirements are applied to concrete cases and the hereby verified class parameters are communicated to the CT manufacturer.

For backward compatibility to IEC 60044-6, the transient factor K_{tf} – analytically calculated from parameters such as time to accuracy limit t'_{al}, duty cycle, etc. – may be applied directly as transient dimensioning factor K_{td} without further protection relay test. This way is not recommended, but may be chosen in situations where the design responsibility is not delegated entirely to the relay manufacturer.

The procedures used to determine the transient dimensioning factor K_{td} on the basis of protection rules can be considered to be the specific know-how of relay specialists, and are not part of this technical report.

In a complementary manner, this report highlights the path from the cycle definition, which still has certain significance, to the definition of a transient dimensioning factor. The analytical formulae in this technical report are extended and diversified. As a consequence, they look much more complex than in IEC 60044-6. But the intention is that they are only applied by a few protection relay developers who then provide the project engineers and the CT manufacturers with design parameters which permit a simpler CT sizing procedure to be applied.

5 Basic theoretical equations for transient designing

5.1 Electrical circuit

5.1.1 General

As an introduction, Figure 2 presents a simplified interaction chain between the main components of the protection circuit: network currents are measured by current transformers, and the values are transmitted to the protection devices.

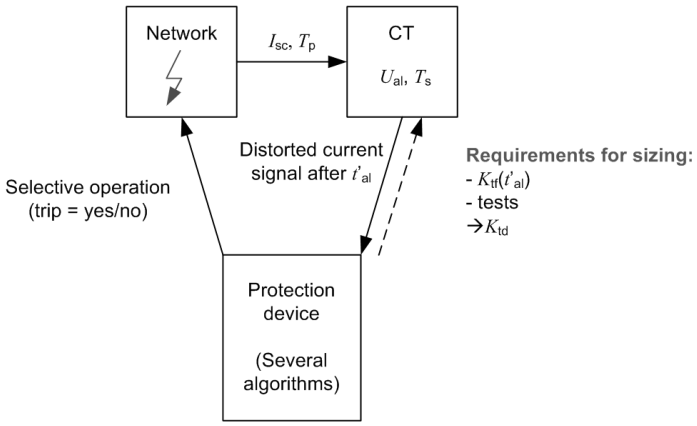

Key

I_{sc}	primary short circuit current
K_{td}	transient dimensioning factor
K_{tf}	transient factor
T_p	specified primary time constant
T_s	secondary loop time constant
t'_{al}	specified time to accuracy limit in the first fault
U_{al}	rated equivalent limiting secondary voltage

Figure 2 – Components of protection circuit

Protection relay development:

– Find out worst case scenarios in typical networks for short circuit currents with I_{sc}, T_p.
– Define needed K_{ssc} and start with analytical calculation of $K_{tf}(t'_{al}, t''_{al}, t', t_{fr}, T_p, T_s)$.
– Verify first results by tests: Numerical CT simulation (software) and protection relay (hardware). If necessary, correct K_{ssc} and K_{tf} and include safety factors.
– Publish results in protection relay manual for the significant worst case scenario(s).
Now the transient factor K_{tf} (from protection point of view) becomes the transient dimensioning factor K_{td} (for CT sizing and construction point of view), where K_{td} includes safety margins M: $K_{td} = K_{tf} * M$.
After the tests, K_{td} does not need to have correlations with the original K_{tf} if tests show different behaviour.

NOTE Protection relay manufacturers normally perform tests with complete protection IEDs (software and hardware) to decide and publish the CT requirements as a total transient dimensioning factor K_{tot}. Depending on the protection function and the application, this factor considers the minimum necessary time to saturation, the remanence factor and also others. In these tests, the fault inception angle covers the complete defined range and is not limited to only the theoretical worst case. For more information, refer to 8.2.

Project engineering:

– Consider the protection relay manual for CT requirements.
– Find the worst case scenarios in the projected network with short circuit currents with I_{sc}, T_p. Find out if these worst case scenarios are considered in the manual.
– Calculate the rated primary currents I_{pr}, K_{ssc}, burdens R_b, etc. and specify the needed CT parameters, applying the K_{td} from protection relay manual.
– The CT manufacturer applies the specified parameters without considering t'_{al}, t''_{al}, t', t_{fr}, T_p, etc.

Backward compatibility to IEC 60044-6:

Alternatively, K_{tf} (t'_{al}, t''_{al}, t', t_{fr}, T_p, T_s) can be calculated and applied directly as K_{td} without tests, where the responsibility lies with the involved project parties.

– Calculate rated primary currents I_{pr}, K_{ssc}, burdens R_b, etc., and specify the needed CT parameters (class, t'_{al}, t''_{al}, t', t_{fr}, T_p).
– The CT manufacturer may calculate $K_{td} = K_{tf}$ as a function of t'_{al}, t''_{al}, t', t_{fr}, T_p.

The more detailed electrical circuit (Figure 3), which has to be considered for current transformer designing, contains

– the primary network represented by the equivalent short circuit diagram;
– the current transformer (CT);
– the protection device as burden.

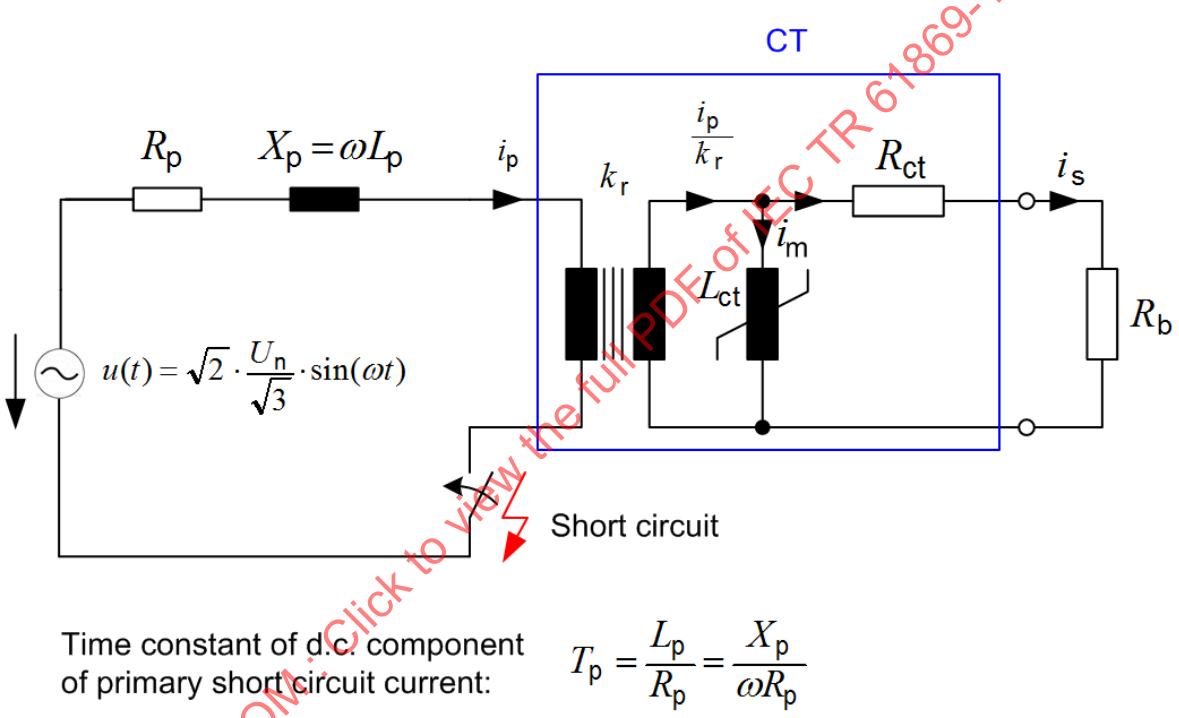

Key

i_p primary current
i_m excitation current
i_s secondary current
k_r rated transformation ratio
L_{ct} nonlinear inductance of the current transformer
L_p inductance of the primary circuit
R_b rated resistive burden
R_{ct} secondary winding resistance
R_p resistive part of the impedance of the primary circuit
u primary voltage
U_n phase-to-phase operating voltage
T_p specified primary time constant
X_p inductive part of the impedance of the primary circuit
ω angular frequency

Figure 3 – Entire electrical circuit

The primary equivalent short circuit diagram represents the whole primary circuit according to IEC 60909-0:2001 and introduces the primary short circuit current $i_p(t)$, composed of an AC component and a DC component, which is declining exponentially with a primary time constant T_p (see Figure 4). For simplification, only the far-from-generator short circuit is treated here.

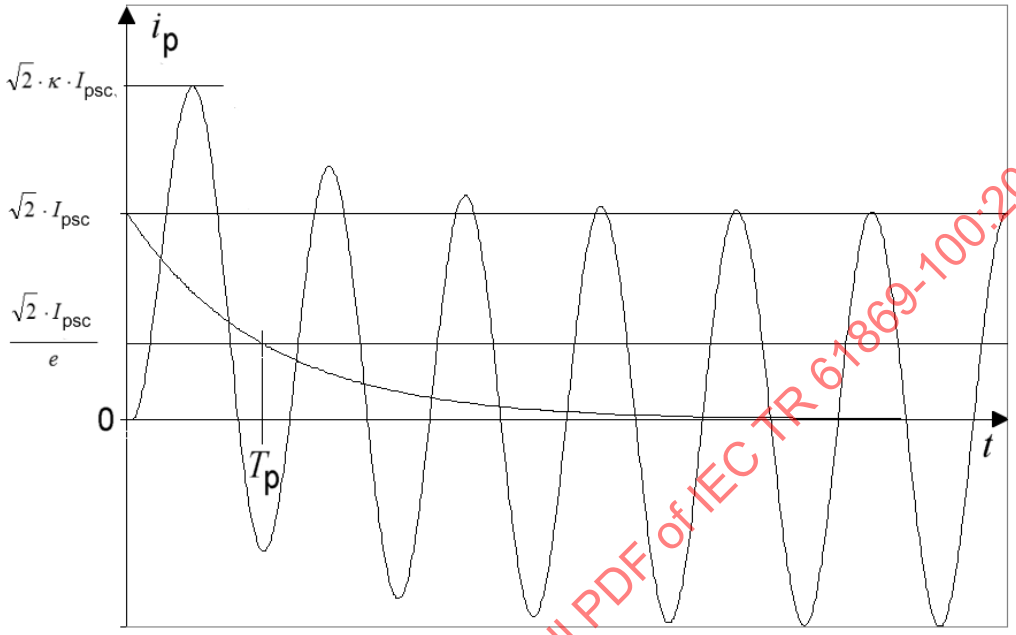

Key

i_p	primary current
I_{psc}	rated primary short circuit current
e	base of natural logarithm
t	time
T_p	specified primary time constant
κ	factor for the calculation of the peak short circuit current according to IEC 60909-0:2001. It attains its maximum value $\kappa = 2$ if T_p tends towards ∞.

Figure 4 – Primary short circuit current

In IEC 61869-2, the standard value for I_{dyn} is defined as 2,5 I_{th}. This value does not correspond strictly to the worst-case value of $\sqrt{2} \cdot \kappa \cdot I_{psc}$, which is 2,83 $\cdot I_{psc}$.

EXAMPLE At 50 Hz, the factor κ = 2,5 / √2 = 1,77 corresponds to an X_p / R_p value of 11 and a T_p value of 35 ms only.

5.1.2 Current transformer

The current transformer is represented by the current ratio k_r, the non-linear inductance L_{ct} with magnetizing curve and winding resistance R_{ct}.

Figure 5 shows the time dependent magnetizing curve of a typical CT core as flux $\psi(t)$ in the non-linear inductance L_{ct} versus magnetizing current $i_m(t)$ (see Figure 3) gained by measurement with an indirect test (primary side with open terminals, excitation and measurement from secondary terminals). If a voltage of rated frequency (e.g. 50 Hz) is applied, the grey curves are the result for steady-state excitations with different magnitudes. If the excitation is performed with DC voltage (see DC method in IEC 61869-2) starting with a demagnetised CT core, the red curve is the result. If the excitation with DC voltage starts with positive remanence, the blue initial curve is the result (see also Figure 51). The main

difference between the DC and the AC curve is mainly caused by higher eddy currents in the AC case.

Such measurements show the magnetizing curve:

- with a steep linear part which is limited by magnetic saturation,
- with ascending and descending curves which are shifted because of hysteresis.

The result is an ambiguous curve, which depends on frequency and antecedence.

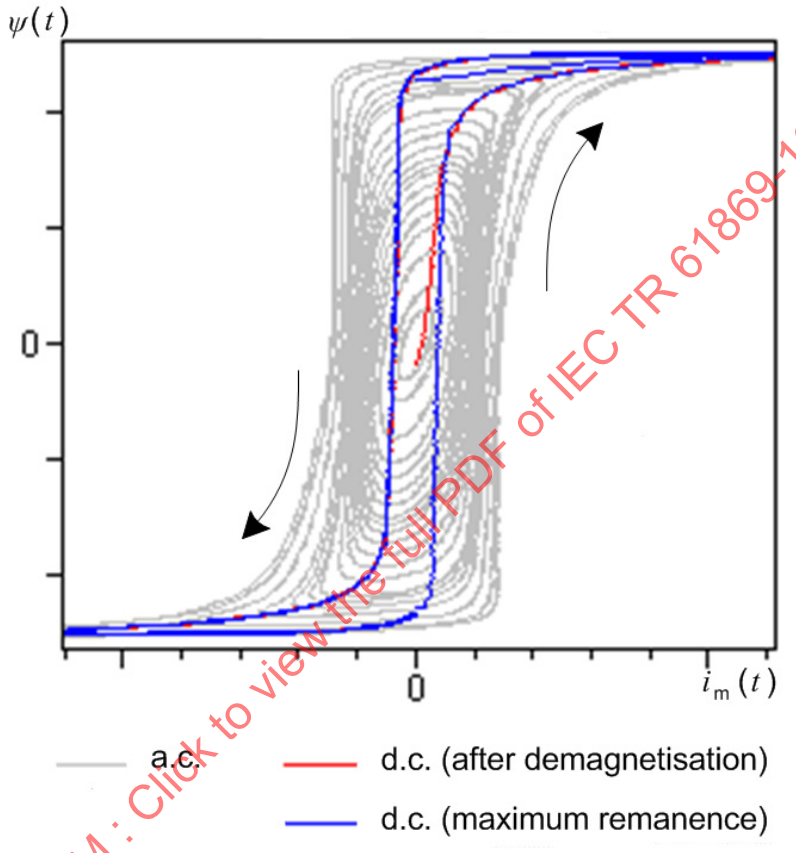

Key

ψ magnetic flux in the current transformer core

i_m magnetizing current

t time

Figure 5 – Non-linear flux of L_{ct}

Such a non-linear physical behaviour is very difficult to describe, so simplifications are necessary. Therefore, at first the hysteresis is neglected and the magnetizing characteristic is simplified to an origin curve with its saturation (dotted line in Figure 6).

In a second step, this curve can be typically represented by a simplified model with one single constant inductance L_m as the slope of the linear part of the magnetizing curve (Figure 6), so the saturation is neglected too (solid red line in Figure 6).

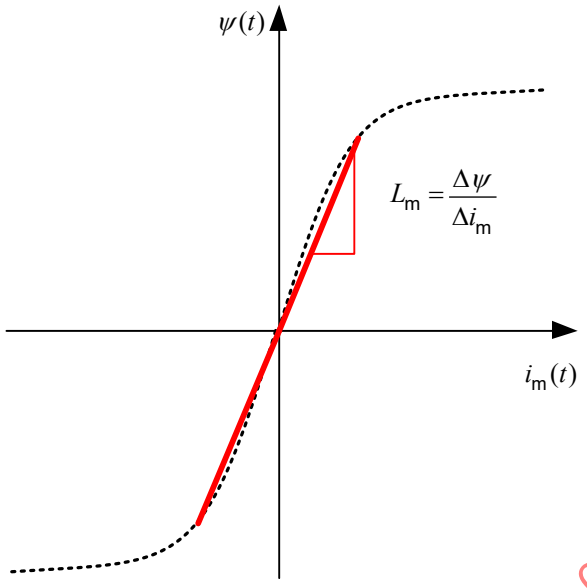

Key

ψ	magnetic flux in the current transformer core
i_m	magnetizing current
L_m	linearized inductance
t	time

Figure 6 – Linearized magnetizing inductance of a current transformer

With such a simplified linear analytical theory, the magnetic behaviour is only described correctly

– for CT demagnetised cores (no remanence), or gapped cores where remanence is significantly reduced,

– up to the time of the first saturation or up to the accuracy limit t'_{al}.

Two simplification steps are therefore needed:

– neglecting the hysteresis phenomena,

– neglecting saturation.

5.2 Transient behaviour

5.2.1 General

As an example, in Figure 7, the short circuit behaviour is simulated with a non-linear model, considering the following configuration:

Current transformer: 500/1 A, 2,5 VA, 5P20, R_{ct} = 2 Ω
real burden = rated burden

Short circuit: I_{psc} = 10 kA = 20 × I_{pr}, T_p = 50 ms

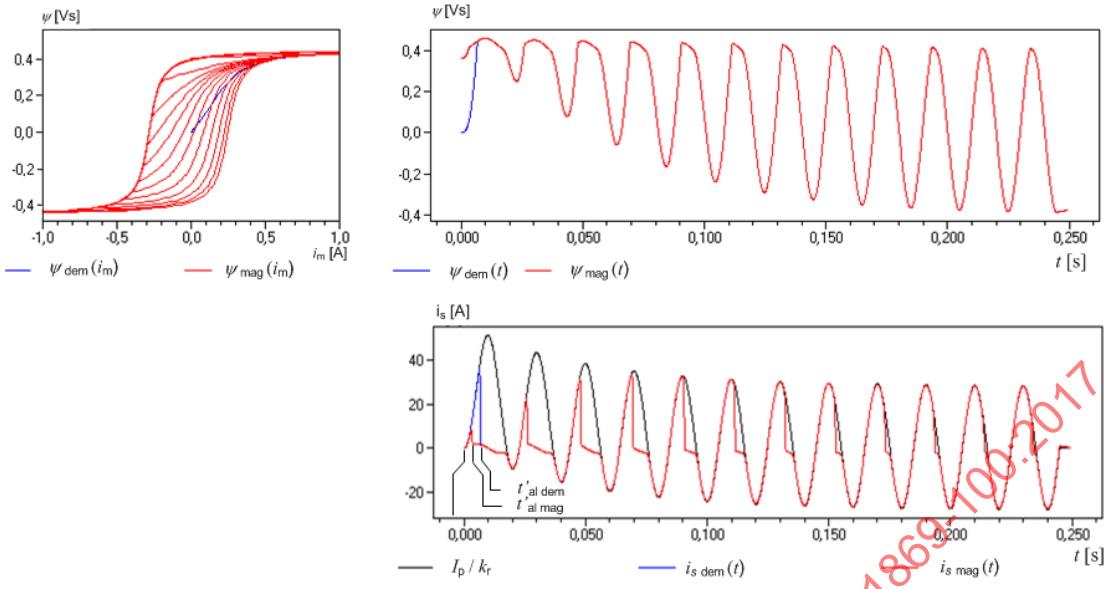

Key

I_p	primary current
$i_{s\ dem}$	secondary current in an initially demagnetized core
$i_{s\ mag}$	secondary current in an initially magnetized core
k_r	rated transformation ratio
t	time
$t'_{al\ dem}$	maximum possible t'_{al} value in an initially demagnetized core
$t'_{al\ mag}$	maximum possible t'_{al} value in an initially magnetized core
ψ	magnetic flux in the current transformer core
ψ_{dem}	magnetic flux in an initially demagnetized core
ψ_{mag}	magnetic flux in an initially magnetized core

Figure 7 – Simulated short circuit behaviour with non-linear model

The simulation in Figure 7 is performed in phase L1 with a maximum DC component and with an AC component I''_k of 20 times the rated primary current I_{pr}. This CT core with protection class 5P20 is correctly dimensioned for the symmetrical steady state case, when the DC component has declined. Saturation occurs, however, shortly after fault inception due to the DC component, regardless of whether the core is demagnetised or not. Therefore the transient performance CT classes TPX, TPY, TPZ with an additional transient dimensioning factor K_{td} were created.

The simulation starts with a demagnetized CT core (blue lines) as well as with a saturated core (90 % remanence, red lines). The left image shows the magnetic flux $\psi(t)$ versus magnetizing current $i_m(t)$. It shows hysteresis and saturation. The magnetic flux can only alternate between the positive and negative limits due to saturation. Starting without remanence (demagnetised case), the first saturation is reached at $t'_{al,dem}$ = 6,5 ms. With remanence, the first saturation is reached much earlier at $t'_{al,mag}$ = 3 ms. In some cases, this could lead to maltrips by some protection relays, e.g. differential protection function. In other cases, e.g. overcurrent protection, it does not result in a maltrip. It may however result in a slower reaction of the protection system.

Negative effects for certain protection functions due to remanence can be avoided easily by application of gapped CT cores. In this case, hysteresis is neglected for simplification purposes (first simplification step).

From the point of view of protection functions, the requirement for the signal quality of the CT secondary current is given by the time to accuracy limit t'_{al}. This value is defined as the

minimum saturation-free time interval, beginning at the first fault inception. Within this time span, the magnetic flux shall be in the linear range of the magnetizing curve, and the protection function shall decide whether to trip or not. The time after the first saturation is then out of the scope in this consideration. With the required time t'_{al}, the transient factor K_{tf} and the transient dimensioning factor K_{td} are calculated and/or determined by testing with the protection relay respectively (see Clause 9). Therefore, for such purposes, only the linear range of the magnetizing curve is interested. The physical problem can be further reduced and simplified to a linear one by neglecting the saturation too (second simplification step). With the constant inductance L_{ct} in the linear problem, the differential Equation (1) can be solved with acceptable mathematical complexity.

5.2.2 Fault inception angle

In the simulation of Figure 7 with a single phase and demagnetised core, a switching angle is chosen to achieve the highest DC component. Under this understanding, a time to accuracy limit t'_{al} of approximately 6,5 ms is obtained.

It shall be kept in mind that this t'_{al} value is valid for one phase only. In cases of multi-phase short circuits, other phases shall also be considered. The above simulation was complemented correspondingly, applying the same preconditions.

In Figure 8, the DC component of phase L1 is at its highest value, while the DC component of other phases L2, L3 is considerably lower. Despite this fact, one can observe that saturation occurs earlier in phase L2 ($t'_{al} \cong 5$ ms) than in phase L1. Therefore, further detailed considerations of the variation of the fault inception or switching angle are necessary.

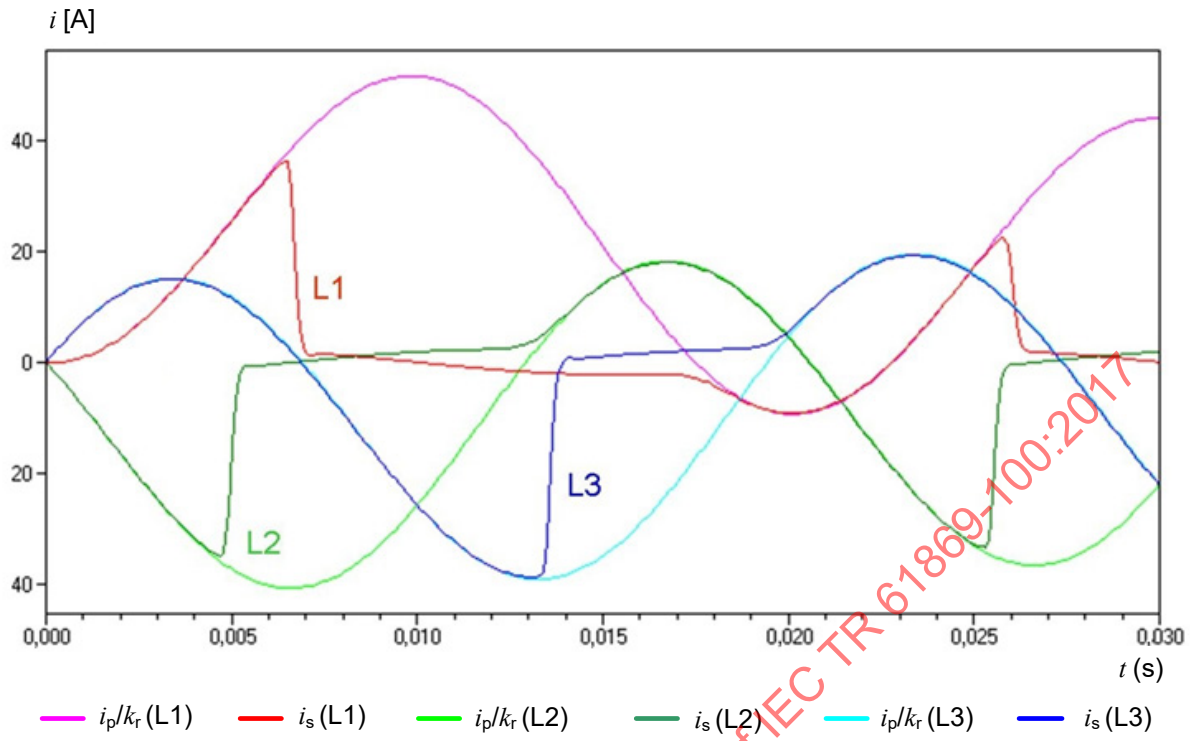

Key

i	current
i_p	primary current
i_s	secondary current
k_r	rated transformation ratio
t	time

Figure 8 – Three-phase short circuit behaviour

5.2.3 Differential equation

Based on the two simplifications above, with the constant inductance L_{ct} in the linear physical problem, the linear differential equation of the first order is formulated for the magnetizing current i_m and the primary current $i_p(t)$ (see Figure 3):

$$T_s \frac{di_m(t)}{dt} + i_m(t) = i_p(t) \qquad i_m(0) = 0 \tag{1}$$

The magnetic behaviour can then be described by the analytical formula for the secondary linked flux:

$$\psi(t) = L_{ct}\, i_m(t) \tag{2}$$

The flux contains a transient part (due to the DC component of the primary short circuit current), and a steady state AC part. Figure 9 presents these parts in a simplified form.

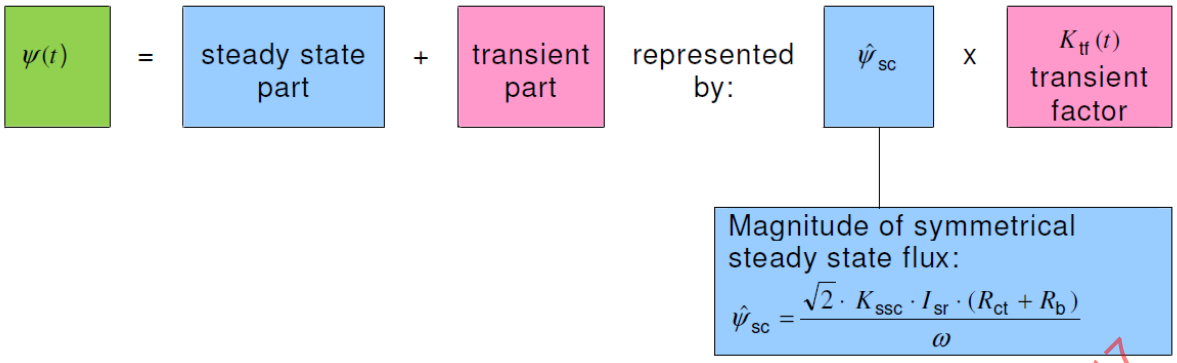

Key

I_{sr}	rated secondary current
K_{tf}	transient factor
K_{ssc}	rated symmetrical short circuit current factor
R_b	rated resistive burden
R_{ct}	secondary winding resistance
t	time
ψ	secondary linked flux
$\hat{\psi}_{sc}$	peak value of the secondary linked flux in the current transformer core at symmetrical short circuit condition
ω	angular frequency

Figure 9 – Composition of flux

The transient part with two time constants T_p and T_s is represented by the time-dependent transient factor $K_{tf}(t)$. This factor scales up the magnitude $\hat{\psi}_{sc}$ from the peak value of the AC component to the peak value of the transient curve.

As it will be shown below, $K_{tf}(t)$ is expressed by several formulae and represents only the magnetic linear theory. For transient performance, the physical requirement for the CT, resulting from the protection algorithms, can be expressed by the single parameter t'_{al} (time to accuracy limit). t'_{al} again is used to calculate K_{tf}, which defines the flux limit, up to which the CT core shall not saturate.

For the algorithms of modern protection devices, it is not sufficient just to provide the CT requirements as the only parameters, such as t'_{al}. In some cases, this value is not constant. It can be a function of further parameters, e.g. the magnitude of the fault current, its inception angle γ (determining the DC component, decaying with the primary time constant T_p) and the protection settings. Therefore it is recommended to test the protection relays with different CT sizes and significant worst-case conditions with a numerical non-linear CT model also containing hysteresis. The analytically calculated transient factor K_{tf} and the additional relay tests lead to the final transient dimensioning factor K_{td} of the CT, which leads to the rated equivalent limiting secondary e.m.f. E_{al} according to the definition in IEC 61869-2:2012, 3.4.237:

$$E_{al} = K_{ssc} \times K_{td} \times (R_{ct} + R_b) \times I_{sr} \quad (3)$$

In this regard, K_{td} differs from the definition in the previous standard: IEC 60044-6: The formulae in IEC 61869-2:2012 consider also very small time to accuracy limit values t'_{al}, as well as the worst-case fault inception angles resulting from the requirements of modern protection relays.

They provide a basis for the relay tests, which should be performed by protection manufacturers in order to provide simpler CT requirements in the relay manuals. These simpler requirements have to be applied by end users in projects and CT designing. In this regard, the technical responsibility for CT requirements is shifted somewhat away from the

end users toward the relay manufacturers and thus the requirements become simpler for the end user.

The protection device as the burden of the CT measures low operational currents as well as higher overcurrents at the highest desirable accuracy. The input signal of the protection device is the CT secondary current, which should correspond to the primary current. In modern protection devices, multiple measuring and protection algorithms are implemented, which require different accuracy classes and transient performances from the CT, where a compromise has to be found between CT size, maximum accuracy and the best performance.

6 Duty cycles

6.1 Duty cycle C – O

6.1.1 General

The following equations refer to a C – O duty cycle. The general expression for the instantaneous value of a primary short circuit current may be defined as:

$$i_{sc}(t) = \sqrt{2}\ I_{psc}\left[e^{-t/T_p}\cos(\gamma-\varphi) - \cos(\omega t+\gamma-\varphi)\right] \quad (4)$$

with the equivalent voltage source of the primary short circuit

$$u(t) = -U_{max}\cos(\omega t+\gamma) \quad (5)$$

where

I_{psc} is the r.m.s. value of primary symmetrical short circuit current $I_{psc} = K_{ssc} \cdot I_{pr}$;

$T_p = \frac{L_p}{R_p}$ is the primary time constant;

γ is the switching angle or fault inception angle (see 3.1.9);

$= \arctan\frac{X_p}{R_p} = \arctan(\omega T_p)$ is the phase angle of the system short circuit impedance.

For simplification purposes, the fault inception angle and system short circuit impedance angle can be summed up into one single angle θ, which makes the calculation easier to understand:

$$\theta = \gamma - \varphi \quad (6)$$

$$i_{sc}(t) = \sqrt{2}\ I_{psc}\left[e^{-t/T_p}\cos(\theta) - \cos(\omega t+\theta)\right] \quad (7)$$

The angles θ and γ both describe the possibility of varying the fault inception angle and therefore can be applied alternatively, but according to their definition.

Figure 10 shows two typical primary short circuit currents:

a) The red one occurs with a fault inception angle of $\gamma = 90°$ which leads to the highest peak current and the highest peak of secondary linked flux for long t'_{al} (Figure 11).

b) The blue one occurs with $\gamma = 140°$ which leads to a lower asymmetry. These cases are important for short t'_{al}, because, during the first half cycle, the current and flux are temporarily higher than in the case of $\gamma = 90°$.

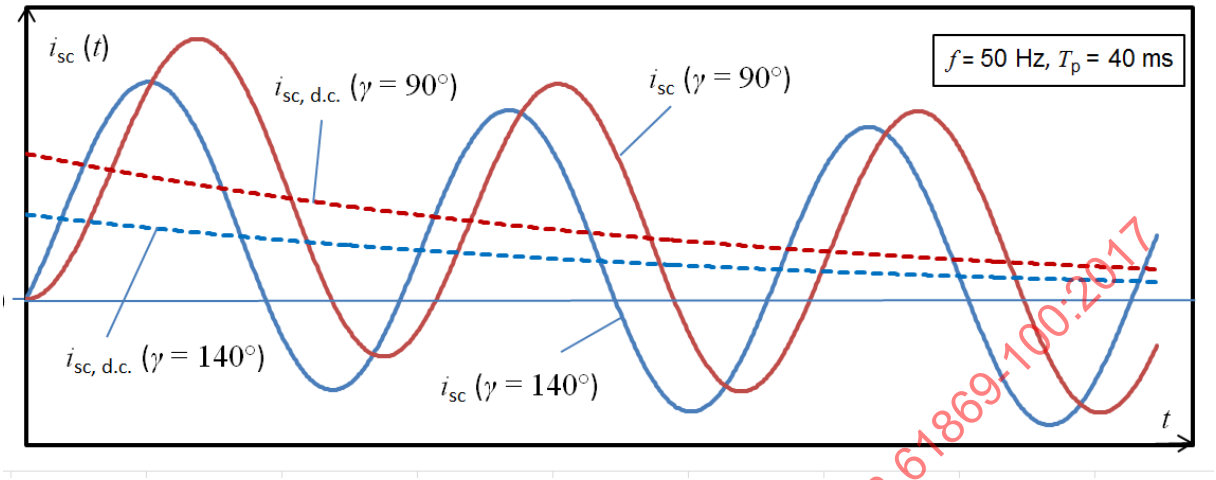

Key

f	frequency
T_p	specified primary time constant
γ	fault inception angle
i_{sc}	instantaneous value of a primary short circuit current
$i_{sc,,d.c.}$	DC component of the instantaneous value of a primary short circuit current
t	time

Figure 10 – Short circuit current for two different fault inception angles

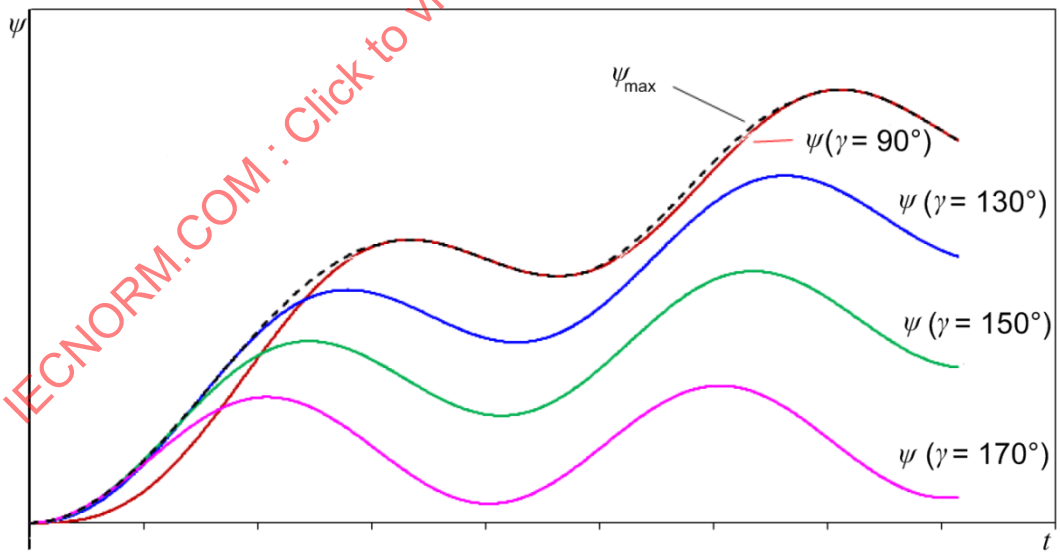

Key

t	time
γ	fault inception angle
ψ	secondary linked flux
ψ_{max}	highest possible flux value at a given time point, considering all fault inception angles γ in a defined range

Figure 11 – ψ_{max} as the curve of the highest flux values

It is easier to evaluate and plot the formulae in the calculations described in 6.1.2 and 6.1.3 with a software tool. For the more complex formulae, the programming code is given in Annex A.

6.1.2 Fault inception angle

Table 1 shows the four significant cases of short circuit current inception angles (here described for positive current polarity only. The negative polarity occurs by inversion of the values at the origin point; all angles increased by 180°.

Table 1 – Four significant cases of short circuit current inception angles

Case no.	Meaning	θ condition	equivalent γ condition	example for φ = 70° (Figure 12)
1	maximum DC component	$\theta = 0°$	$\gamma = \varphi$	$\gamma = 70°$
2	maximum peak of short circuit current: $\hat{\imath}_p = \sqrt{2}\cdot\kappa\cdot I_{psc}$ fault inception at voltage zero crossing	$\theta = 90° - \varphi$	$\gamma = 90°$	$\gamma = 90°$
3	no DC component	$\theta = 90°$	$\gamma = 90° + \varphi$	$\gamma = 160°$
4	fault inception at voltage maximum	$\theta = 180° - \varphi$	$\gamma = 180°$	$\gamma = 180°$

Case 4 is the one with the highest initial flux increase, and therefore the worst-case for very small values of t'_{al}.

Figure 12 shows the current curves for these 4 cases. The phase angle φ of the system short circuit impedance has been chosen extremely low, in order to point out the differences between the different cases.

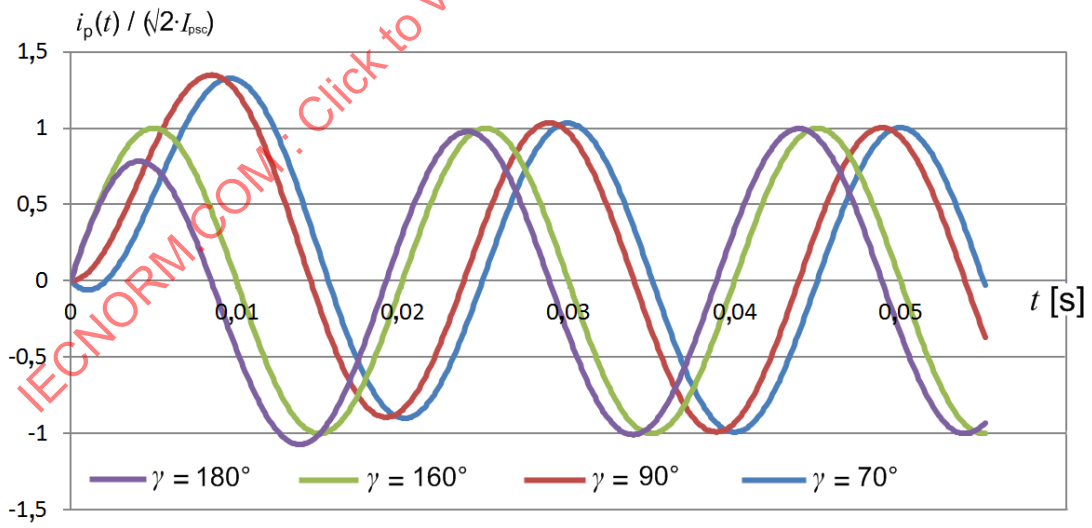

Key

i_p primary current

I_{psc} rated primary short circuit current

t time

γ fault inception angle

Figure 12 – Primary current curves for the 4 cases for 50 Hz and φ = 70°

Figure 13 shows these four cases in a polar diagram.

γ_m is the lowest value of γ to be considered in the designing of the current transformer. The possible limiting of the range of the current inception angle is discussed in 6.1.4.

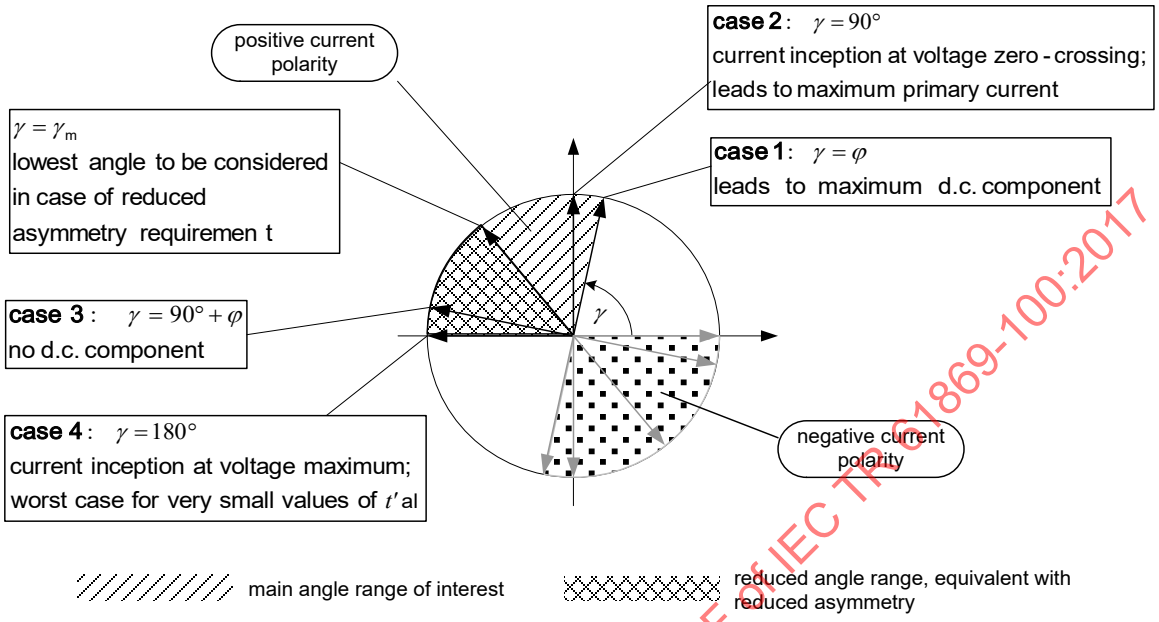

Key

γ_m lowest fault inception angle to be considered in case of a reduced asymmetry requirement

t'_{al} specified time to accuracy limit in the first fault

γ fault inception angle

φ phase angle of the system short circuit impedance

Figure 13 – Four significant cases of short circuit currents with impact on magnetic saturation of current transformers

6.1.3 Transient factor K_{tf} and transient dimensioning factor K_{td}

6.1.3.1 General

The transient dimensioning factor K_{td} is the final parameter for the core designing and is given on the rating plate. It can be calculated as different functions of the transient factor K_{tf} as given in the equations below and later shown in Figure 14.

In 6.1.3, the determination of the transient dimensioning factor K_{td} is discussed under the condition that every fault inception angle γ may occur. In some special cases, a reduced range of fault inception angle (expressed by γ_m) may lead to a reduced factor K_{td} (see 6.1.4).

6.1.3.2 Equations for K_{tf}

The transient factor K_{tf} given in this section is derived from the differential equation for the equivalent circuit (Figure 3) with the constant inductance L_{ct} of the current transformer core, with an ohmic burden and without consideration of hysteresis, losses and remanence. With the exact solution $i_\varepsilon(t)$ of the differential equation, the transient factor $K_{tf}(t)$ is gained from the magnetic flux ratio

$$K_{\mathrm{tf}}(t) = \frac{\psi(t)}{\hat{\psi}_{\mathrm{sc}}} = \frac{L_{\mathrm{ct}}\, i_{\varepsilon}(t)}{\hat{\psi}_{\mathrm{sc}}} \tag{8}$$

where

$\hat{\psi}_{\mathrm{sc}}$ is the peak value of the AC component of the flux during short circuit;

L_{ct} is the linearized inductance (see Figure 6).

Similarly to the magnetic flux, K_{tf} also depends on time and, finally, on the time to accuracy limit t'_{al} as required by the protection system. When calculating using the linear inductivity, the solution is only valid up to the first saturation of the current transformer.

Strictly speaking, the time to accuracy limit t'_{al} is the only physical parameter which acts as an interface between the protection relay and the current transformer and is decisive for the proper and stable operation of the relay. In many cases, t'_{al} is assumed to be constant, independent of other physical parameters. But, in some cases, due to complex algorithms and functions, the protection system may require a t'_{al} which is not constant and which depends on different parameters of the short circuit current. Therefore, the transient dimensioning factor K_{td} can also be tested and defined directly by the manufacturer of the protection system according to the physical basics described in this technical report. For logical reasons, the perfect function of the protection is then the protection manufacturer's responsibility.

The actual transient K_{tf} containing the AC component is

$$K_{\mathrm{tf}}(t) = \omega\, T_{\mathrm{s}} \left[\frac{\mathrm{e}^{-t/T_{\mathrm{s}}}}{T_{\mathrm{p}} - T_{\mathrm{s}}} \left(\begin{array}{l} \cos(\theta)\, T_{\mathrm{p}}\, \mathrm{e}^{(t/T_{\mathrm{s}} - t/T_{\mathrm{p}})} \\ + \dfrac{\omega\, T_{\mathrm{s}}\, \sin(\theta)\left(T_{\mathrm{p}} - T_{\mathrm{s}}\right) - T_{\mathrm{s}}\, \cos(\theta)\left(1 + \omega^2\, T_{\mathrm{s}}\, T_{\mathrm{p}}\right)}{1 + \omega^2\, T_{\mathrm{s}}^2} \end{array} \right) - \frac{\omega\, T_{\mathrm{s}}\, \sin(\omega\, t + \theta) + \cos(\omega\, t + \theta)}{1 + \omega^2\, T_{\mathrm{s}}^2} \right] \tag{9}$$

A simplified formula for K_{tf} exists as follows:

$$K_{\mathrm{tf}}(t) = \frac{\omega T_{\mathrm{s}} T_{\mathrm{p}}}{T_{\mathrm{p}} - T_{\mathrm{s}}} \cos(\theta) \left(\mathrm{e}^{-t/T_{\mathrm{p}}} - \mathrm{e}^{-t/T_{\mathrm{s}}} \right) + \sin(\theta) \mathrm{e}^{-t/T_{\mathrm{s}}} - \sin(\omega t + \theta) \tag{10}$$

For extremely low parameters of T_{p}, T_{s}, and t'_{al}, the K_{tf}. value of Equation (10) is lower than the one of Equation (9), and therefore not on the safe side.

With θ = 0 (equivalent to $\gamma = \varphi$), Equation (10) leads to the well-known formula in the former IEC 60044-6, which is given here for backward compatibility (with index "dc"):

$$K_{\mathrm{tf,\,dc}}(t) = K_{\mathrm{tf}}(\theta = 0°) = \frac{\omega T_{\mathrm{p}} T_{\mathrm{s}}}{T_{\mathrm{p}} - T_{\mathrm{s}}} \left(\mathrm{e}^{-t/T_{\mathrm{p}}} - \mathrm{e}^{-t/T_{\mathrm{s}}} \right) - \sin(\omega\, t) \tag{11}$$

When calculating the transient factor necessary for designing purposes, Equation (9) is modified by assuming the worst case condition $\sin(\omega t) = -1$. The result is the envelope curve K_{tfp} for peak values of the transient factor.

$$K_{\mathrm{tfp}}(t) = \omega T_{\mathrm{s}} \left[\frac{\mathrm{e}^{-t/T_{\mathrm{s}}}}{T_{\mathrm{p}} - T_S} \left(\cos(\theta)\, T_{\mathrm{p}}\, \mathrm{e}^{(t/T_{\mathrm{s}} - t/T_{\mathrm{p}})} + \frac{\omega T_{\mathrm{s}} \sin(\theta)\left(T_{\mathrm{p}} - T_{\mathrm{s}}\right) - T_{\mathrm{s}} \cos(\theta)\left(1 + \omega^2 T_{\mathrm{s}} T_{\mathrm{p}}\right)}{1 + \omega^2 T_{\mathrm{s}}^2} \right) + \frac{1 + \omega T_{\mathrm{s}}}{1 + \omega^2 T_{\mathrm{s}}^2} \right] \tag{12}$$

A simplified formula is given in Equation (13):

$$K_{\mathrm{tfp}}(t) = \frac{\omega T_{\mathrm{s}} T_{\mathrm{p}}}{T_{\mathrm{p}} - T_{\mathrm{s}}} \cos(\theta)\left(\mathrm{e}^{-t/T_{\mathrm{p}}} - \mathrm{e}^{-t/T_{\mathrm{s}}}\right) + \sin(\theta)\mathrm{e}^{-t/T_{\mathrm{s}}} + 1 \tag{13}$$

With θ = 0, we get the formula for K_{td} in IEC 60044-6, now indicated as $K_{\mathrm{tfp,dc}}$ (14):

$$K_{\mathrm{tfp,dc}}(t) = \frac{\omega T_{\mathrm{p}} T_{\mathrm{s}}}{T_{\mathrm{p}} - T_{\mathrm{s}}}\left(\mathrm{e}^{-t/T_{\mathrm{p}}} - \mathrm{e}^{-t/T_{\mathrm{s}}}\right) + 1 \tag{14}$$

The maximum values occur at the time $t = t_{\mathrm{tfp,max}}$ (15) and $t = t_{\mathrm{tfp,dc,max}}$ (16):

$$t_{\mathrm{tfp,max}} = \frac{T_{\mathrm{p}} T_{\mathrm{s}}}{T_{\mathrm{p}} - T_{\mathrm{s}}} \ln \frac{\frac{T_{\mathrm{p}}}{T_{\mathrm{s}}}\cos(\theta) + \frac{T_{\mathrm{s}} - T_{\mathrm{p}}}{\omega T_{\mathrm{s}}^2}\sin(\theta)}{\cos(\theta)} \tag{15}$$

$$t_{\mathrm{tfp,dc,max}} = \frac{T_{\mathrm{p}}\, T_{\mathrm{s}}}{T_{\mathrm{p}} - T_{\mathrm{s}}} \ln \frac{T_{\mathrm{p}}}{T_{\mathrm{s}}} \tag{16}$$

The corresponding values $K_{\mathrm{tfp,max}}$ and $K_{\mathrm{tfp,dc,max}}$ are given in Equations (17) and (18) as

$$K_{\mathrm{tfp,max}} = \left(\omega T_{\mathrm{p}} \cos(\theta) + \frac{T_{\mathrm{p}} + T_{\mathrm{s}}}{T_{\mathrm{s}}} \sin(\theta)\right) \cdot \left[\frac{\frac{T_{\mathrm{p}}}{T_{\mathrm{s}}}\cos(\theta) + \frac{T_{\mathrm{s}} - T_{\mathrm{p}}}{\omega T_{\mathrm{s}}^2}\sin(\theta)}{\cos(\theta)} \right]^{\frac{T_{\mathrm{p}}}{T_{\mathrm{s}} - T_{\mathrm{p}}}} + 1 \tag{17}$$

$$K_{\mathrm{tfp,\,dc,\,max}} = \omega\, T_{\mathrm{p}} \left(\frac{T_{\mathrm{p}}}{T_{\mathrm{s}}}\right)^{\frac{T_{\mathrm{p}}}{T_{\mathrm{s}} - T_{\mathrm{p}}}} + 1 \tag{18}$$

In Figure 14, curve $K_{\mathrm{tf},\psi\mathrm{max}}$ is plotted as “overall transient factor”, that means as transient factor regarding all specified current inception angles. It is defined as the $\psi_{\mathrm{max}}(t)$ curve (Figure 11) divided by the peak value of the steady-state flux $\hat{\psi}_{\mathrm{sc}}$ (Figure 9). The behaviour of the upper envelope K_{tfp} of the curve $K_{\mathrm{tf},\psi\mathrm{max}}$ leads to the definition of three time ranges described in 6.1.3.3 to 6.1.3.5.

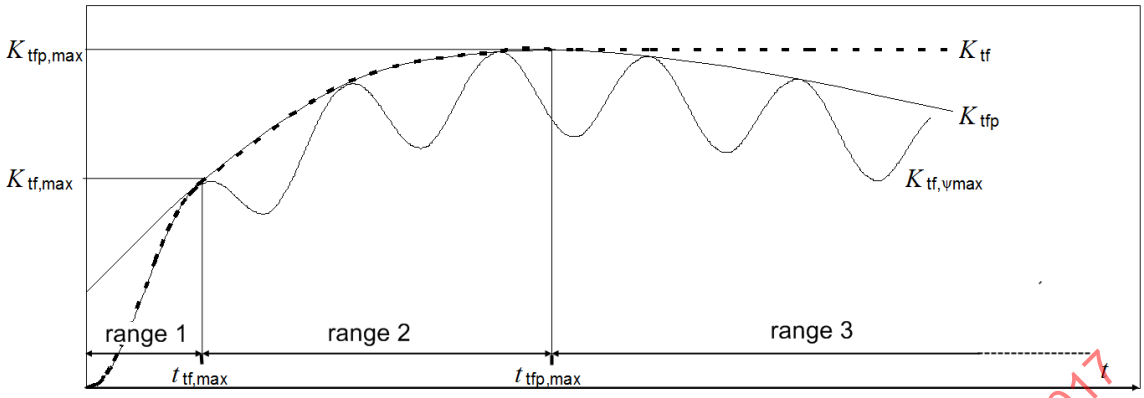

Key

$K_{tf,\psi max}$	overall transient factor
K_{tfp}	envelope of the curve $K_{tf,\psi max}(t)$
$K_{tfp,max}$	highest value of the curve $K_{tfp}(t)$
$K_{tf,max}$	K_{tf} value where the curve $K_{tf,\psi max}$ (t) touches its envelope $K_{tfp}(t)$ for the first time
K_{tf}	resulting transient factor, depending on the required saturation free time
t	time
$t_{tf,max}$	time point, where the curve $K_{tf,\psi max}$ (t) touches its envelope $K_{tfp}(t)$ for the first time
$t_{tfp,max}$	time point of the highest occurring K_{tfp} value

Figure 14 – Relevant time ranges for calculation of transient factor

6.1.3.3 Range 1: $0 \le t'_{al} \le t_{tf,max}$

$t_{tf,max}$ is the time, where the $K_{tf}(t)$ curve touches the envelope curve $K_{tfp}(t)$ for the first time (see Figure 14).

At this point in time, the following condition is fulfilled:

$$\sin(\omega t_{tf,max} + \gamma - \quad) = -1$$

This equation is equivalent to

$$t_{tf,max} = \frac{3\pi/2 - \gamma +}{\omega} \tag{19}$$

where

$= \arctan(\omega T_p)$.

In Figure 15, $t_{tf,max}$ is plotted versus the primary time constant T_p for several fault inception angles γ. $t_{tf,max}$ is practically constant for higher values of T_p, what occurs in common practice.

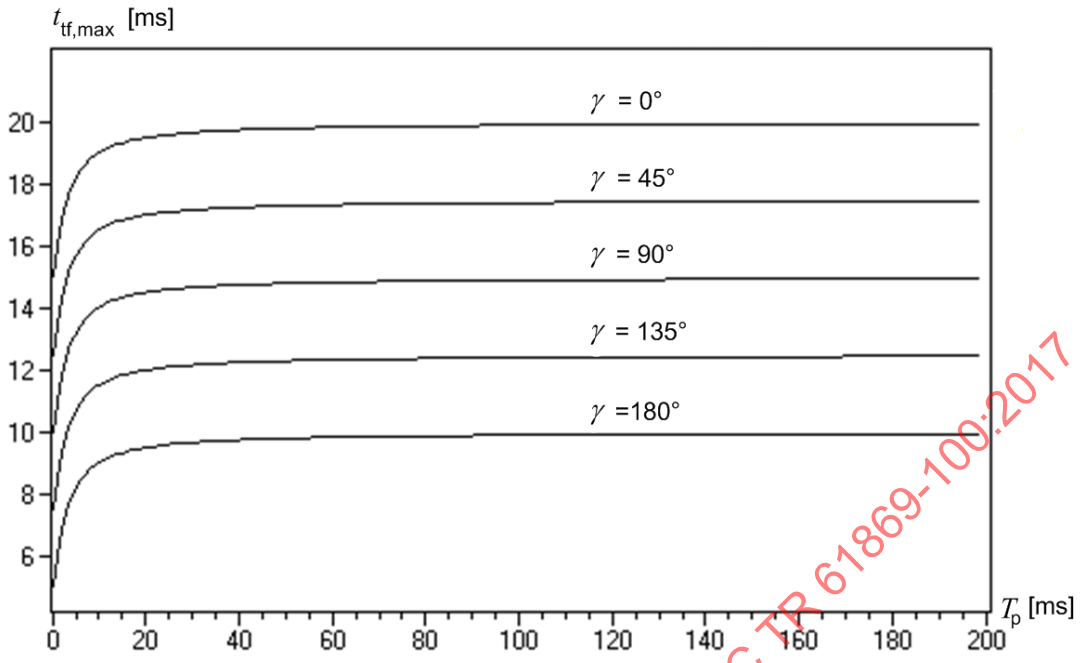

Key

$t_{tf,max}$	time point, where the curve $K_{tf,\psi max}$ (t) touches its envelope K_{tfp}(t) for the first time
T_p	specified primary time constant
γ	fault inception angle

Figure 15 – Occurrence of the first flux peak depending on T_p, at 50 Hz

For every t'_{al}, there exists a certain worst-case angle $\theta(t'_{al})$, which leads to the highest flux $\psi_{max}(t'_{al})$ at time t'_{al}.

This angle can be found by calculating the extreme value of K_{tf} in Equations (9) or (10) for $t = t'_{al}$, with θ as the dependent variable. This defines the angle $\theta_{tf,\psi max}$ and the corresponding fault inception angle $\gamma_{tf,\psi max}$:

$$\theta_{tf,\,\psi max} = \arctan\frac{Y}{X} \tag{20}$$

where

$$Y = \omega T_s - e^{t/T_s}\left[\omega T_s \cos(\omega t) - \sin(\omega t)\right]$$

$$X = \frac{1}{T_p - T_s}\left[T_p\left(1+\omega^2 T_s^2\right)e^{(t/T_s - t/T_p)} - T_s\left(1+\omega^2 T_s T_p\right)\right] - e^{t/T_s}\left[\cos(\omega t) + \omega T_s \sin(\omega t)\right]$$

and

$$\gamma_{tf,\psi max} = \theta_{tf,\psi max} + \varphi \tag{21}$$

The normal arctan function only provides results for $-\pi/2 < \theta < \pi/2$. Results for angles $|\theta| > \pi/2$ (see Figure 16, Figure 17, Figure 18) can be found with an arctan function which considers all four quadrants. In many mathematical software packages, such a function is known as θ = arctan2(x,y), where x and y are coordinates.

Introducing this angle in Equation (9) or Equation (10), we obtain the highest dimensioning factor for the current transformer for the specified time to accuracy limit t'_{al}.

$$K_{tf,\psi max} = K_{tf}(t'_{al}, \theta_{tf,\psi max}) \tag{22}$$

In Figure 16, the angle $\theta_{tf,\psi max}$ is plotted against the primary time constant T_p, for several values of t'_{al} and for two extreme cases of T_s, whereby the relation between T_s and the phase displacement $\Delta\varphi$ is given by

$$T_S[s] = \frac{3438}{2\pi \cdot 50[Hz] \cdot \Delta\varphi[min]}$$

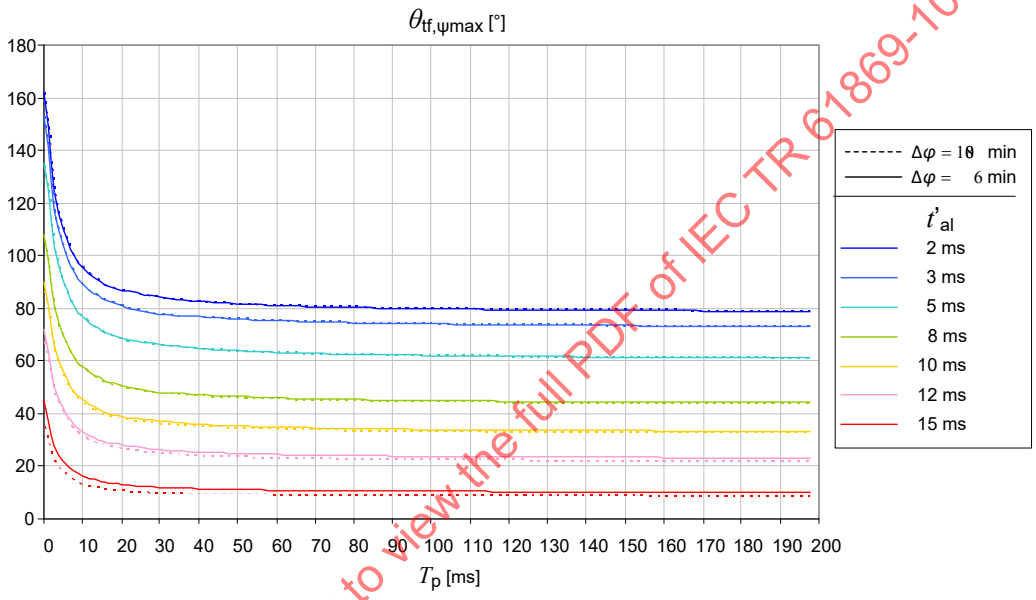

Key

T_p specified primary time constant

t'_{al} specified time to accuracy limit in the first fault

$\Delta\varphi$ phase displacement

$\theta_{tf,\psi max}$ worst-case fault inception angle (alternative definition), which leads to the highest flux at time t'_{al}

Figure 16 – Worst-case angle $\theta_{tf,\psi max}$ as function of T_p and t'_{al}

In Figure 17, $\theta_{tf,\psi max}$ is replaced by $\gamma_{tf,\psi max}$, see Equation (21).

The appropriate values of $K_{tf,\psi max}$ are given in Figure 18.

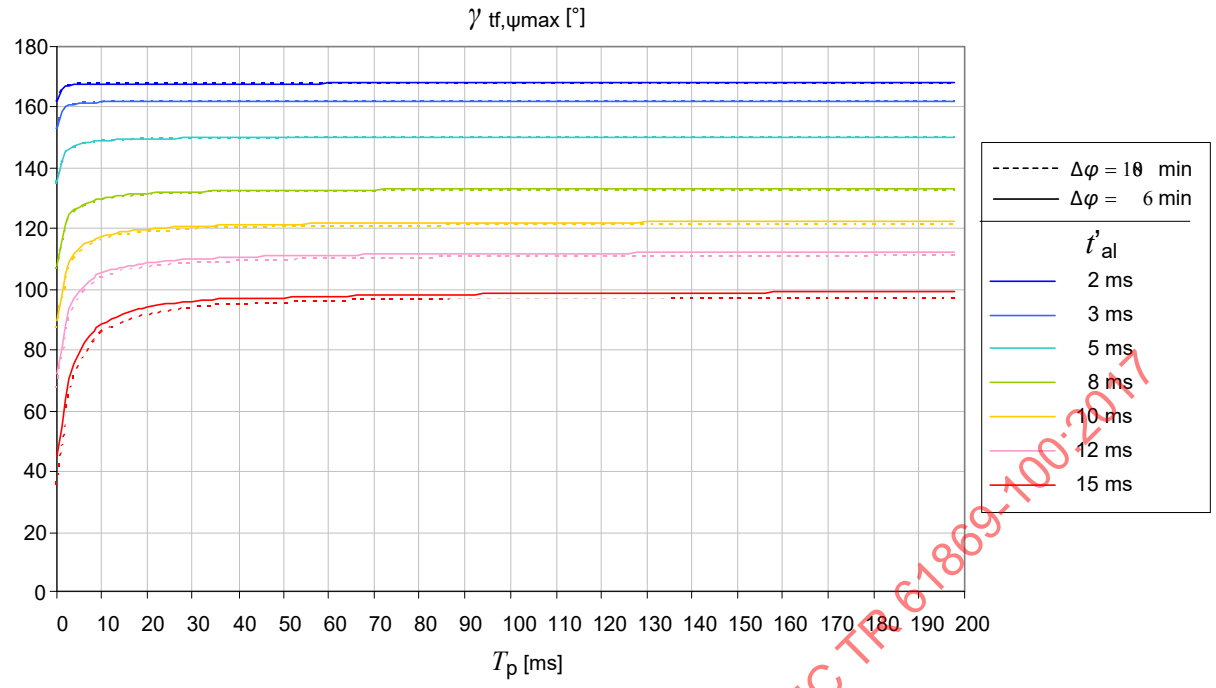

Key

T_p	specified primary time constant
t'_{al}	specified time to accuracy limit in the first fault
$\gamma_{tf,\psi max}$	worst-case fault inception angle which leads to the highest flux at time t'_{al}
$\Delta\varphi$	phase displacement

Figure 17 – Worst-case fault inception angle $\gamma_{tf,\psi max}$ as function of T_p and t'_{al}

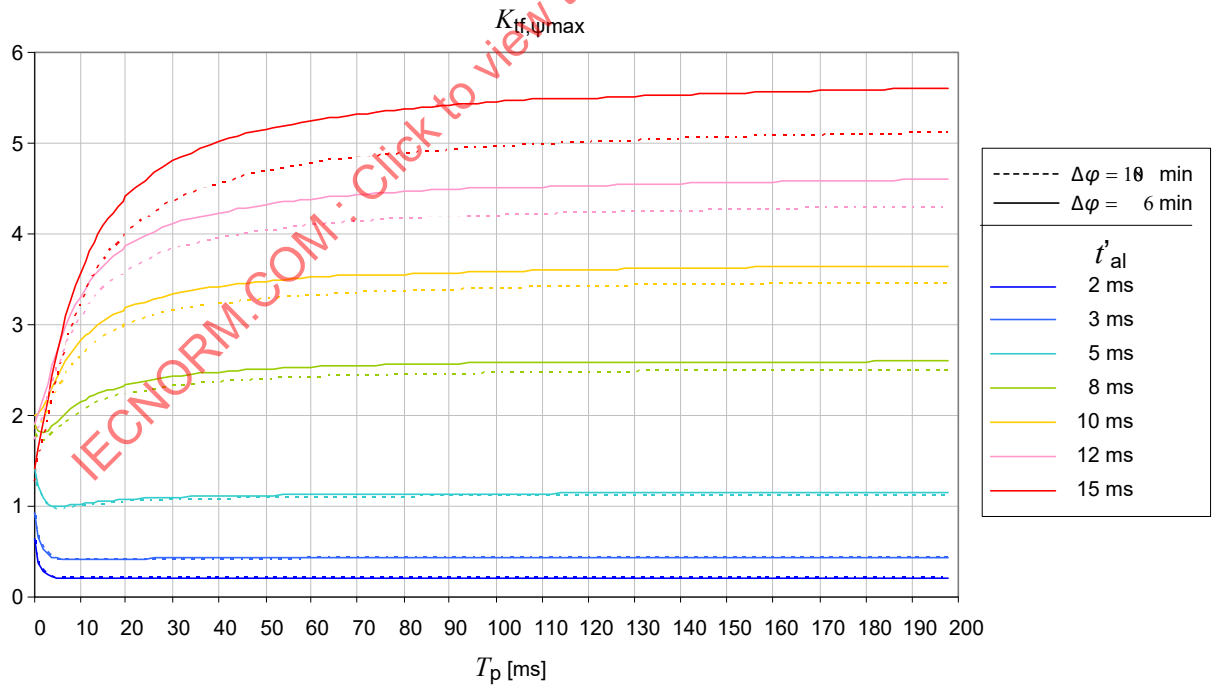

Key

$K_{tf,\psi max}$	overall transient factor, see Figure 14
T_p	specified primary time constant
t'_{al}	specified time to accuracy limit in the first fault
$\Delta\varphi$	phase displacement

Figure 18 – $K_{tf,\psi max}$ calculated with worst-case fault inception angle $\theta_{\psi max}$

In Figure 18, some curves intersect at a very low primary time constant T_p, but some of those curve values are actually not part of time range 1, they belong to time range 2. This effect is corrected and eliminated in Figure 20.

For a better understanding, $K_{tf,\psi max}$ and $\gamma_{tf,\psi max}$ are plotted in a polar diagram (Figure 19), similar to the one in Figure 13, with T_p as parameter.

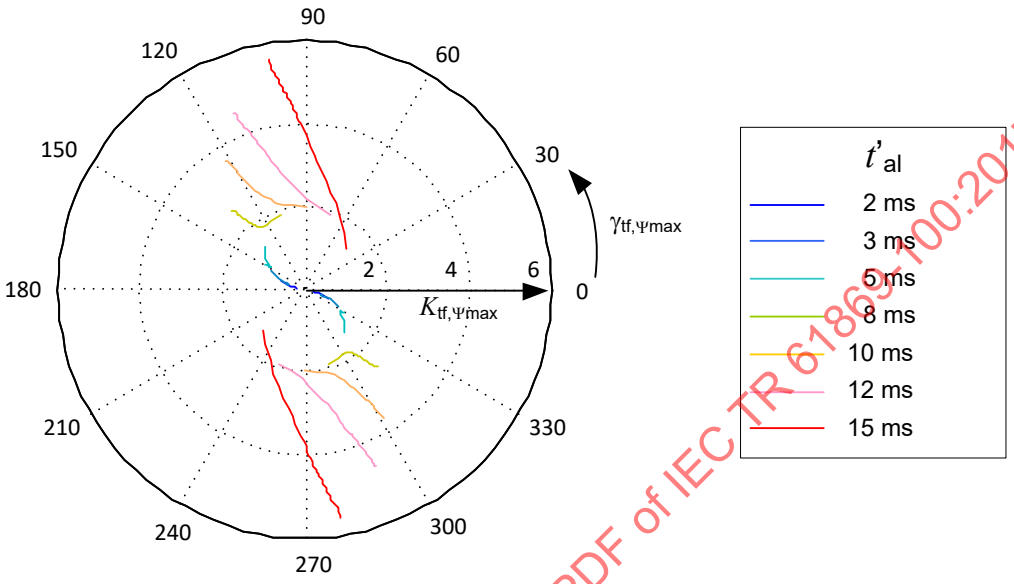

Key

$K_{tf,\psi max}$	overall transient factor, see Figure 14
$\gamma_{tf,\psi max}$	worst-case fault inception angle which leads to the highest flux at time t'_{al}
t'_{al}	specified time to accuracy limit in the first fault

Figure 19 – Polar diagram with $K_{tf,\psi max}$ and $\gamma_{tf,\psi max}$

Due to the complexity and the potential mistakes that can be made in daily application, the function $K_{tf,\psi max} = K_{tf}(\gamma_{tf,\psi max}(t'_{al}))$ is shown in Figure 20 as curves for different t'_{al} and secondary time constants T_s plotted against the primary time constant T_p for given configurations of secondary time constant and frequency.

Due to the complexity of the relationships, potential mistakes can be made in the daily application. Therefore, Figure 20, shows the function $K_{tf,\psi max}$ versus the primary time constant T_p, as an array of curves with the array parameter t'_{al}.

The sub-figures a) to i) cover 3 frequency values and, for each frequency value, 3 values of the secondary time constant T_s.

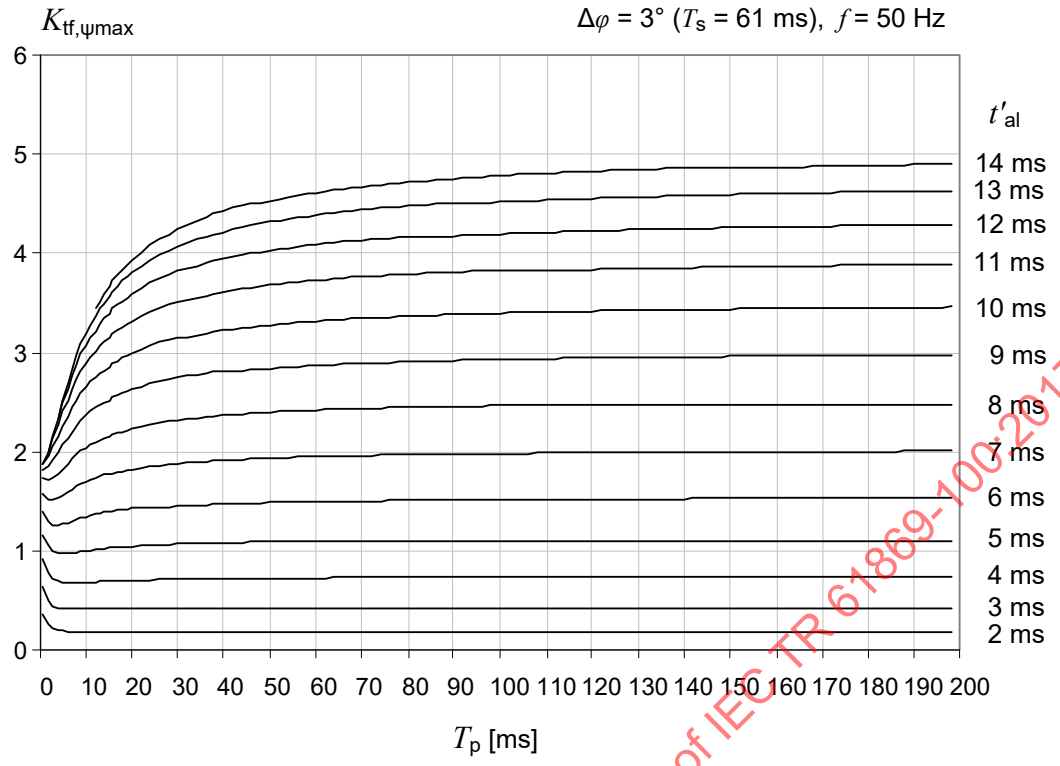

a) T_s = 61 ms at 50 Hz

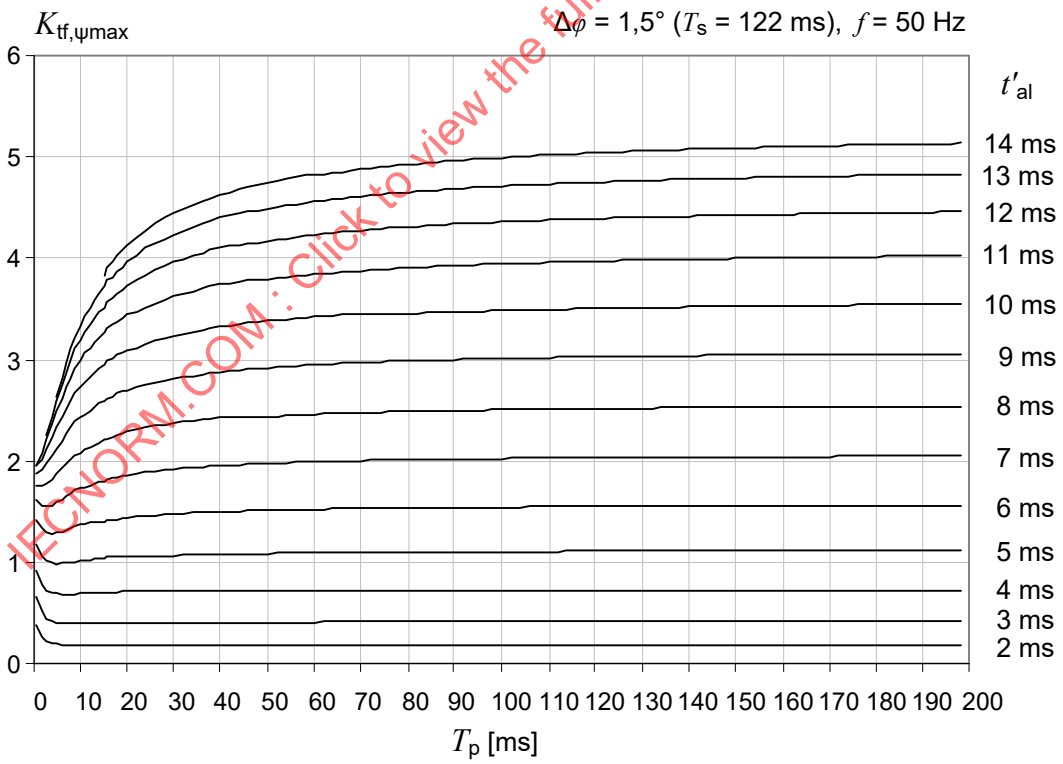

b) T_s = 122 ms at 50 Hz

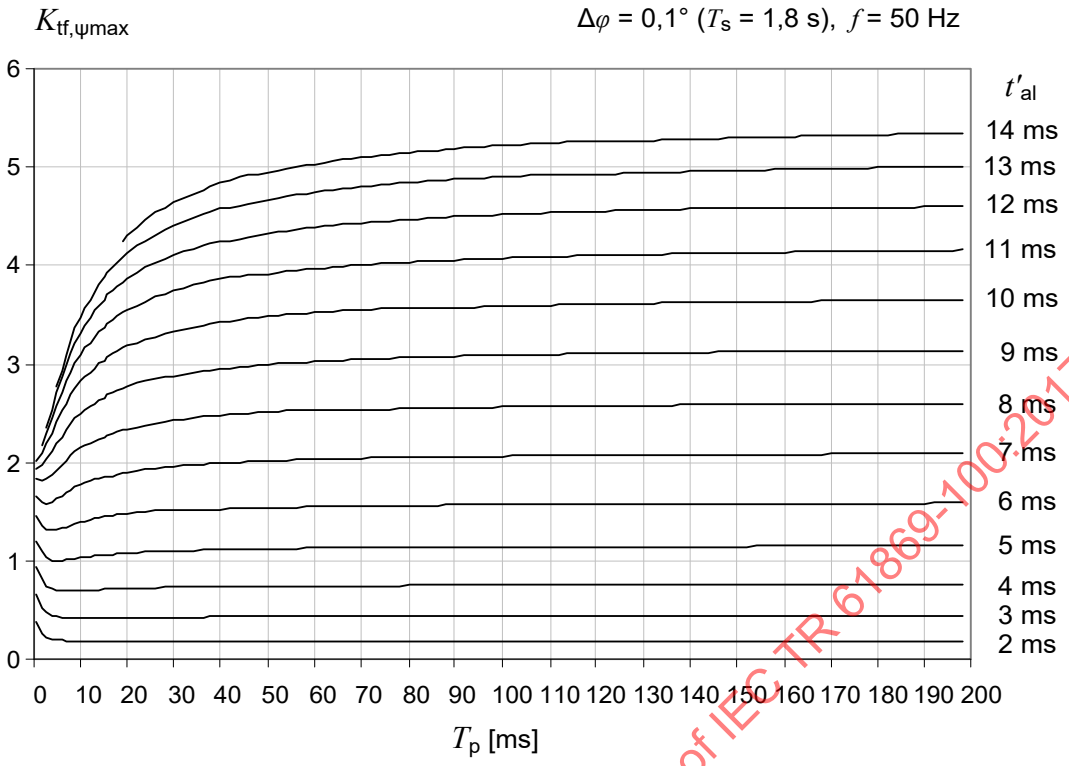

c) T_s = 1,8 s at 50 Hz

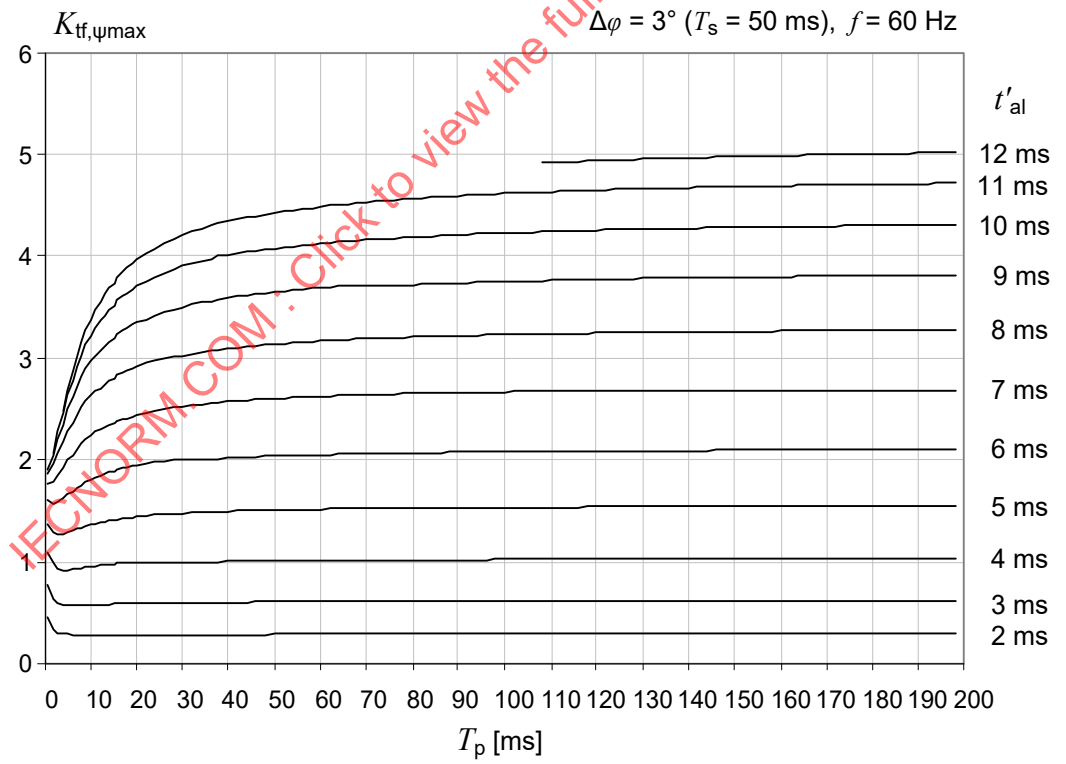

d) T_s = 50 ms at 60 Hz

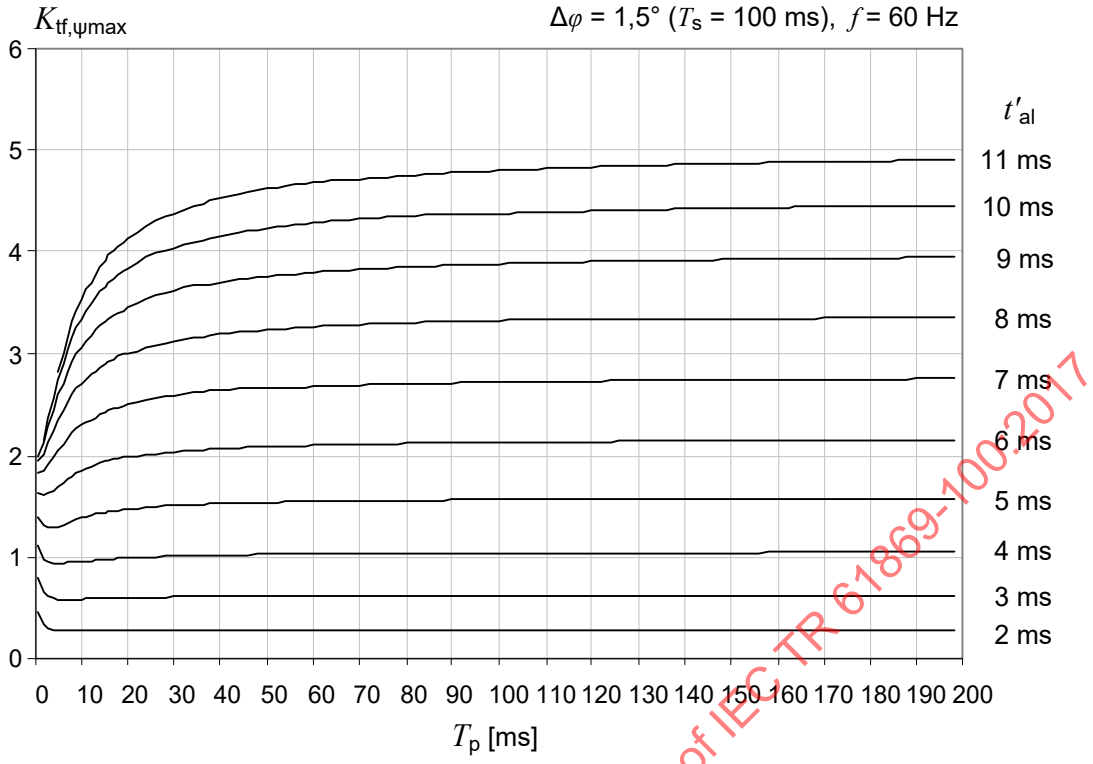

e) T_s = 100 ms at 60 Hz

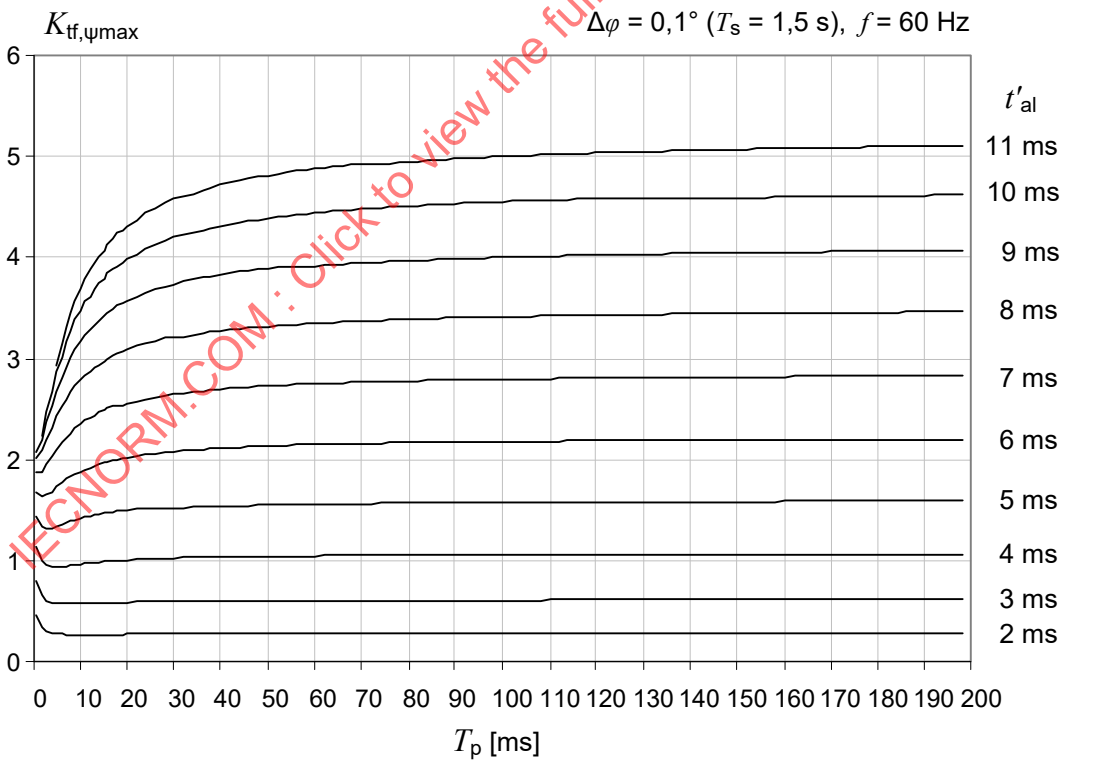

f) T_s = 1,5 s at 60 Hz

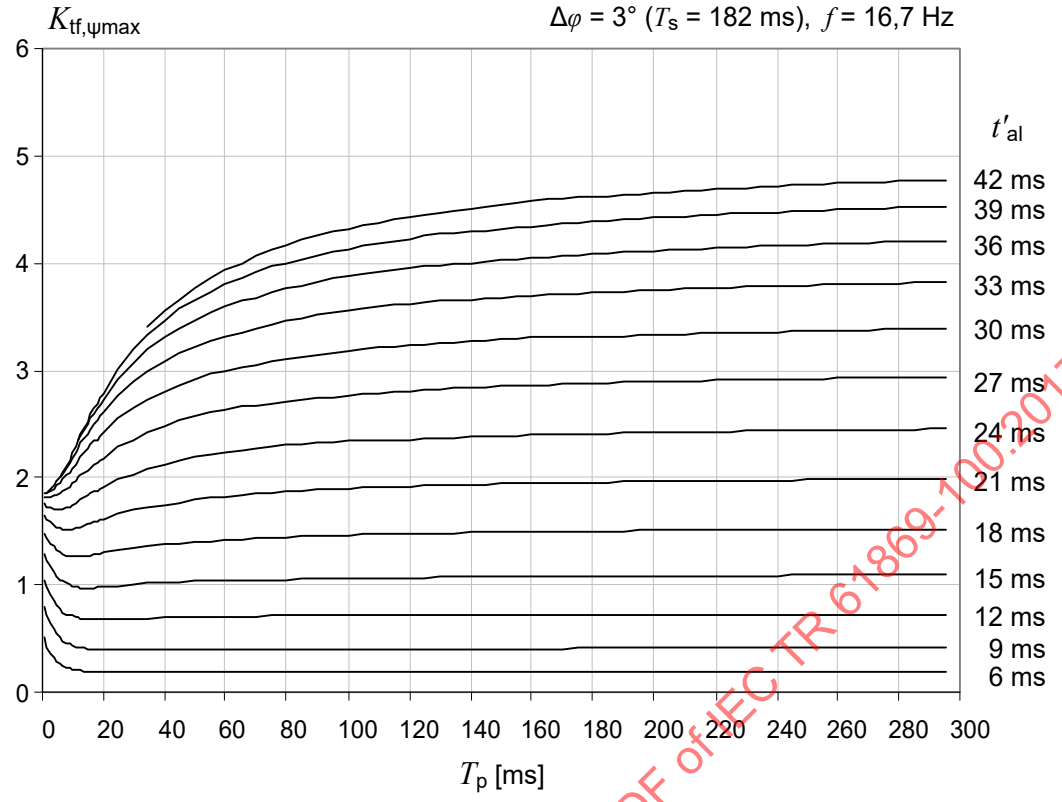

g) T_s = 182 ms at 16,7 Hz

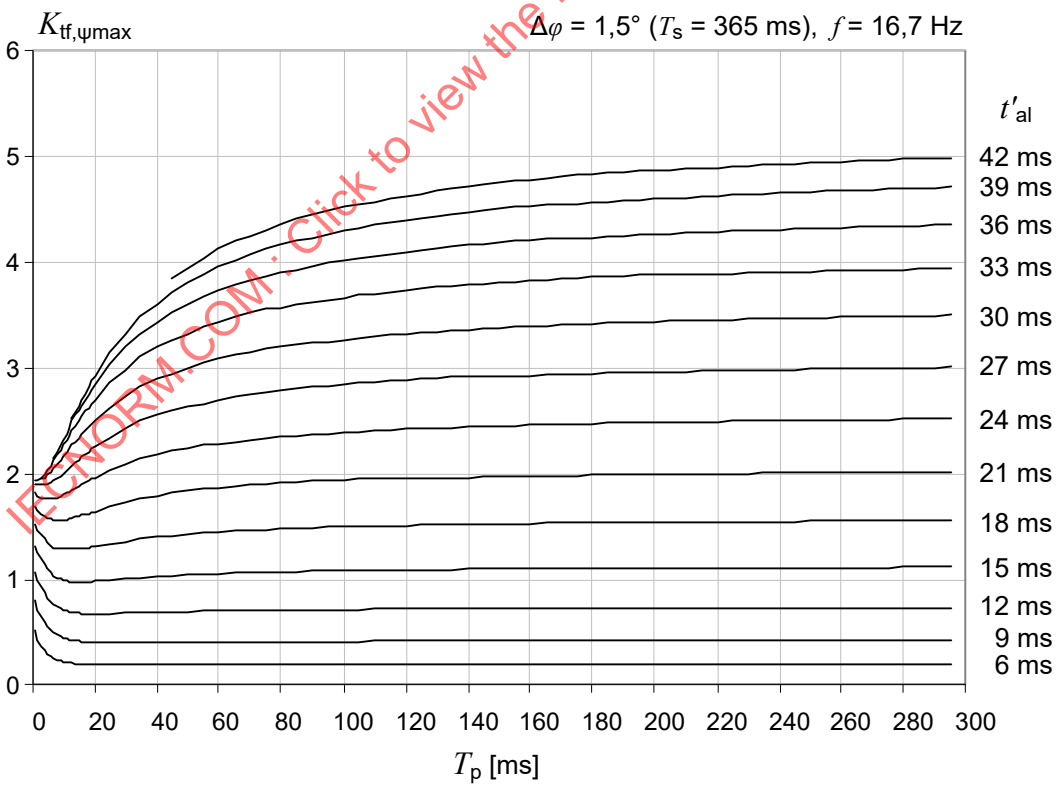

h) T_s = 365 ms at 16,7 Hz

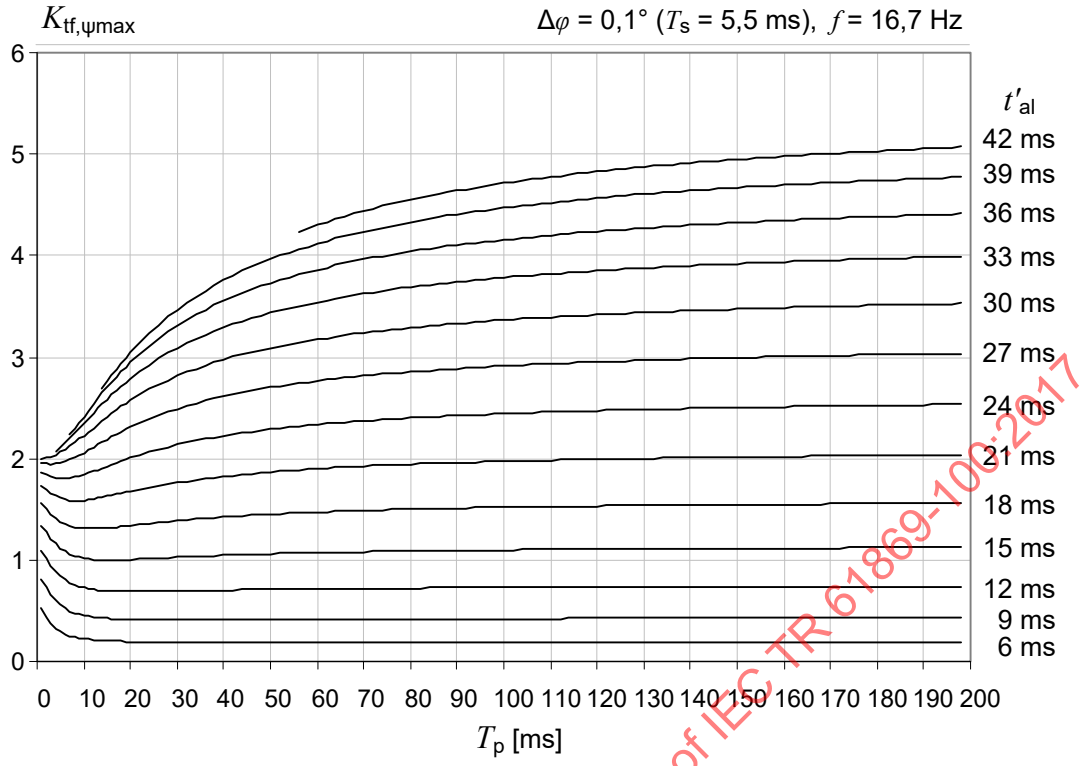

i) T_s = 5,5 s at 16,7 Hz

Key

f	frequency
$K_{tf,\psi max}$	overall transient factor, see Figure 14, in range 1 identical with K_{tf}
T_p	specified primary time constant
T_s	secondary loop time constant
t'_{al}	specified time to accuracy limit in the first fault
$\Delta\varphi$	phase displacement

Figure 20 – Determination of K_{tf} in time range 1

Usually, the normalized slope of the total primary current curve at time t=0 is between 0 (maximum DC component) and 1 (no DC component). A very small T_p, together with a negative DC component, leads to a slope higher than 1 (see Figure 21), and therefore to much earlier CT saturation. Therefore, the K_{tf} curves for short t'_{al} are higher for very short T_p. T_p is directly correlated to the X/R ratio as a finite value given by the conductor geometry of the primary circuit. For medium and high voltage networks, such low X/R ratios may be more theoretical cases, whereas, in low voltage networks, values of T_p down to 1 ms are possible and realistic. The curve i_{sin} is given as a reference, in order to compare the gradients in the first few milliseconds.

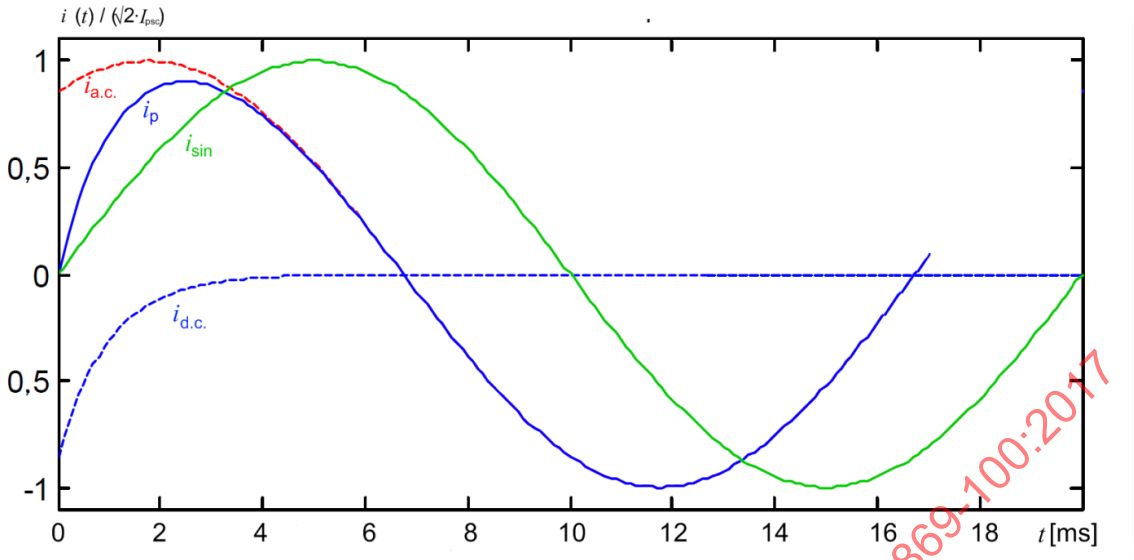

Key

$i_{a.c.}$	AC component of the i_p curve
$i_{d.c.}$	DC component of the i_p curve
i_{sin}	primary current
i_p	sinus curve, as reference
t	time

Figure 21 – Primary current curves for 50Hz, T_p = 1 ms, $\gamma_{\psi max}$ = 166° for t'_{al} = 2 ms

6.1.3.4 Range 2: $t_{tf,max} \leq t'_{al} \leq t_{tfp,max}$

$t_{tfp,max}$ is given in Equation (15), $t_{tf,max}$ in Equation (19).

The worst-case angle $\theta_{tfp,\psi max}$ for the peak curve $K_{tfp}(t,\theta)$ according to Equation (13) is given by Equation (23).

$$\theta_{tfp,\psi max} = \arctan \frac{\omega T_s (T_p - T_s)}{T_p \left(1+\omega^2 T_s^2\right) e^{(t/T_s - t/T_p)} - T_s \left(1+\omega^2 T_s T_p\right)} \quad (23)$$

The appropriate maximum value $K_{tfp,\psi max}$ is calculated as follows:

$$K_{tfp,\psi max} = K_{tfp}(t'_{al}, \theta_{tfp,\psi max}) \quad (24)$$

6.1.3.5 Range 3: $t_{tfp,max} \leq t'_{al}$

In the third time range, K_{tf} assumes the constant value $K_{tfp,max}$, given in Equation (17). It is defined as the maximum value of the K_{tfp} curve.

6.1.3.6 Consolidation and explanation of borderline cases

NOTE Subclause 6.1.3.6 provides supplementary information. It is intended for readers who are highly interested in the theoretical understanding of the matter, and who like to delve into the mathematical background of K_{tf} determination.

For f = 50 Hz, T_p = 50 ms and T_s = 61 ms, Figure 22 shows the worst-case fault inception angles:

for the K_{tf} curve: $\gamma_{tf,\psi max}$

for the K_{tfp} curve:, $\gamma_{tfp,\psi max}$

$\gamma_{tf,\psi max}$ is derived from the real transient factor K_{tf} and therefore also contains the sinusoidal AC component, but for CT designing it is only valid for time range 1 until the time $t_{tf,max}$.

$\gamma_{tfp,\psi max}$ is derived from the envelope K_{tfp}, and doesn't contain any AC component. It is only valid for time range 2 between $t_{tf,max}$ and $t_{tfp,max}$.

Time range 3 continues with the maximum value $K_{tfp,max}$ for times higher than $t_{tfp,max}$.

Therefore, the calculation of worst-case fault inception angles for $t > t_{tfp,max}$ is irrelevant.

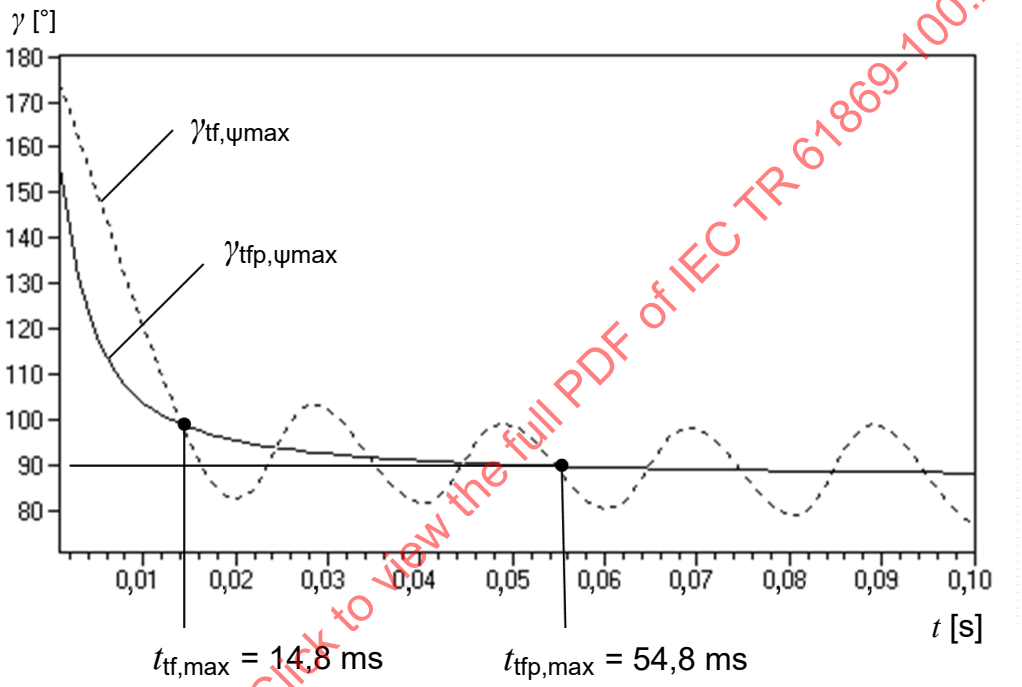

Key

t	time
$t_{tf,max}$	end of time range 1
$t_{tfp,max}$	end of time range 2
γ	fault inception angle
$\gamma_{tf,\psi max}$	worst-case fault inception angle which leads to the highest flux at time $t = t'_{al}$ in time range 1
$\gamma_{tfp,\psi max}$	worst-case fault inception angle which leads to the highest flux at time $t = t'_{al}$ in time range 2

Figure 22 – worst-case fault inception angles for 50Hz, T_p = 50 ms and T_s = 61 ms

Figure 23 shows the K_{tf} and K_{tfp} curves again for f = 50 Hz, T_p = 50 ms and T_s = 61 ms:

K_{tf}, based on the worst-case fault inception angle $\gamma_{tf,\psi max}$ as a function of time, and

K_{tfp}, based on the worst-case fault inception angle $\gamma_{tfp,\psi max}$ as a function of time,

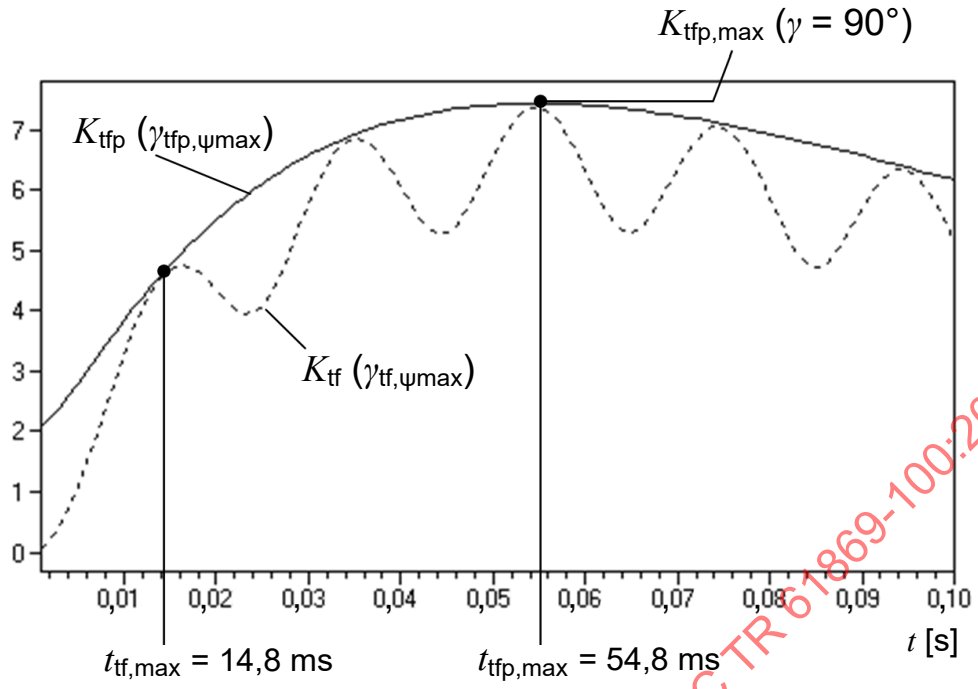

Key

$t_{tf,max}$	end of time range 1
$t_{tfp,max}$	end of time range 2
$\gamma_{tf,\psi max}$	worst-case fault inception angle which leads to the highest flux at time t'_{al} in time range 1
$\gamma_{tfp,\psi max}$	worst-case fault inception angle which leads to the highest flux at time t'_{al} in time range 2
$K_{tfp}(\gamma_{tfp,\psi max})$	K_{tfp} value, resulting from $\gamma_{tfp,\psi max}$
$K_{tf}(\gamma_{tf,\psi max})$	K_{tf} value, resulting from $\gamma_{tf,\psi max}$
$K_{tfp,max}$	highest point of the curve $K_{tfp}(t)$

Figure 23 – transient factor for different time ranges

In this example, it is important to show that generally $\gamma_{tf,\psi max}$ is a very steep function as it depends highly on the time in time range 1, whereas $\gamma_{tfp,\psi max}$ is a flat function of time in time range 2, and assumes typical values between 100° and 90°. The latter one is always 90° at the end of time range 2 for $t_{tfp,max}$, when the flux reaches the maximum value (the fault inception angle γ = 90° corresponds to the primary current with the highest peak, see Figure 10; Figure 11 and Figure 13).

Therefore, in IEC 61869-2, in range 2, γ = 90° is generally used for simplification purposes, where the deviation from the exact formula is not significant. For more detailed and exact calculations, it is recommended to use the exact formulae in Equations (12), (23) and (24).

For better illustration, Figure 24 shows the diagram similar to Figure 20 (graphical K_{tf} determination in time range 1) for δ = 3° (T_s = 61 ms, class TPZ), but for all three time ranges (range 1 in blue, range 2 in green, range 3 in red).

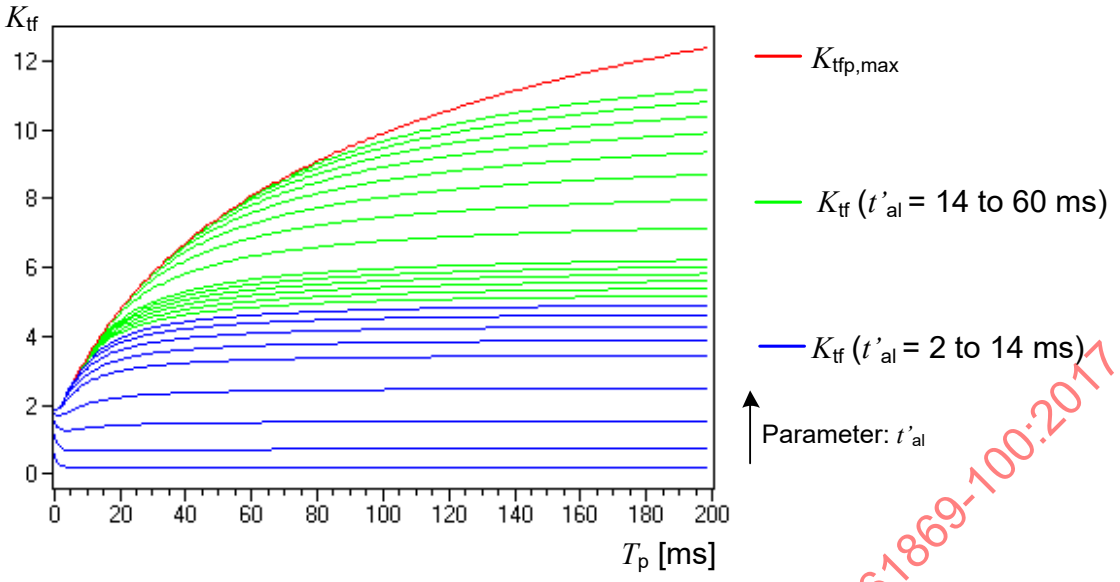

Key

K_{tf}	transient factor
$K_{tfp,max}$	highest point of the curve K_{tf}; end of time range 2
t'_{al}	specified time to accuracy limit in the first fault
T_p	primary time constant

Figure 24 – K_{tf} in all time ranges for T_s = 61 ms at 50 Hz with t'_{al} as parameter

The following diagram is presented only to explain some curiosities of the transient curves in Figure 20. Figure 25 zooms in for the very low range of T_p where the curves for t'_{al} = 13 ms and t'_{al} = 14 ms start at higher T_p in time range 1. The green curve (time range 2) for t'_{al} = 14 ms augments the corresponding blue one in time range 1.

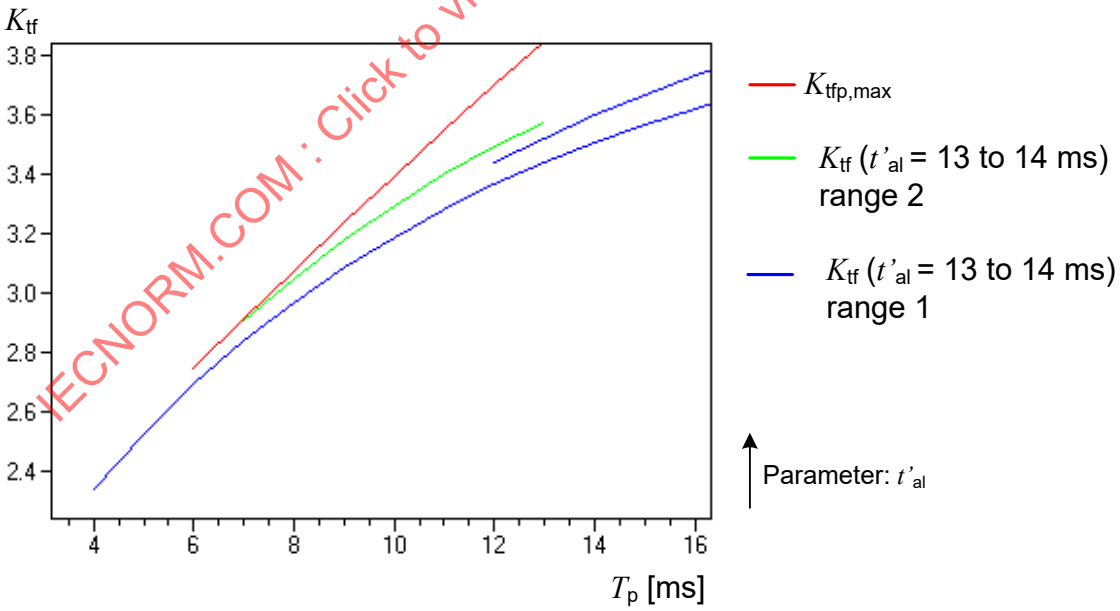

Key

K_{tf}	transient factor
$K_{tfp,max}$	highest point of the curve K_{tf}; end of time range 2
t'_{al}	specified time to accuracy limit in the first fault
T_p	primary time constant

Figure 25 – Zoom of Figure 24

Figure 25 also shows that for very low T_p and certain t'_{al}, the factors K_{tf} and K_{tfp} seem to be undefined.

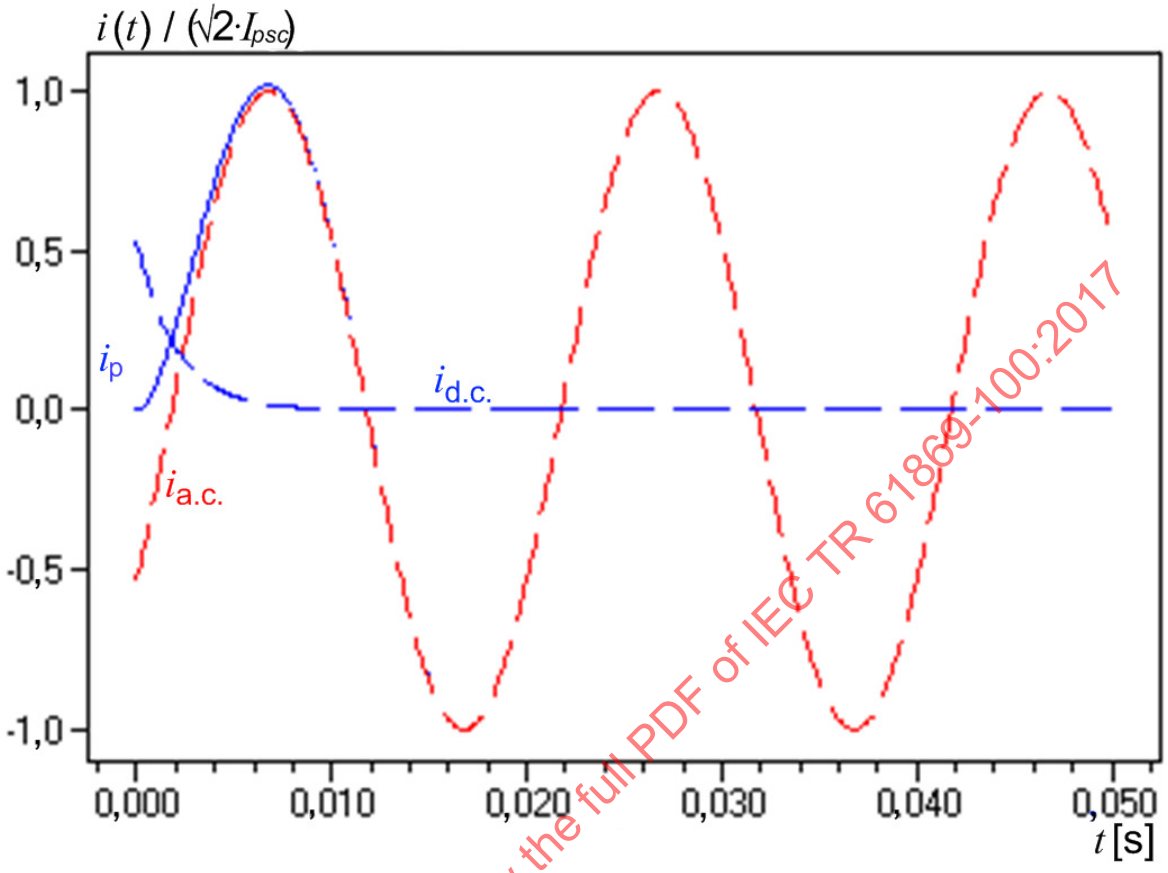

Key

i	current
i_p	primary current
i_{psc}	rated primary short circuit current
$i_{a.c.}$	AC component of the i_p curve
$i_{d.c.}$	DC component of the i_p curve
t	time

Figure 26 – Primary current for a short primary time constant

Such an exceptional case is shown in Figure 27 for T_p = 2 ms (primary current in Figure 26), where time range 2 doesn't exist, because the maximum $K_{tfp\ max}$ of the envelope K_{tfp} occurs before the maximum of K_{tf} at time $t_{tf\ max}$. This envelope and its maximum have no physical relevance in such cases. For $t'_{al} \geq t_{tf\ max}$ the maximum $K_{tf\ max}$ of K_{tf} is relevant for time range 3.

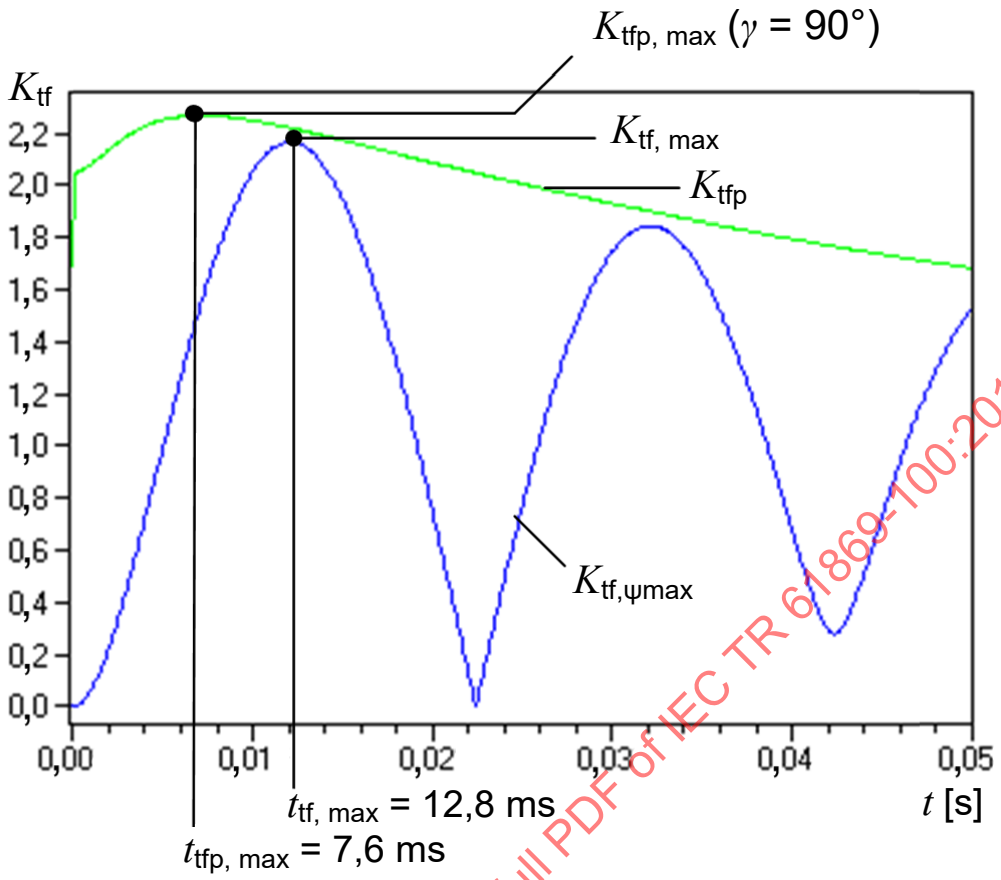

Key

K_{tf}	transient factor
$t_{tf,max}$	end of time range 1
$t_{tfp,max}$	end of time range 2
$K_{tfp,max}$	K_{tf} value at end of time range 2
$K_{tf,max}$	K_{tf} value at end of time range 1
$K_{tf,\psi max}$	overall transient factor
K_{tfp}	envelope of the curve $K_{tf,\psi max}(t)$
t	time

Figure 27 – K_{tf} values for a short primary time constant

Configurations with very low primary time constants T_p occur mainly in low voltage networks, where the current transformers for overcurrent protection are not dimensioned with transient dimensioning factors, i.e. the primary time constant T_p is not considered.

6.1.3.7 Example

A hypothetical differential protection relay requires t'_{al} = 5ms (quarter cycle) for stable and selective operation. The fault inception angle which leads to the highest flux at 5 ms for T_s = 10 s and a wide range of T_p is $\gamma_{tf,\psi max}$ = 150° (Figure 17).

Figure 28 shows three general possible short circuit currents where T_p = 20 ms has been chosen low in this example in order to make some differences clear.

- For times shorter than approximately 9,5 ms, the highest peak current for γ = 90° is slightly higher than the one for maximum DC component.
- The highest peak current for $\gamma_{tf,\psi max}$ = 150° is lower than that for the other two, but the instantaneous current is higher for times shorter than 6 ms in this example. The magnetic flux of a current transformer excited by such a primary current as the latter will rise higher

during the first milliseconds but remains later at a lower level. For current transformers which have to be dimensioned for short t'_{al} values, Equation (10) should be used. The required transient dimensioning factor is

$$K_{td} = K_{tf}(t'_{al} = 5\,\text{ms}, \gamma_{tf,\psi max} = 150°) = 1{,}1$$

For t'_{al} = 5 ms, this value is

– much higher than $K_{tf,dc}$ = 0,4, which would be obtained by considering the curve leading to the highest DC component;

– much lower than $K_{tfp,dc}$ = 2,4 which is too conservative for this short time range and would lead to cores that would be too large.

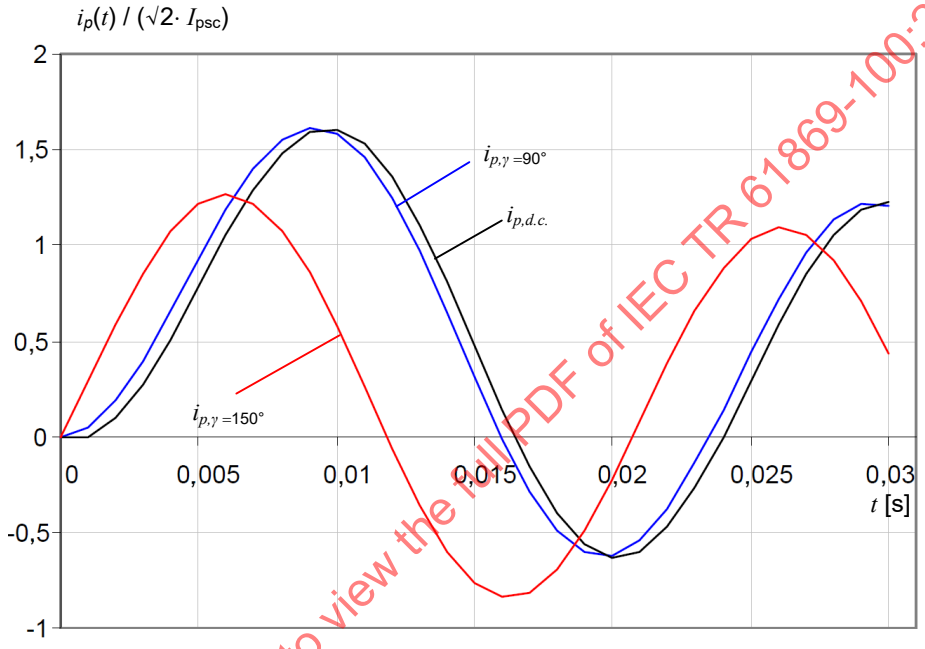

Key

i	current
i_{psc}	rated primary short circuit current
$i_{p,d.c.}$	primary current resulting from a current inception angle leading to the highest DC component
$i_{p,\gamma=90°}$	primary current resulting from a current inception angle of 90°
$i_{p,\gamma=150°}$	primary current resulting from a current inception angle of 150°
t	time

Figure 28 – Short circuit currents for various fault inception angles

Additionally, Figure 29 shows a fictive transient factor $K_{tf,\psi max}(\gamma_{tf,\psi max}(t))$ where, for every time step t, the worst-case fault inception angle $\gamma_{tf,\psi max}$ has been considered (see Figure 30). The resulting curve is the envelope for all possible curves $K_{tf}(t'_{al})$, each calculated for one specific time to accuracy limit t'_{al}.

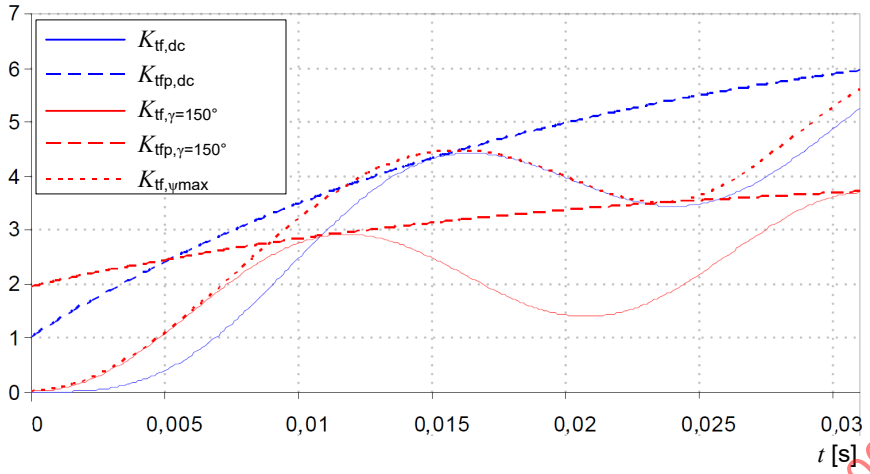

Key

$K_{tf,dc}$	transient factor for highest d.c. component
$K_{tf,\gamma=150°}$	transient factor for fault inception angle 150°
$K_{tfp,dc}$	envelope curve of transient factor for highest d.c. component
$K_{tfp,\gamma=150°}$	envelope curve of transient factor for fault inception angle 150°
$K_{tf,\psi max}$	overall transient factor
t	time

Figure 29 – Transient factors for various fault inception angles (example)

The curve $K_{tf,\psi max}$ is higher than $K_{tfp,dc}$ at 14 ms in this case, because the short circuit current with the highest peak i_p with fault inception at $\gamma = 90°$ leads to the absolute highest flux and not, as often stated, the current with the highest DC component.

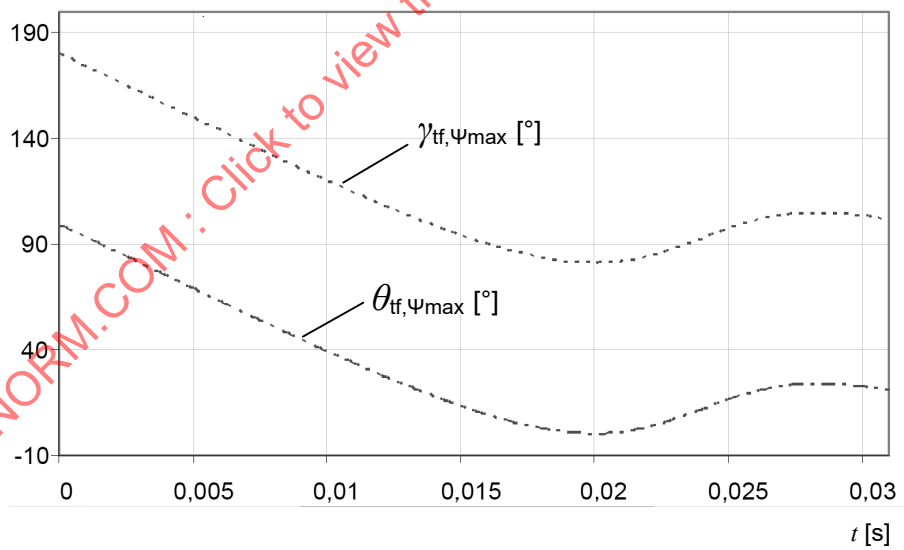

Key

$\gamma_{tf,\psi max}$	worst-case fault inception angle which leads to the highest flux at time t'_{al} in time range 1
$\theta_{tf,\psi max}$	worst-case fault inception angle (alternative definition) which leads to the highest flux at time t'_{al} in time range 1
t	time

Figure 30 – Worst-case fault inception angles for each time step (example for 50 Hz)

This effect is more dominant for an example with 16,67 Hz, where Ktfp,dc is even negative during the first milliseconds (Figure 31).

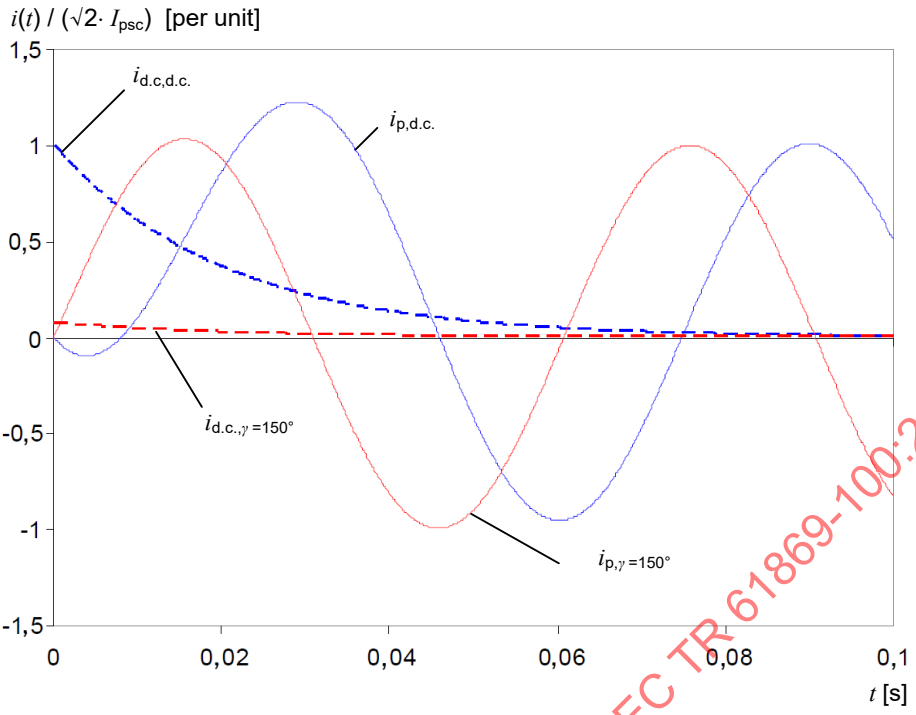

Key

i	current
i_{psc}	rated primary short circuit current
$i_{p,d.c.}$	primary current resulting from a current inception angle leading to the highest DC component
$i_{d.c.,d.c}$	DC component of the $i_{p,d.c}$ curve
$i_{p,\gamma=150°}$	primary current resulting from a current inception angle of 150°
$i_{d.c.,\ \gamma=150°}$	DC component of the $i_{p,\ \gamma=150°}$ curve
t	time

Figure 31 – Primary current for two different fault inception angles (example for 16,67 Hz)

Figure 32 shows the fictive transient factor $K_{tf,\psi max}(\gamma_{tf,\psi max}(t))$ where, for every time step t, the worst-case fault inception angle $\gamma_{tf,\psi max}$ has been considered (see Figure 33).

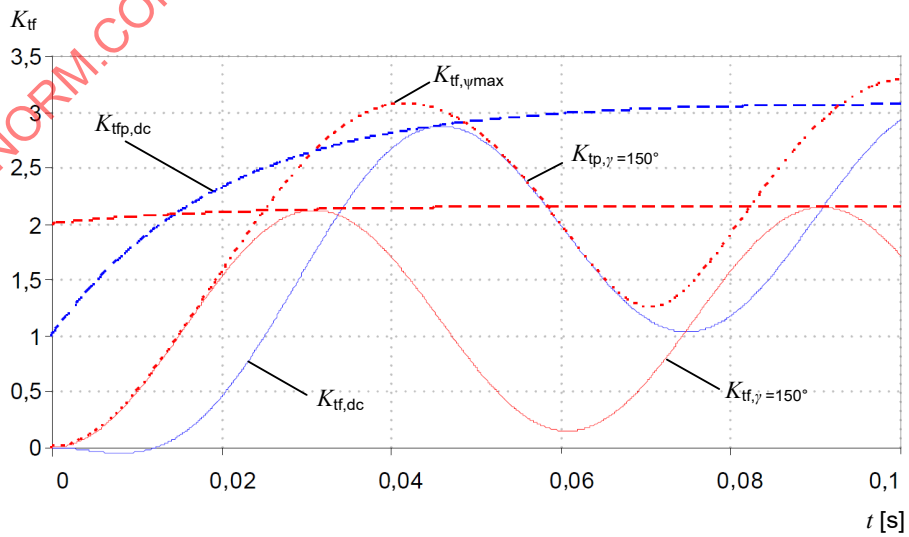

Key

K_{tf}	transient factor
$K_{tf,dc}$	transient factor for highest d.c. component
$K_{tf,\gamma=150°}$	transient factor for fault inception angle 150°

$K_{tfp,dc}$ envelope curve of transient factor for highest d.c. component

$K_{tfp,\gamma=150°}$ envelope curve of transient factor for fault inception angle 150°

$K_{tf,\psi max}$ overall transient factor

t time

Figure 32 – Transient factors for various fault inception angles (example for 16,67 Hz)

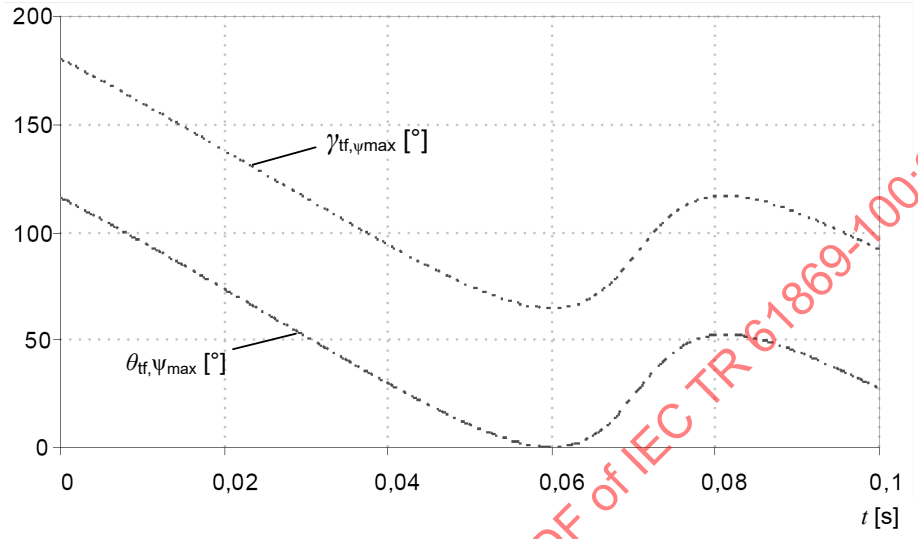

Key

$\gamma_{tf,\psi max}$ worst-case fault inception angle which leads to the highest flux at time t'_{al} in time range 1

$\theta_{tf,\psi max}$ worst-case fault inception angle (alternative definition) which leads to the highest flux at time t'_{al} in time range 1

t time

Figure 33 – Worst-case fault inception angles for every time step (example for 16,67 Hz)

6.1.4 Reduction of asymmetry by definition of the minimum current inception angle

From experience in high voltage systems, it is known that many faults are insulation faults and occur before and close to the voltage maximum, whereas faults with full offset are relatively seldom. As stated by Warrington in [1][2]: "Over 95 % of faults occur within 40° before voltage maximum" (Figure 34).

In Equation (5), this angle corresponds to the angle γ = 140° to 180° with γ_m = 140° as minimum current inception angle. The corresponding angle γ = 320° to 360° occurs for mirroring to the opposite polarity (see Figure 13).

2 Numbers in square brackets refer to the Bibliography.

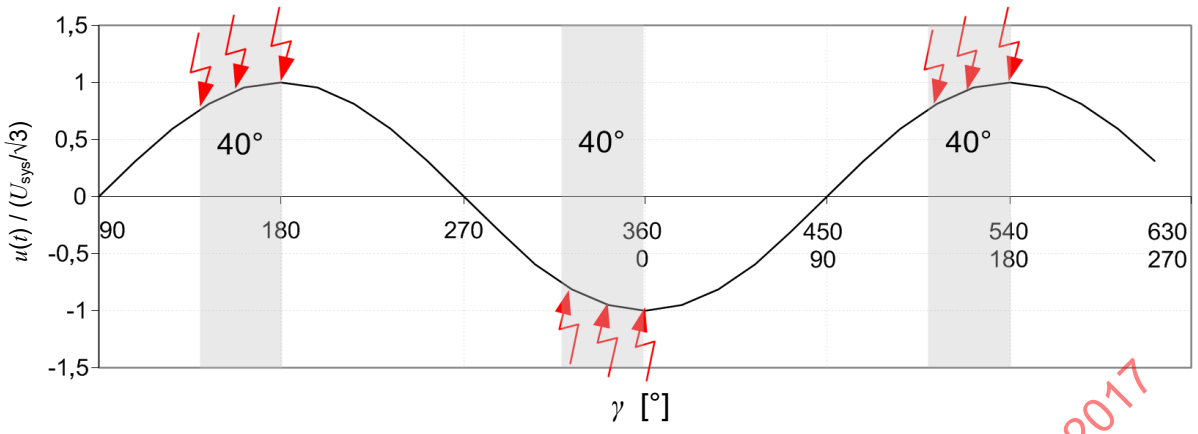

Key

u	primary voltage
u_{sys}	highest voltage for system
t	time
γ	fault inception angle

Figure 34 – Fault occurrence according to Warrington

But, the fault inception mechanisms are different in networks with different voltage levels (high or medium voltage), overhead lines or cables, or different star point connection (isolated, resistance, resonant or solidly earthed).

Furthermore, it is not known which kind of these networks have led to Mr. Warrington's conclusions. Therefore, it is recommended that statistical methods be used to determine the dependency of the majority of faults on inception angle γ for the network concerned. A risk estimation can be made in order to find the compromise between CT size (possibly reduced by asymmetry) and faulty relay operation due to saturation of the under-dimensioned CT.

Figure 35 (only as exemplary template) shows a possible accumulation of faults against the fault inception angle γ for a hypothetic utility evaluated over a longer period of time. The angle area from 0° to 360° is reduced to 0° to 180°. For our consideration, it could be reduced to 90° to 180°. Faults with 90° (highest peak current, high DC component) do not occur as often as faults closer to 0° and 180° (symmetrical, low or no DC component). The example in Figure 35 shows a slight fault accumulation for γ < 50° (after maximum) and, for γ > 140° (before maximum), a significant one.

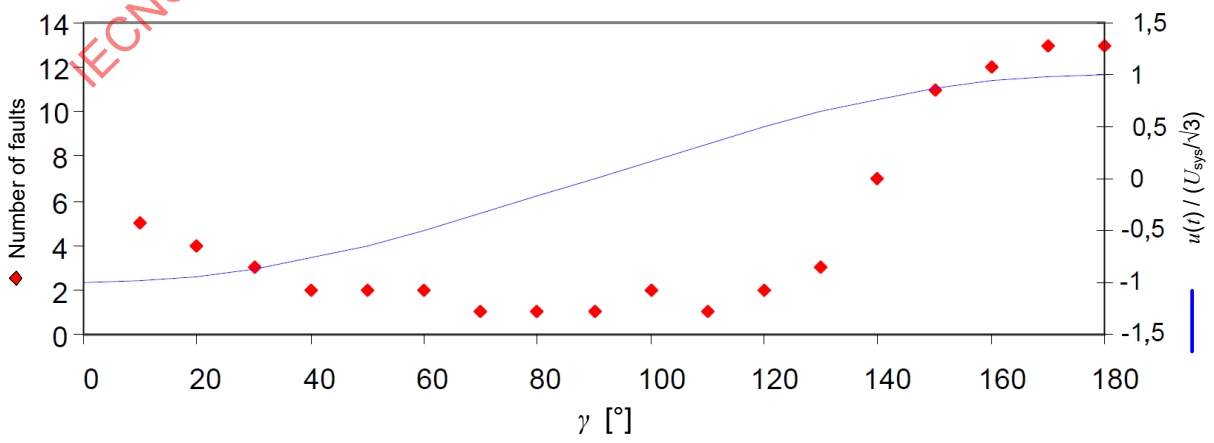

Key

u	primary voltage

u_{sys} highest voltage for system

t time

γ fault inception angle

Figure 35 – estimated distribution of faults over several years

A possibly reduced range of fault inception angle ($\gamma_m \geq 90°$) leads to reduced asymmetry and may lead to a reduced factor K_{td} in some special cases.

According to IEC 61869-2:2012, 2B.1.1, it is possible to define and calculate K_{td} with a minimum fault inception angle γ_m which is higher than 90°, thus reducing the maximum possible asymmetry of the short circuit current: $90° \leq \gamma_m \leq 180°$.

The simplest way to define the degree of asymmetry is by using the physical basis, the fault inception angle γ. If desired, this restriction has to be assessed by the customer who should evaluate the probability of asymmetrical faults in his network by using statistical methods. Such evaluation depends on the type and operation of the network (overhead lines or cables, climate, etc.). If the factor K_{td} can be reduced by using $\gamma_m > 90°$, a possibly unselective operation of the protection system has to be considered. This could occur because of current transformer saturation caused by a possibly unexpected high asymmetrical short circuit current.

NOTE These days, controlled switching of transmission lines is employed to reduce switching overvoltages, especially during fast re-energizing. Based on this technique, which has been utilized for many modern transmission lines, both energizing and re-energizing instants are controlled in a way that make the current when the instantaneous phase to ground voltages close to zero.

In such cases, the determination of fault inception angle based on statistical method (especially where controlled closing method is employed as a new approach) is not recommended and maximum decaying DC of fault current should take into account, as necessary.

It is recommended that reduced asymmetry should be used as restrictively as possible. Therefore, as a recommendation, it should not be applied in time range 1. Figure 36 shows the transient factor $K_{tf}(\gamma,t'_{al})$ for t'_{al} = 2 ms to 16 ms. (Compare with Figure 13 and Figure 19.) In this example, for each time t'_{al} represented by one of the curves, the highest K_{tf} value occurs at the worst case fault inception angle $\gamma_{tf,\psi max}(t'_{al})$.

As an example for a longer time t'_{al} = 16 ms, the worst case fault inception angle is $\gamma_{tf,\psi max}$= 90° with the curve maximum $K_{tf,max}$ = 4,5.

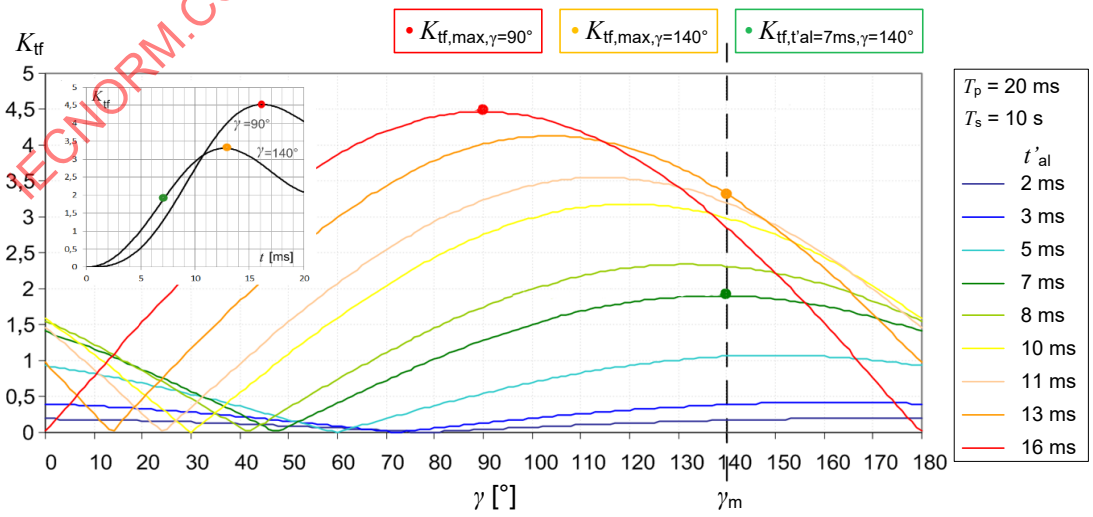

Key

$K_{tf,max\ \gamma=90°}$ maximum value of the $K_{tf,\gamma=90°}$ (t) curve

$K_{tf,max\ \gamma=140°}$ maximum value of the $K_{tf,\gamma=140°}$ (t) curve

$K_{tf,\ t'al=7ms,\gamma=140°}$	K_{tf} value at a given t'_{al} value and at a given current inception angle
T_p	specified primary time constant
T_s	secondary loop time constant
t	time
γ	fault inception angle
γ_m	minimum fault inception angle

Figure 36 – Transient factor K_{tf} calculated with various fault inception angles γ

For lower times t'_{al}, the worst case fault inception angle $\gamma_{tf,\psi max}$ shifts to higher values and the absolute curve maximum declines to lower values. According to Figure 13 and Figure 19, the full angle range is 90° ≤ $\gamma_{tf,\psi max}$ ≤ 180°.

By reducing the fault inception angle range to 140° ≤ $\gamma_{tf,\psi max}$ ≤ 180° (γ_m = 140°), the reduced range of asymmetry leads to a reduction of K_{tf} to a maximum of 3,3 for t'_{al} = 13 ms. This means that all higher values of K_{tf} > 3,3 are expected to occur with low probability only (low dc component), and the smaller core size should not lead to maloperation of the protection system.

For t'_{al} = 0 ms to 7 ms, K_{tf} has maximums for γ_m > 140°, that means in the angle range where faults occur with high probability. For these t'_{al} values and angle range, the reduction of K_{tf} (and core size) to the 140° value does not provide any advantage.

6.2 Duty cycle C – O – C – O

6.2.1 General

The designing for transient auto-reclosure duty cycles has to be done for each cycle according to the equations given above, where the magnetic flux and therefore the transient factor decays exponentially with a secondary time constant T_s during the fault repetition time.

For non-gapped cores having a high secondary time constant (typically TPX cores), the flux may decay to the remanence level (see Figure 53), depending on the fault repetition time t_{fr} and the saturation level. As worst case approximation, the flux is assumed to be constant after t', what will be fulfilled for short t_{fr} values and a flux far from saturation. This means that the second energization always leads to a higher flux value than the one at t' (Figure 37).

$$K_{td,(C-O-C-O)} = K_{td}(t') + K_{td}(t''_{al}) \quad (25)$$

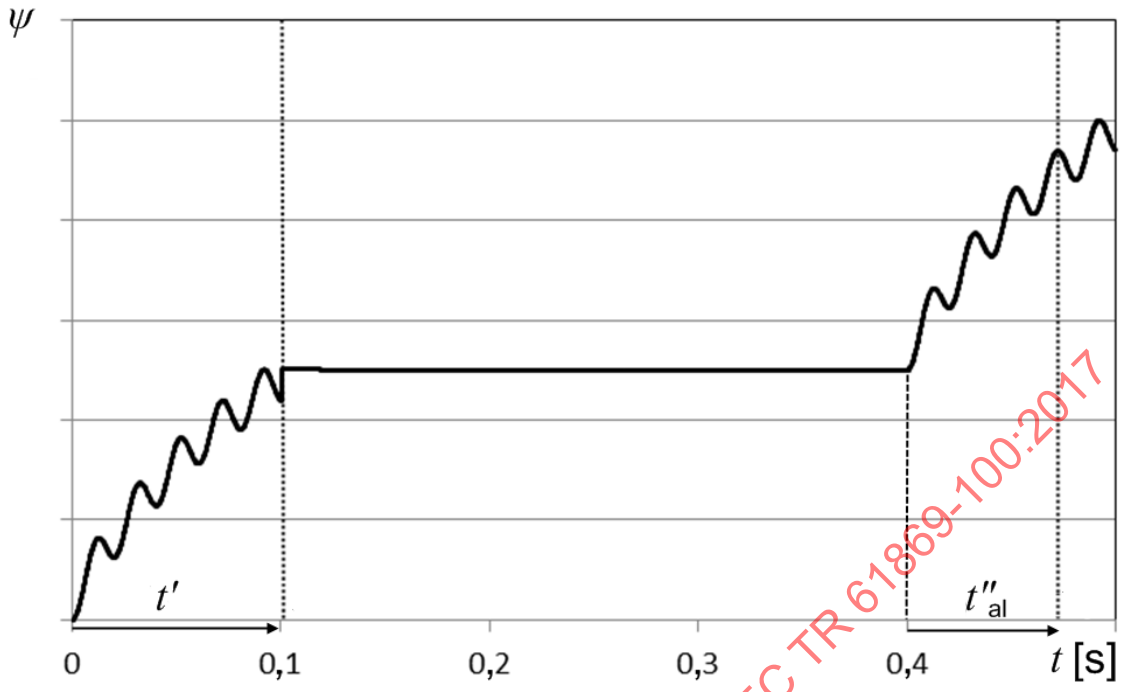

Key

t	time
t'	duration of the first fault
t''_{al}	specified time to accuracy limit in the second fault
ψ	secondary linked flux

Figure 37 – Flux course in a C-O-C-O cycle of a non-gapped core

NOTE The practicality of Equation (25) is also limited, because it can hardly be ensured that the flux starts at zero in the first energization.

For cores having a low secondary time constant (typically TPY and TPZ cores), the flux declines exponentially with the secondary time constant T_s during the fault repetition time t_{fr} (Figure 38). In this case, no analytical formula exists for the time argument t in the term for the first fault, and several case differentiations may be necessary.

6.2.2 Case A: No saturation occurs until t'

Usually, the highest flux occurs in the second energization. In this case, the following formula shall be applied:

$$K_{td,(C-O-C-O)} = K_{td}(t') \cdot e^{-(t_{fr}+t''_{al})/T_s} + K_{td}(t''_{al}) \quad (26)$$

Even with a t'_{al} lower than t', the K_{td} of the first fault shall be calculated for t', because the flux may increase until this point in time.

The term K_{td} (t) means the K_{td} value of a C-O duty cycle, whereby the highest flux value within the time interval from 0 up to time t shall be considered.

In Equation (26), the complete K_{td} determining procedure has to be carried out twice, for both times t' and t''_{al}.

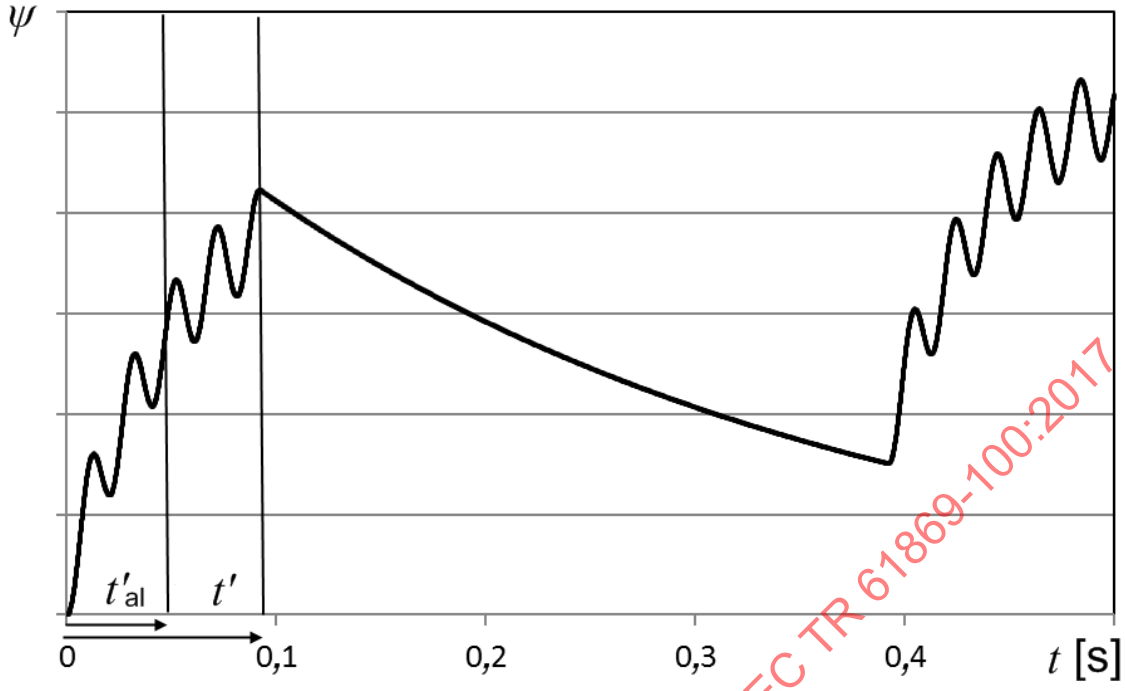

Key

t	time
t'	duration of the first fault
t'_{al}	specified time to accuracy limit in the first fault
ψ	secondary linked flux

Figure 38 – Typical flux curve in a C-O-C-O cycle of a gapped core, with higher flux in the second energization

In some cases, it is possible that the maximum flux value occurs during the first fault (Figure 39). It means that the flux values of both the C-O and the C-O-C-O cycle have to be determined, and the higher value has to be considered:

$$K_{td,(C-O-C-O)max} = \max\{K_{td}(t'_{al}),\ K_{td}(t') \cdot e^{-(t_{fr}+t''_{al})/T_s} + K_{td}(t''_{al})\} \quad (27)$$

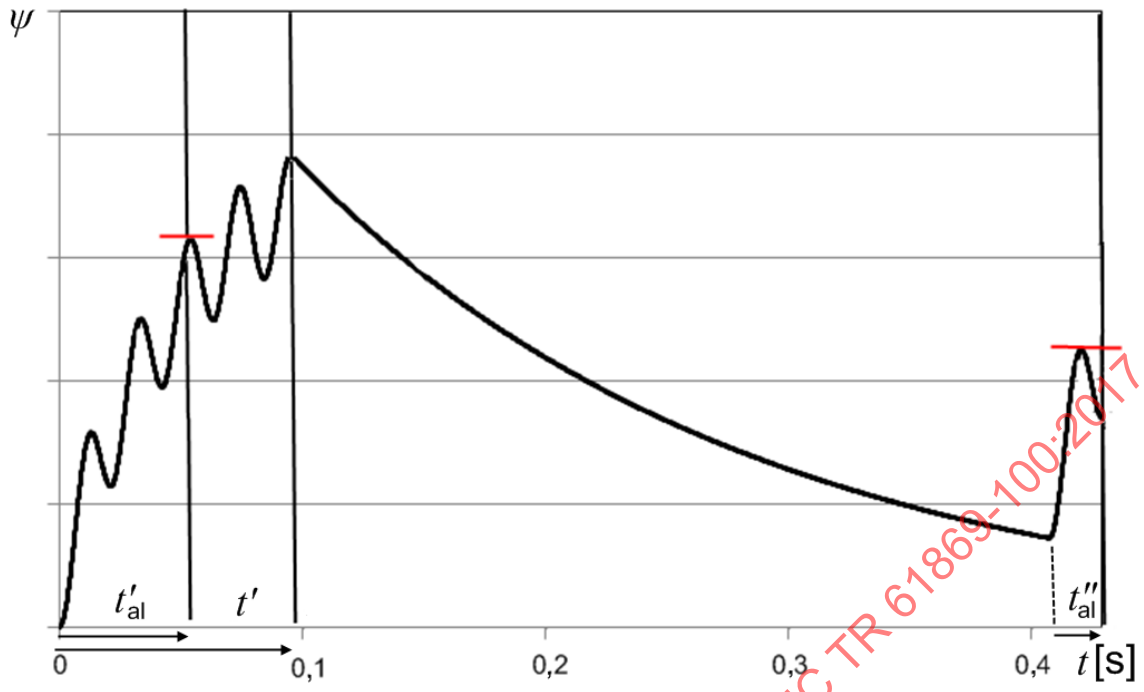

Key

t time

t' duration of the first fault

t'_{al} specified time to accuracy limit in the first fault

ψ secondary linked flux

Figure 39 – Flux curve in a C-O-C-O cycle of a gapped core, with higher flux in the first energization

6.2.3 Case B: Saturation occurs between t'_{al} and t'

In this case, the core saturation limits the flux before the second energization (Figure 40).The CT designer can even utilize core saturation to keep the flux as low as possible. No formula in the clauses above considers this situation.

The highest flux value ψ_{peak} is determined by "scanning" the flux curve from time 0 up to the point in time $t' + t_{fr} + t''_{al}$. In this time interval, no saturation is allowed in the intervals

– between 0 and t''_{al};

– between $t' + t_{fr}$ and $t' + t_{fr} + t''_{al}$.

K_{td} is then determined by dividing the highest flux ψ_{peak} within the two above mentioned intervals by the peak value of the AC flux component of the short circuit current:

$$K_{td,(C-O-C-O)max\ sat} = \frac{\psi_{peak}}{\hat{\psi}_{sc}} \tag{28}$$

where

$$\hat{\psi}_{sc} = \frac{\sqrt{2}\ K_{ssc} \cdot (R_{ct} + R_b) \cdot I_{sr}}{\omega}$$

See also Figure 9.

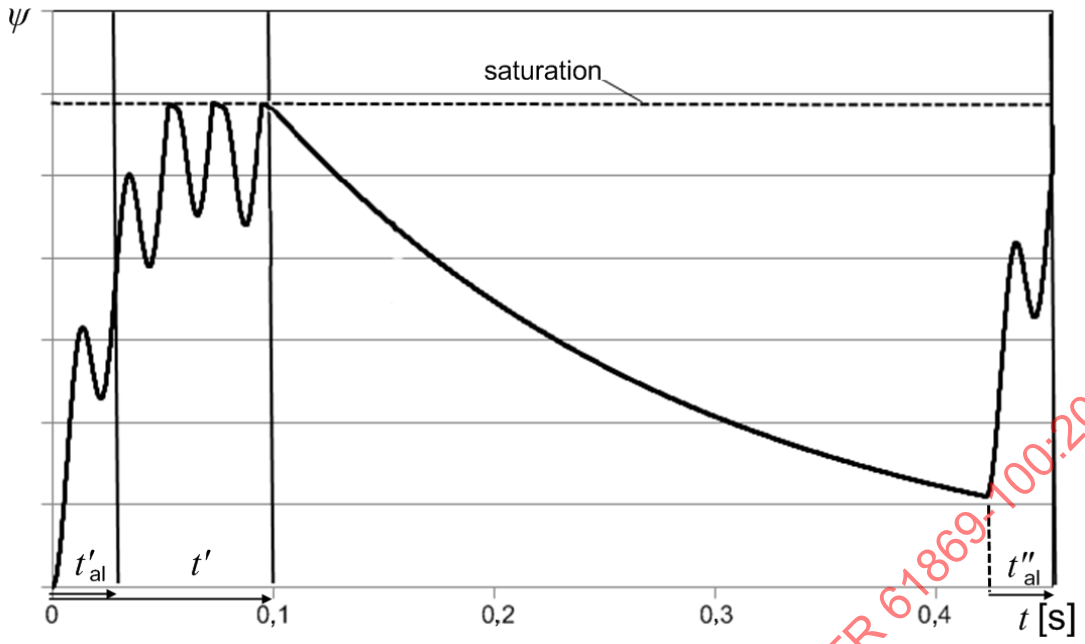

Key

t	time
t'	duration of the first fault
t'_{al}	specified time to accuracy limit in the first fault
t''_{al}	specified time to accuracy limit in the second fault
ψ	secondary linked flux

Figure 40 – Flux curve in a C-O-C-O cycle with saturation allowed

Figure 41 shows such an example. The curve ψ_1 would apply to a much bigger core and, accordingly, to a much higher K_{td} value than necessary. The curve ψ_2 considers saturation as an acknowledged case (because saturation does not occur within the t'_{al} and t''_{al} zones), and makes the choice of a reasonable K_{td} value possible.

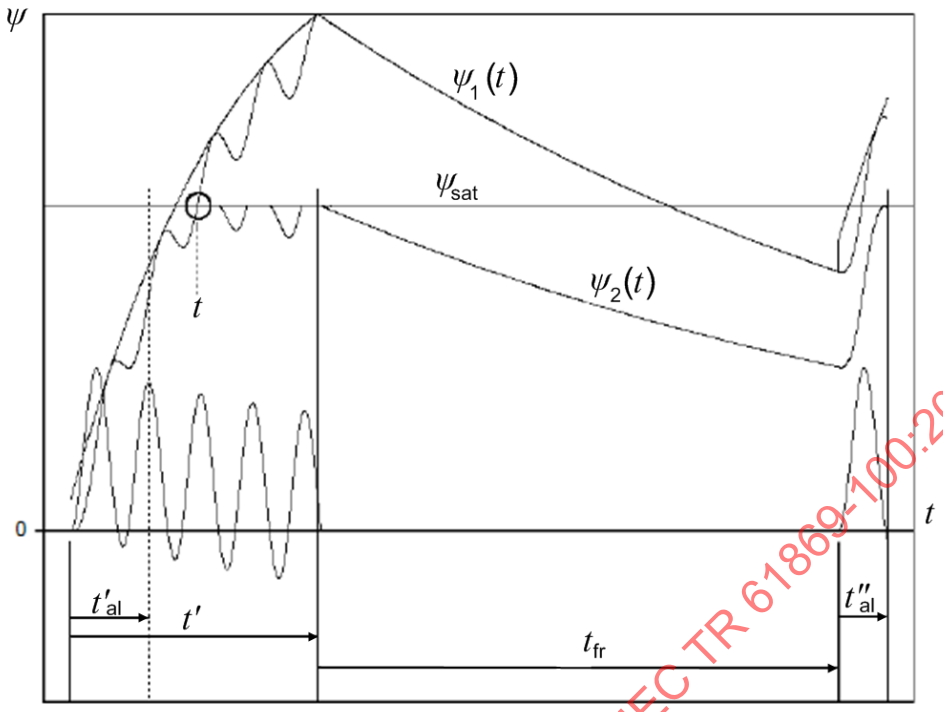

Key

t	time
t'	duration of the first fault
t'_{al}	specified time to accuracy limit in the first fault
t_{fr}	fault repetition time
t''_{al}	specified time to accuracy limit in the second fault
ψ	secondary linked flux
ψ_1	flux if no saturation would occur
ψ_2	flux considering core saturation
ψ_{sat}	saturation flux

Figure 41 – Core saturation used to reduce the peak flux value

6.3 Summary

In order to decide which equation(s) shall be used for designing current transformers for transient performance depending on the required time to accuracy limit t'_{al}, a general overview is given in Figure 42 and Table 2. Due to the consideration of the transient performance, the transient dimensioning factor K_{td} can be lower than 1 for a short time to accuracy limit t'_{al}.

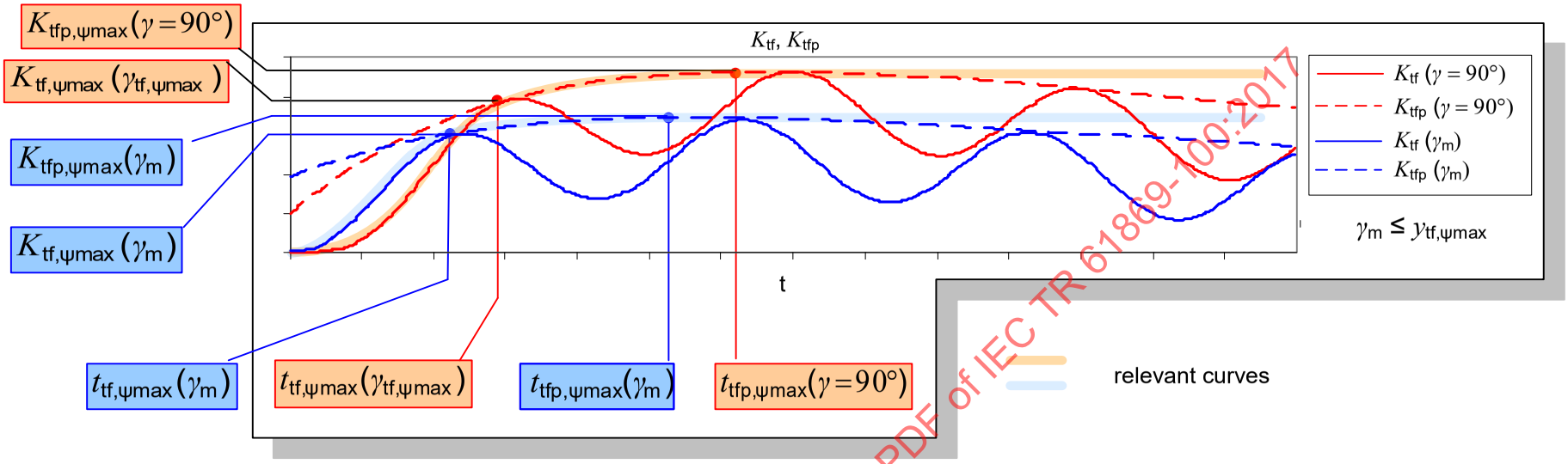

Key

K_{tf}	transient factor as a function of time, at a given fault inception angle γ
K_{tfp}	envelope of the K_{tf} curve
$K_{tfp,\psi max}$	highest value of the K_{tfp} curve
$K_{tf,\psi max}$	K_{tf} value where the curve K_{tf} touches its envelope for the first time
$t_{tf,\psi max}$	time where the curve K_{tf} touches its envelope for the first time
$t_{tfp,\psi max}$	time of the highest value of the K_{tfp} curve
t	time
γ	fault inception angle
γ_m	minimum fault inception angle
$\gamma_{tf,\psi max}$	worst case fault inception angle

Figure 42 – Curves overview for transient designing

Table 2 – Equation overview for transient designing

$t = 0$	Range (1)	$t_{tf,max}$	Range (2)	$t_{tfp,max}$	Range (3)
Exact	$\theta_{tf,\psi max}(t'_{al})$ $\gamma_{tf,\psi max} = \theta_{tf,\psi max} + \varphi$ Equation (20), (21) $K_{tf}(t'_{al}, \gamma_{tf,\psi max})$ Equation (9)		$\theta_{tfp,\psi max}(t'_{al})$ $\gamma_{tfp,\psi max} = \theta_{tfp,\psi max} + \varphi$ Equation (23) Equation (12)	$t_{tfp,max}(\gamma = 90°)$ Equation (15)	$K_{tfp,max}(\gamma = 90°)$ Equation (17)
Simplified	Equation (10)	$t_{tf,max}(\gamma_{tf,\psi max})$ Equation (19)	Equation (13)	---	---
IEC 61869-2	Graphical solution	ditto with $\gamma_{tf,\psi max} = 90°$	ditto with $\gamma_{tfp,\psi max} = 90°$	ditto	ditto
Previous standard (max "dc")	Equation (11), Equation (14)		Equation (16)	Equation (18)	
Reduced asymmetry			Instead of $\varphi \leq \gamma_{tf,\psi max} \leq 90°+\varphi$ reduce angle range to $\gamma_m \leq \gamma_{tf,\psi max} \leq 90°+\varphi$, γ_m from statistical consideration		
Dimension of core size			$E_{al} = K_{td} \cdot K_{ssc} \cdot I_{sr}(R_{ct}+R_b)$ with $K_{td} = K_{tf}$ and protection test		

7 Determination of the transient dimensioning factor K_{td} by numerical calculation

7.1 General

The calculation method in Clause 7 covers only the cases where the cycle parameters are given, or where a definite course of the primary current is given. On this understanding, K_{td} can be calculated.

In IEC 61869-2, several formulae are given to calculate K_{td}. All these formulae were stated in order to provide simple calculation tools, but with the disadvantage of delivering too conservative results in some cases.

In this clause, a numerical approach for the K_{td} factor is introduced. It is easy to understand and to replicate, even for non-specialists. The advantages of this calculation method are:

– extraordinary cases are covered which are based on saturation or reduced range of current inception angle, or even on properties of the duty cycle which are not covered by IEC 61869-2 (e.g. damped primary oscillations);

– giving the non-specialist the sense how a current transformer responds to various input signals.

It does not replace the K_{td} determination of relay manufacturers based on their specific requirements and algorithms.

7.2 Basic circuit

The calculation below is based on the circuit diagram in Figure 43:

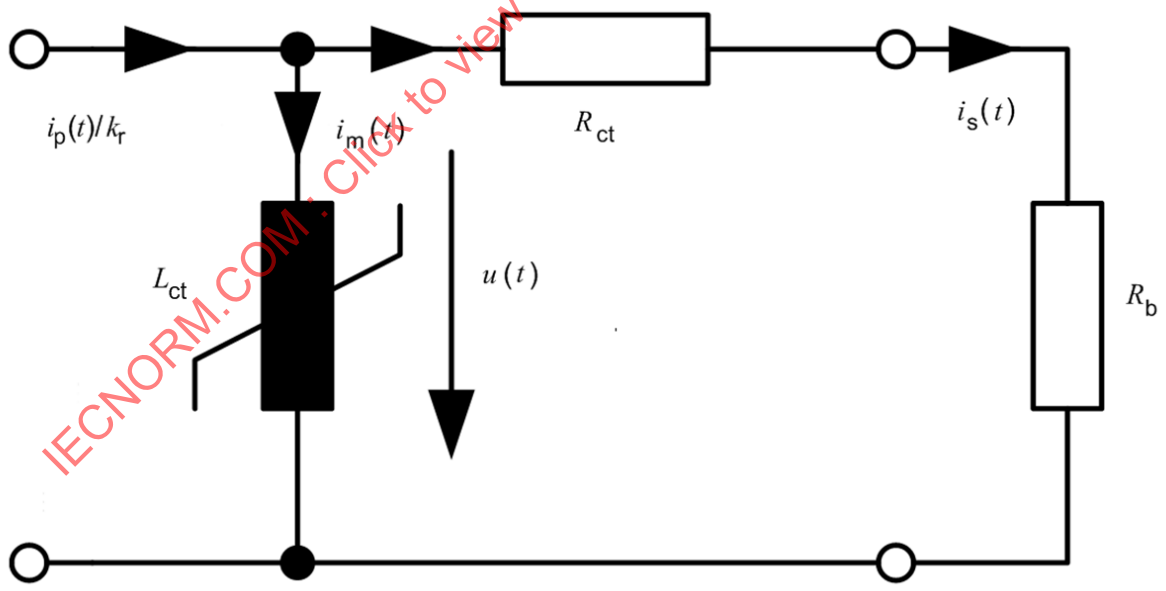

Key

u secondary e.m.f.
i_m magnetizing current
i_m magnetizing current
i_p primary current
i_s secondary current
k_r rated transformation ratio
L_{ct} non-linear inductance

R_b rated resistive burden

R_{ct} secondary winding resistance

t time

Figure 43 – Basic circuit diagram for numerical calculation of K_{td}

With $R_s = R_{ct} + R_b$, the following system of equations can be set up:

$$i_s(t) = \frac{i_p(t)}{k_r} - i_m(t) \tag{29}$$

$$u(t) = R_s \cdot i_s(t) \tag{30}$$

$$\psi(t) = \int_0^t u(t)\, dt \tag{31}$$

For the linear part, represented by L_m of the magnetizing curve:

$$i_m(t) = \frac{\psi(t)}{L_m} \tag{32}$$

With $T_s = L_m/R_s$, Equations (29) to (32) result in

$$\psi(t) = \int_0^t (\frac{R_s}{k_r} i_p(t) - \frac{\psi(t)}{T_s}) dt \tag{33}$$

7.3 Algorithm

With the following algorithm, the values of the following terms can easily be calculated for any waveform of primary current:

– density of the secondary linked flux in the iron core;

– secondary current;

– factor K_{td}.

Equation (33) can be converted into a difference equation, and the flux in the core can be calculated as follows:

$$\psi_{(k)} = \psi_{(k-1)} + (\frac{R_s}{k_r} i_{p(k)} - \frac{\psi_{(k-1)}}{T_s}) \cdot \Delta t \tag{34}$$

When saturation occurs, the actual T_s value has to be modified. Experience has shown that it is sufficient to lower the T_s value by a factor of 1 000 at a pre-defined value of flux ψ_{sat}. For all values of $\psi_{(k-1)} > \psi_{sat}$, Equation (35) is applied.

$$\psi_{(k)} = \psi_{(k-1)} + \left(\frac{R_s}{k_r} i_{p(k-1)} - \left(\frac{\psi_{sat} + (\psi_{(k-1)} - \psi_{sat}) \cdot 1000}{T_s}\right) \cdot \Delta t \right) \quad (35)$$

ψ_{sat} is derived from

$$\psi_{sat} = \frac{\sqrt{2} \cdot E_{al}}{2\pi f_r} \quad (36)$$

7.4 Calculation method

The calculation method is programmed in Visual Basic®, applying an Excel® sheet. In the following, the essential procedures are listed. They may easily be transferred to other programme languages.

The calculation scheme is built as follows:

sub enter_values
assigning values to the variables.

sub data_conditioning
preparing the start conditions.

function current
calculation the actual primary current value for the specified point in time, for specified values of T_p and γ.

sub Calc_ Ip_co, sub Calc_ Ip_coco
calculating curves of the primary short circuit currentfor various current inception angles, whereby angle steps of 10° are sufficient.

sub Calc_psi
calculating the appropriate flux curves for current inception angles γ in the interval between γ_m and 180°.

sub Calc_psimax
selecting the highest flux values for every time point, taking all calculated flux curves into consideration.

sub Calc_psimax_tal
finding the highest flux value (psimax_t) for every time point, considering the time interval from t=0 up to the actual time point. Only the relevant time intervals are considered.

sub Calc_Ktd
calculating

- K_{td}, as ratio between the highest psimax_t value and the peak value of its AC component;
- epsilon_peak for TPY-cores (according to Equation (37)).

sub co_cycle
main routine for calculation a C-O cycle.

sub coco_cycle
main routine for calculation a C-O-C-O cycle.

The time step dt has to be chosen ≤ 10^{-4} s at 50 Hz. At other frequencies, the time interval dt has to be modified; it shall be inversely proportional to the frequency.

The value of E_{al} shall be stated in order to recognize the saturation level. If saturation is reached within the relevant time interval(s), a K_{td} value of 99 999 is returned.

Further explanations are given directly in the description of the procedures.

The programme code is listed in Annex B.

In the appropriate Excel® sheets (Figure 44 to Figure 49), the cells B2 to B13 are input values. The output values are presented in cells B16 and B17. The values in rows E, F and G are generated by the programme, as a database for the graphic representation.

7.5 Reference examples

The following examples are created to provide the user with the possibility of checking his own calculation scheme.

In Figure 44, the maximum possible range of current inception angles φ shall be covered. Therefore, the minimum fault inception angle γ_m is chosen as $\varphi = \arctan(\omega T_p)$. This angle affects the maximum DC component.

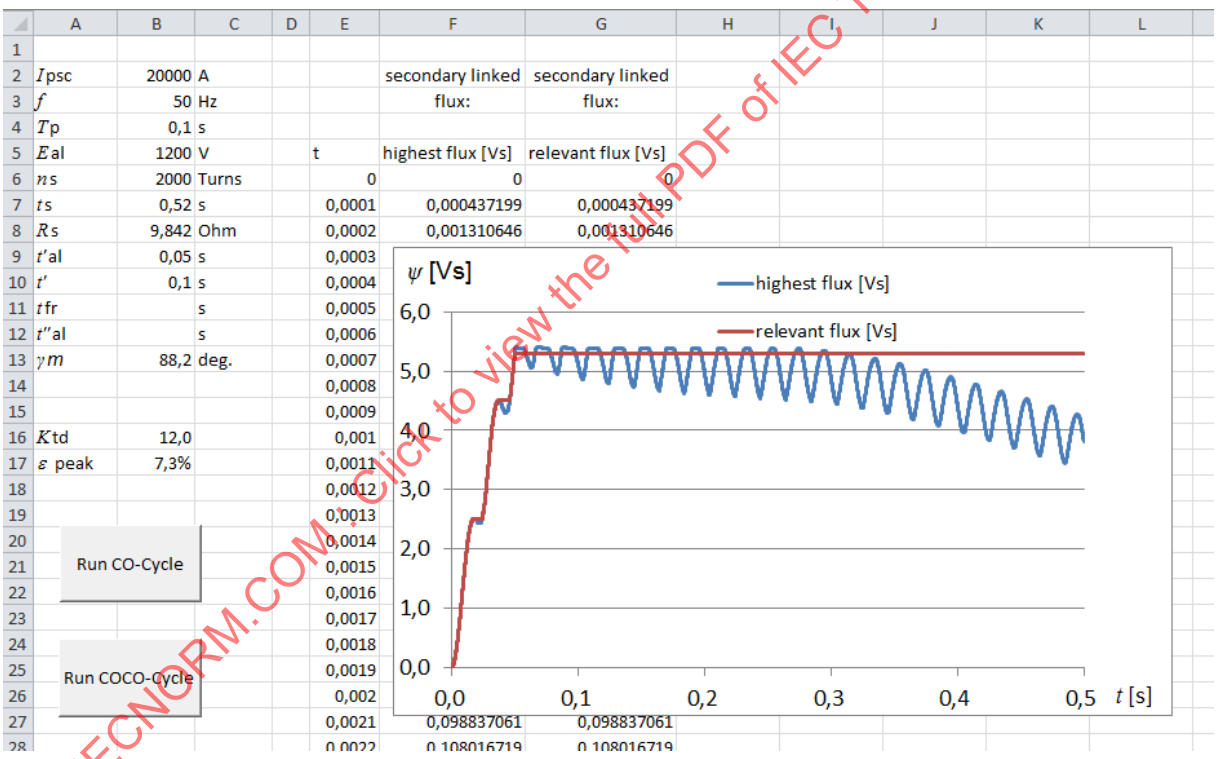

Key

ψ secondary linked flux

t time

All symbols used the spreadsheet are listed in the index of abbreviations 3.2.

Figure 44 – K_{td} calculation for C-O cycle

	A	B	C	D	E	F	G
1							
2	Ipsc	20000	A			secondary linked	secondary linked
3	f	50	Hz			flux:	flux:
4	Tp	0,1	s				
5	Eal	2200	V		t	highest flux [Vs]	relevant flux [Vs]
6	ns	2000	Turns		0	0	0
7	ts	0,74	s		0,0001	0,000437199	0,000437199
8	Rs	9,842	Ohm		0,0002	0,001310671	0,001310671
9	t'al	0,05	s		0,0003		
10	t'	0,1	s		0,0004		
11	$t$fr	0,3	s		0,0005		
12	t"al	0,03	s		0,0006		
13	γm	88,2	deg.		0,0007		
14					0,0008		
15					0,0009		
16	Ktd	20,3			0,001		
17	ε peak	8,8%			0,0011		
18					0,0012		
19					0,0013		
20					0,0014		
21	Run CO-Cycle				0,0015		
22					0,0016		
23					0,0017		
24					0,0018		
25	Run COCO-Cycle				0,0019		
26					0,002		
27					0,0021	0,098875006	0,098875006
28					0,0022	0,108060309	0,108060309

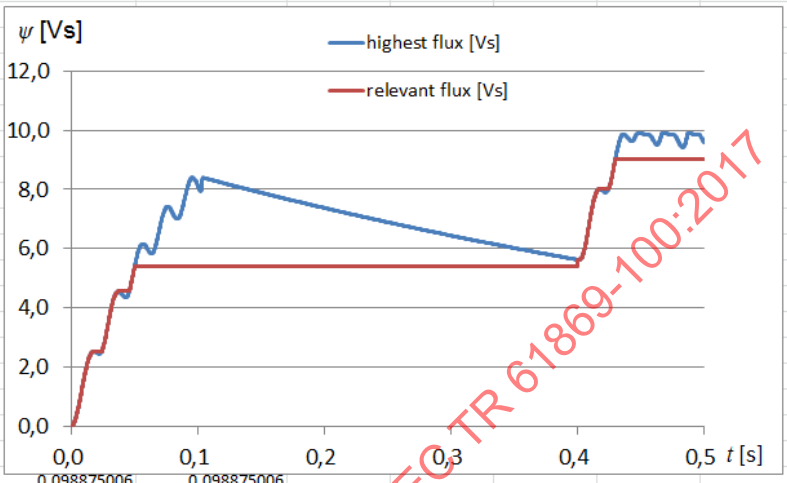

Key

ψ secondary linked flux

t time

All symbols used the spreadsheet are listed in the index of abbreviations 3.2.

Figure 45 – K_{td} calculation for C-O-C-O cycle without core saturation in the first cycle

	A	B	C	D	E	F	G
1							
2	Ipsc	20000	A			secondary linked	secondary linked
3	f	50	Hz			flux:	flux:
4	Tp	0,1	s				
5	Eal	1500	V		t	highest flux [Vs]	relevant flux [Vs]
6	ns	2000	Turns		0	0	0
7	ts	0,582	s		0,0001	0,000418453	0,000418453
8	Rs	9,42	Ohm		0,0002	0,001254457	0,001254457
9	t'al	0,05	s		0,0003		
10	t'	0,1	s		0,0004		
11	$t$fr	0,3	s		0,0005		
12	t''al	0,025	s		0,0006		
13	γm	88,2	deg.		0,0007		
14					0,0008		
15					0,0009		
16	Ktd	15,0			0,001		
17	ε peak	8,2%			0,0011		
18					0,0012		
19					0,0013		
20					0,0014		
21					0,0015		
22					0,0016		
23					0,0017		
24					0,0018		
25					0,0019		
26					0,002		
27					0,0021	0,09461219	0,09461219
28					0,0022	0,103400183	0,103400183

Run CO-Cycle

Run COCO-Cycle

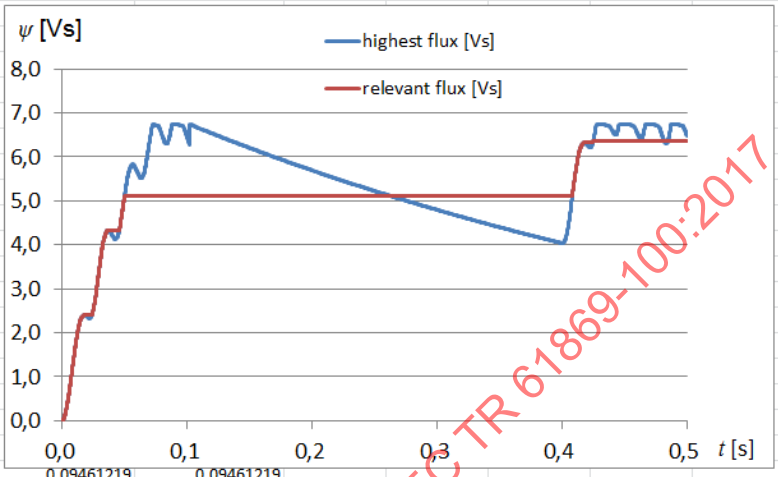

Key

ψ secondary linked flux

t time

All symbols used the spreadsheet are listed in the index of abbreviations 3.2.

Figure 46 – K_{td} calculation for C-O-C-O cycle considering core saturation in the first cycle

	A	B	C	D	E	F	G
1							
2	Ipsc	20000	A			secondary linked	secondary linked
3	f	50	Hz			flux:	flux:
4	Tp	0,1	s				
5	Eal	1500	V		t	highest flux [Vs]	relevant flux [Vs]
6	ns	2000	Turns		0	0	0
7	ts	0,582	s		0,0001	0,000418453	0,000418453
8	Rs	9,42	Ohm		0,0002	0,001254457	0,001254457
9	t'al	0,05	s		0,0003		
10	t'	0,1	s		0,0004		
11	$t$fr	0,3	s		0,0005		
12	t''al	0,04	s		0,0006		
13	γm	140	deg.		0,0007		
14					0,0008		
15					0,0009		
16	Ktd	14,0			0,001		
17	ε peak	7,7%			0,0011		
18					0,0012		
19					0,0013		
20					0,0014		
21	Run CO-Cycle				0,0015		
22					0,0016		
23					0,0017		
24					0,0018		
25	Run COCO-Cycle				0,0019		
26					0,002		
27					0,0021	0,094715113	0,094715113
28					0,0022	0,103571954	0,103571954

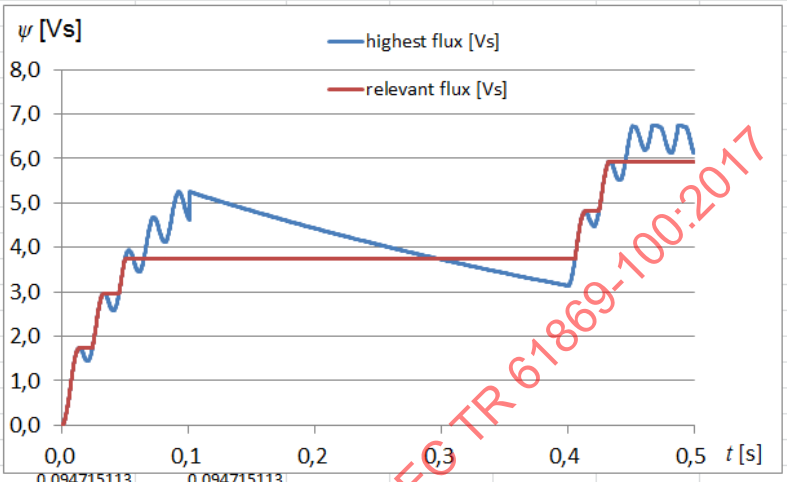

Key

ψ secondary linked flux

t time

All symbols used the spreadsheet are listed in the index of abbreviations 3.2.

Figure 47 – K_{td} calculation for C-O-C-O cycle with reduced asymmetry

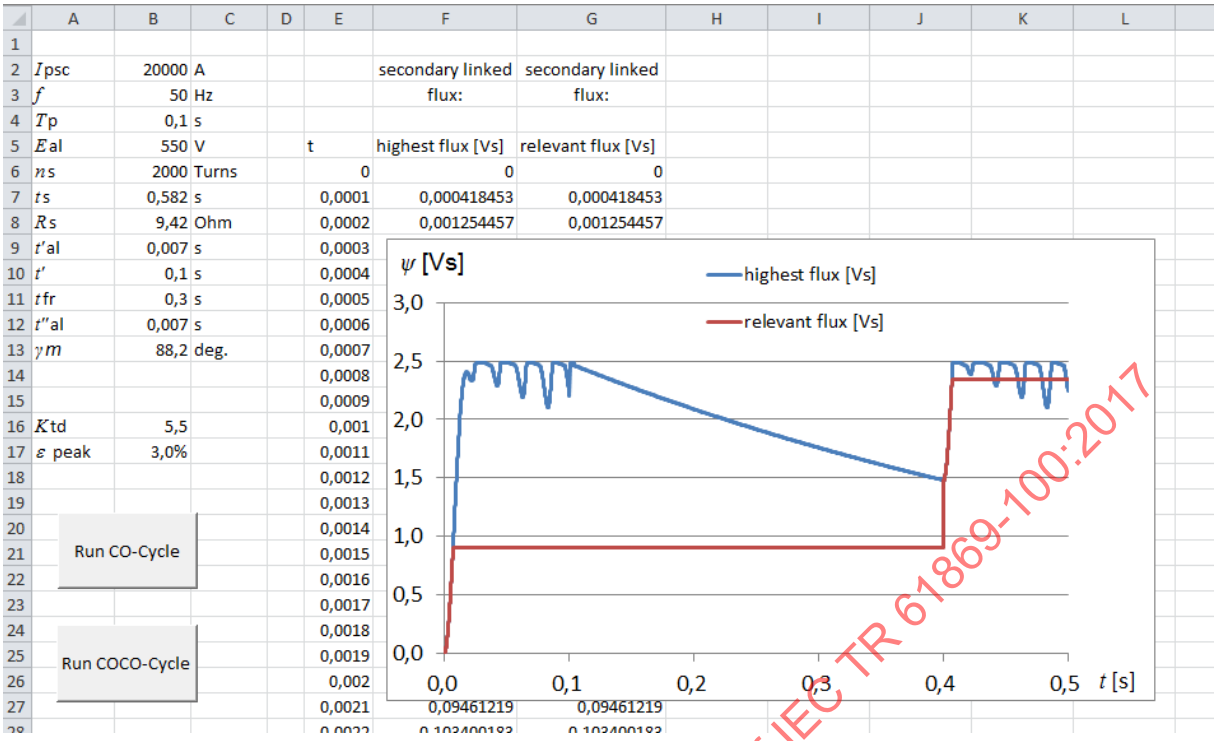

Key

ψ secondary linked flux

t time

All symbols used the spreadsheet are listed in the index of abbreviations 3.2.

Figure 48 – K_{td} calculation for C-O-C-O cycle with short t'_{al} and t''_{al}

In Figure 49, the behaviour of a TPX core is calculated. The result has to be assessed carefully by the following reasons:

- Remanence is not considered. To obtain reasonable results regarding remanence, the exact course of the remanence curve of the core material ought to be incorporated.
- In the case of saturation during the first fault, there is a rather rapid drop of the flux to remanence level during t_{fr}. The available flux interval after the first fault will always be at least the flux difference between saturation level and the remanence level.
- The secondary time constant T_s has been chosen high enough, preventing the flux from decaying during the fault repetition time. In practice, the flux may decay to the remanence level within a reasonable time interval.
- The model does not cover the current practice to consider the flux drop to remanence level of non-gapped cores after reaching full saturation.

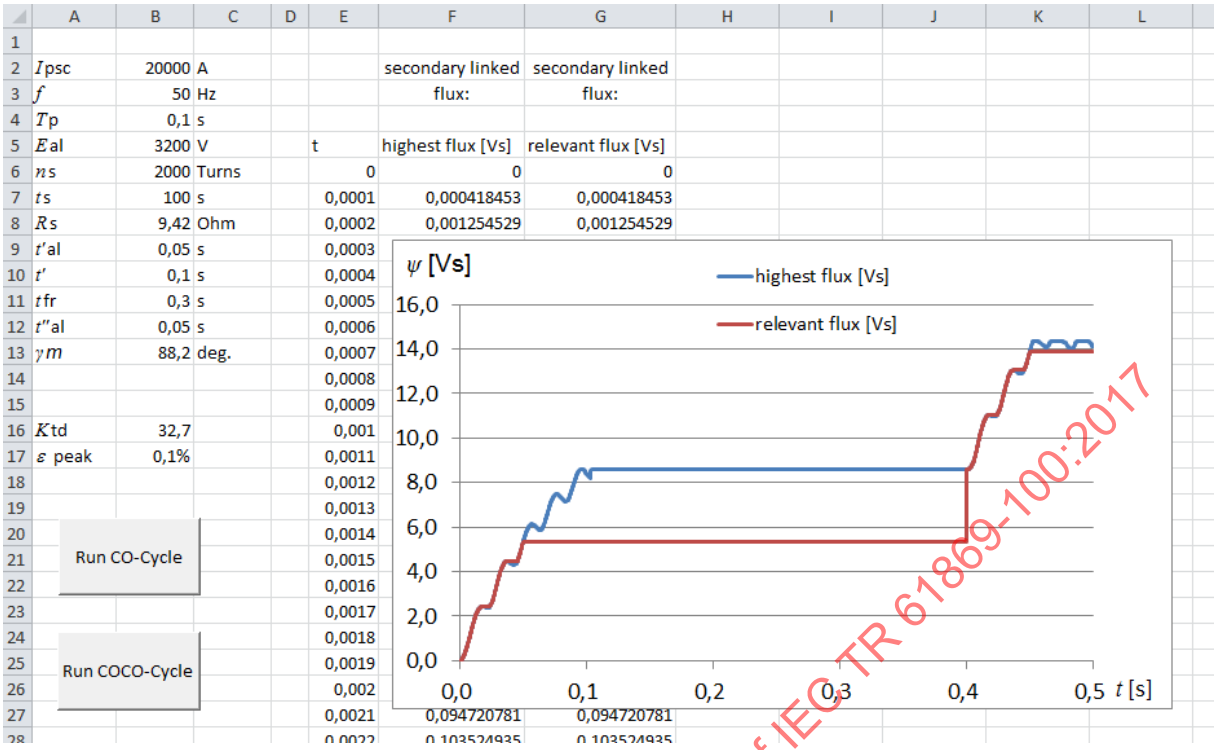

Key

ψ secondary linked flux

t time

All symbols used the spreadsheet are listed in the index of abbreviations 3.2.

Figure 49 – K_{td} calculation for C-O-C-O cycle for a non-gapped core

8 Core saturation and remanence

8.1 Saturation definition for common practice

8.1.1 General

Various proposals for the definition of the saturation flux have been made in the past. In the following, three approaches are discussed.

8.1.2 Definition of the saturation flux in the preceding standard IEC 60044-1 [3]

In IEC 60044-1:1996/AMD1:2000, 2.3.6, the saturation flux was defined as: “that peak value of the flux which would exist in a core in the transition from the non-saturated to the fully saturated condition and deemed to be that point on the B-H characteristic for the core concerned at which a 10 % increase in B causes H to be increased by 50 %”.

This definition gained no acceptance because the saturation value was too low, and led to misunderstandings and contradictions. According this previous definition, the remanence factor, which is defined as remanence flux divided by saturation flux, could achieve values higher than 100 %. See Figure 50.

3 Withdrawn and replaced by IEC 61869-2:2012.

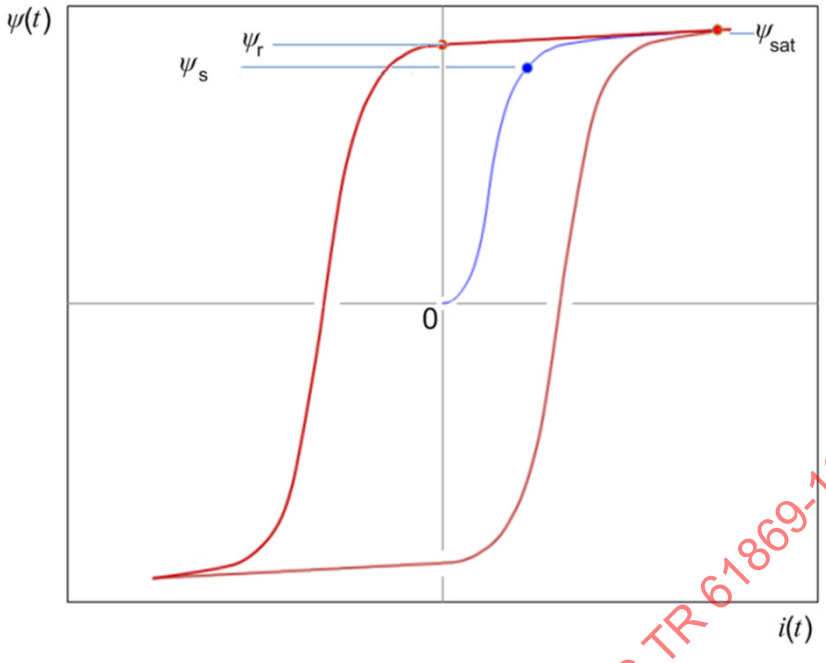

Key

i	secondary current (while primary circuit open)
ψ_r	remanent flux
ψ_s	saturation flux according to the preceding standard IEC 60044-1
ψ_{sat}	saturation flux according to the standard IEC 61869-2

Figure 50 – Comparison of the saturation definitions according to IEC 60044-1 and according to IEC 61869-2

Nevertheless, to confirm the remanence condition of a gapped core (< 10 %), the result of this method will provide a result on the safe side. Figure 51 shows exemplarily the flux course of a non-gapped core in the case of a demagnetized core (red curves) and of magnetised core (blue curve, remanence in the same direction as magnetization).

One can note that the calculation of the remanence factor K_r (with lower case index) according to the old standard IEC 60044-6 with the knee point method (50 % current rise resulting in 10 % flux rise) leads to the factor K_r = 119 % (Figure 51). It is clear that remanence factor values higher than 100 % are physically absurd.

Therefore the definition of the saturation flux has been changed in the standard IEC 61869-2. This leads always to remanence factor values K_R (with capital index) lower than 100 %. In the case of Figure 51, the remanence factor K_R is 90 % according to the new definition.

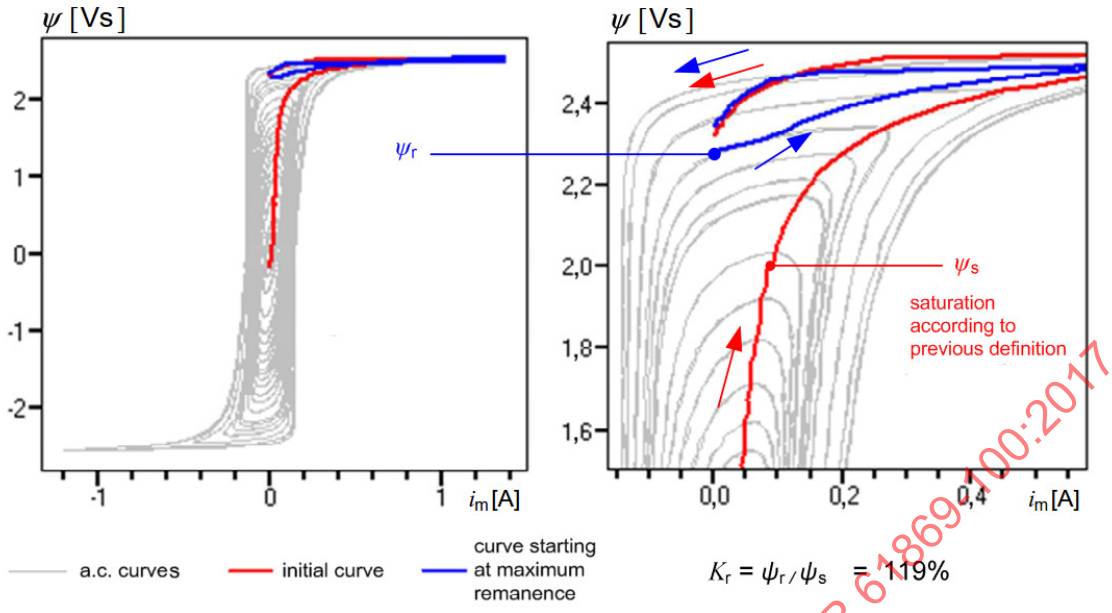

Key

i_m Excitation current

ψ secondary linked flux

ψ_r remanent flux

ψ_s saturation flux according to the preceding standard IEC 60044-1

K_r saturation flux according to the preceding standard IEC 60044-1

Figure 51 – Remanence factor K_r according to the previous definition IEC 60044-1

8.1.3 Definition of the saturation flux in IEC 61869-2

In IEC 61869-2:2012, 3.4.210, the saturation flux is defined as the "maximum value of secondary linked flux in a current transformer, which corresponds to the magnetic saturation of the core material" with the following note: "The most suitable procedure for the determination of the saturation flux Ψ_{sat} is given with the DC saturation method described in 2B.2.3."

This definition is not as mathematically strict as the previous one; on the other hand, it is more suitable for practical use. The examples in Figure 52 and Figure 53 show a print-out of a real laboratory test. It demonstrates how saturation is given by the evident value of the horizontal line.

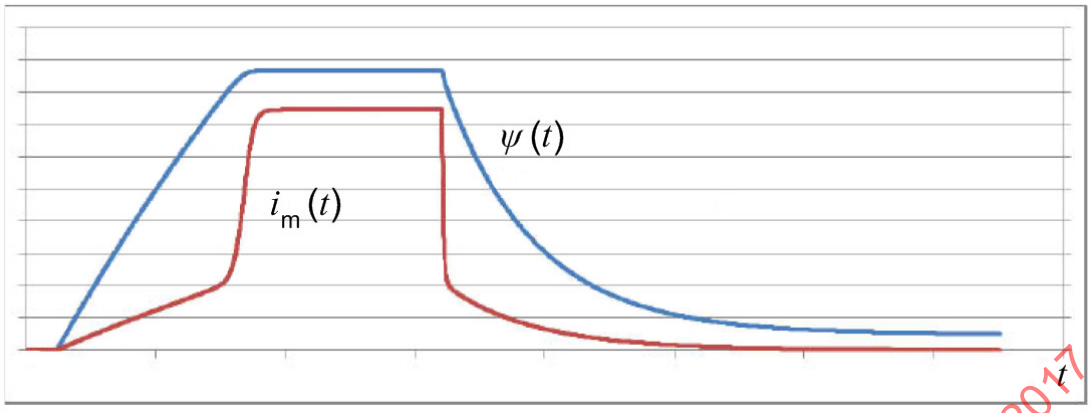

Key

$\psi(t)$ magnetic flux in the current transformer core

$i_m(t)$ magnetizing current

t time

Figure 52 – Determination of saturation and remanence flux using the DC method for a gapped core

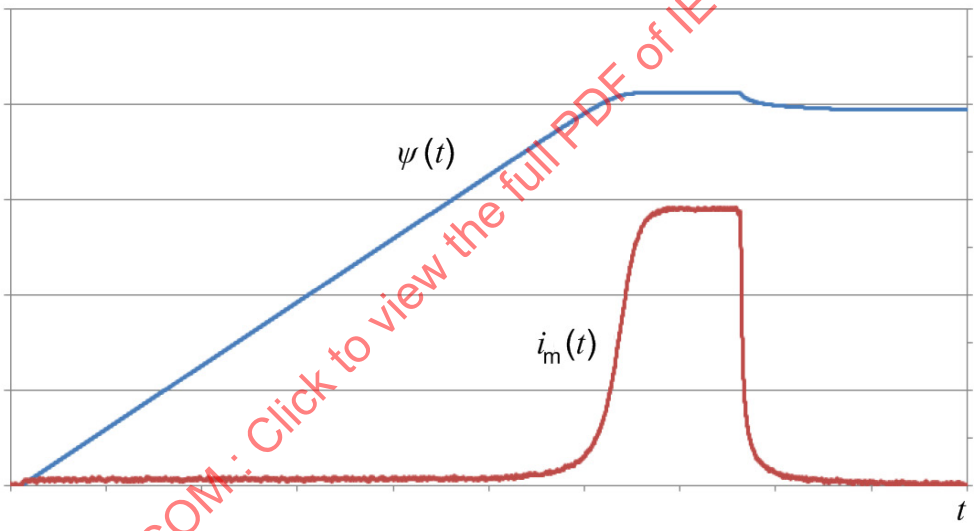

Key

$\psi(t)$ magnetic flux in the current transformer core

$i_m(t)$ magnetizing current

t time

Figure 53 – Determination of saturation and remanence flux using DC method for a non-gapped core

8.1.4 Approach "5 % – Factor 5"

For non-gapped cores, the following simplified saturation definition was proposed in the maintenance team MT40. "The peak value of the flux which exists in a core as close as possible below the fully saturated condition". It is deemed to be the point on the flux-current characteristic of the concerned core at which 5 % decrease in flux causes the current to be reduced by factor 5."

Measurements were made to verify the suitability of this method (Table 3). The hereby obtained values remain about 0 % to 3 % below the saturation flux obtained according to

IEC 61869-2. Please take note that the saturation behaviour is given by the physical designing. With given ratio and class, different physical solutions may be possible.

Table 3 – Comparison of saturation point definitions

Ratio	Class	Method IEC 61869-2	Method "5 %-Factor 5"	Ratio	Remark
		$\Psi_{\text{sat DC}}$	$\Psi_{\text{sat 5 \%-factor 5}}$	$\Psi_{\text{sat 5 \%-factor 5}} / \Psi_{\text{sat DC}}$	
		Vs	Vs		
800 / 1 A	5VA 0,2S FS5	0,1198	0,1182	98,7 %	
1000 / 5 A	75VA 0,5 FS5	0,2802	0,2790	99,6 %	
1600 / 5 A	45VA 0,5 FS10	0,2930	0,2916	99,5 %	
400 / 5 A	30VA 5P20	0,6196	0,6144	99,2 %	1
2 500 / 1 A	30VA 5P20	2,8782	2,8357	98,5 %	
1 200 / 1 A	60VA 5P30	8,6527	8,3687	96,7 %	
2 400 / 1 A	120VA 5P30	17,265	16,719	96,8 %	
2 400 / 1 A	120VA 5P30	17,266	16,725	96,9 %	2
1 000 / 5 A	50VA 5PR20	2,0406	2,0466	100,3 %	
300 / 1 A	15VA 10P20	1,7139	1,6623	97,0 %	1
1 000 / 1 A	15VA 10P20	1,8829	1,8436	97,9 %	
2 000 / 1 A	30VA 10P30	9,0819	8,8258	97,2 %	
2 000 / 1 A	30VA 10P30	9,0823	8,8265	97,2 %	2
1 000 / 5 A	PX	2,7781	2,6940	97,0 %	1
1 000 / 5 A	PX	2,7768	2,6883	96,8 %	2
3 000 / 1 A	PX	4,5348	4,4591	98,3%	
3 000 / 1 A	PX	4,5004	4,4594	99,1 %	2
2 500 / 1 A	PX	14,556	14,167	97,3 %	
3 000 / 1 A	PX	29,85	27,49	92,1 %	

1 Real maximum value not detected, max read value used.

2 Same test object as line above (reproducibility check).

8.2 Gapped cores versus non-gapped cores

Nowadays, the majority of applications still work well with the conventional classes. However, several protection applications where remanence appears can be handled much more easily and safely with gapped cores and reasonable core sizes.

Practically, the maximum remanence factor of non-gapped cores is typically in the range of 60 % to 95 %, and it depends on the applied magnetic core material and its alloy constituents. Many references for protective current transformers classify non-gapped cores with a remanence factor K_R of 75 % to 80 % as "high remanence cores". This implies that remanence factors higher than 80 % are impossible. But nowadays several core materials with a remanence factor up to 95 % have been found.

For instance, during some refurbishment projects, the remanence level of old CT cores (manufactured between 1930 and 1940) was measured (Table 3 "old CT cores"). CT cores manufactured until 1980 showed similar results. In contrast to this result, CT cores manufactured after about 1990 (this year is a rough indication only, the change is more smooth in a longer time span) show remanence factors up to 95 % (Table 3 "new CT cores"). This does not mean that nowadays only such "newer, very high remanence type materials"

are applied, but they are part of a set of several different materials which have been developed further through the last decades and have been optimized for certain criteria. The high remanence is an unwanted result within such an optimization process. Therefore, as the worst case, one has to consider such high remanence as the possible maximum.

Table 4 – Measured remanence factors

	Old CT cores (1930 to 1990)	New CT cores since 1995
Maximum remanence[a]	75 % to 77 %	88 % to 95 %
Actual remanence[b]	70 % to 75 %	85 % to 87 %

[a] Maximum possible remanence limited by hysteresis curve.

[b] Actual residual remanence measured after de-energization, commissioning or other tests (maximum values within some test series where lower values and values close to zero are found too).

When non-gapped cores for protection purposes are dimensioned considering the influence of remanence, the high starting point of flux reduces the operational flux range of the magnetizing curve at the beginning of the fault inception. In the calculation of the required saturation e.m.f., the relay manufacturers consider this reduction of the flux range due to high remanence with an additional overdimensioning factor K_{h}.

$$K_{\mathrm{h}} = \frac{1}{1 - K_{\mathrm{R}}}$$

The required voltage E_{al} is then

$$E_{\mathrm{al}} = K_{\mathrm{h}} \cdot K_{\mathrm{td}} \cdot K_{\mathrm{ssc}} \cdot I_{\mathrm{sr}} \cdot \left(R_{\mathrm{ct}} + R_{\mathrm{b}}\right) = K_{\mathrm{tot}} \cdot K_{\mathrm{ssc}} \cdot I_{\mathrm{sr}} \cdot \left(R_{\mathrm{ct}} + R_{\mathrm{br}}\right)$$

with $K_{\mathrm{tot}} = K_{\mathrm{h}} \cdot K_{\mathrm{td}}$.

It is obvious that the overdimensioning factor for remanence K_{h} is highly dependent on the maximum possible remanence factor K_{R} of the magnetic core material, which in most practical cases is unknown.

Generally, remanence is not considered for dependability cases (cases when a protection system shall operate for an internal power system fault). The possible consequences of remanence can be an additional time delay, which is normally not of importance. As long as a CT does not saturate for AC current (K_{tot} = 1) the remanence behaviour will never cause a failure to operate. Lack of security (unwanted operation of protection for faults outside the protected zone) is never accepted and therefore the remanence shall be considered for these cases.

Examples:

- For the case in Figure 51 – Remanence factor Kr according to the previous definition IEC 60044-1
- with K_{R} = 90 %, the overdimensioning factor K_{h} is 10.
- In the worst cases, K_{R} equals to 95 %. This leads to an overdimensioning factor K_{h} = 20, which is considerable high and its usage would lead to unfeasible large CTs.
- If the highest remanence factor K_{R} is assumed to be lower than 80 %, the overdimensioning factor K_{h} is only 5.

Therefore, when current transformers have to be chosen to suit a new protection scheme, the following two ways can be applied:

- When existing non-gapped current transformers shall suit the new protection scheme, the usage of such a factor K_h is possible for CT cores with maximum remanence factors lower than 80 %. The overdimensioning factor K_h against remanence scales the range of the linear part of the magnetizing curve to the part between maximum remanence and saturation.
- For new projects where new CT core materials can lead to maximum remanence factors higher than 80 %, gapped cores are recommended if the relay function or algorithm is sensitive to distorted signals due to remanence. In general, at least differential protection functions are predestined to such issues but the final decision shall be found by protection relay tests.

  As the remanence factor K_R of anti-remanence core classes PR, PXR and TPY is limited to 10 %, the effective and remaining linear range of the magnetizing curve is then reduced to minimum 90 %. The overdimensioning factor against remanence is then

$$K_h = \frac{1}{1-K_R} = \frac{1}{1-0,1} = 1,11$$

  During protection relay tests, project engineering, CT core sizing and construction, the consideration of safety factors is the usual procedure. If the safety factors in total are deemed too narrow, the factor K_h = 1,11 may be applied.

Anti-remanence classes PR, PXR and TPY normally have a secondary time constant T_s higher than 1 s (T_s may be specified additionally with a lower value for special purposes). The transient performance of a simple anti-remanence class (without specification of T_s) is very similar to that of non-gapped core classes. Therefore the application of anti-remanence classes do not result in any disadvantages concerning the transient performance compared to the similar non-gapped core with the same saturation voltage E_{al} or knee point E_k. The parameters of class TPZ and classes PR, PXR and TPY with specified low T_s shall be geared individually on the relay function/algorithm.

Summarizing, it is proposed to use gapped cores as a rule for any new protection application (of low impedance type). Gapped cores do not have the drawback of an unpredictable remanence level. Typically, they can be dimensioned with a size less or equal to that of equivalent non-gapped cores.

Within high impedance protection schemes, there is neither necessity to use gapped cores (because saturation due to remanence is stabilised by the stabilising resistor) nor to use the overdimensioning factor K_h (for more details on high impedance protection scheme see 11.5.6).

8.3 Possible causes of remanence

Remanence persists until the core is demagnetised.

Demagnetizing only occurs when high primary currents with suitable polarity lead to a high burden voltage. Causes for remanence in CTs are:

a) from the CT primary side:
   - interruption of fault currents, particularly fault currents with DC component;
   - geomagnetic induced currents (GIC) with very low frequency (quasi DC) induced into the phase-earth loops of overhead lines due to solar flares;
   - varying loads with fluctuating DC components (e.g. arc furnaces).

     Figure 54 shows the fault records (three phases L1, L2, L3) of an arc furnace transformer. The filtered DC component $i_{d.c.}$ of $i(t)$ shows the pulsating shape and leads very easily to core saturation and remanence.

NOTE The DC component on the primary side is not completely transformed to the CT secondary side, so the fault record does not show the full DC component which may cause saturation problems here.

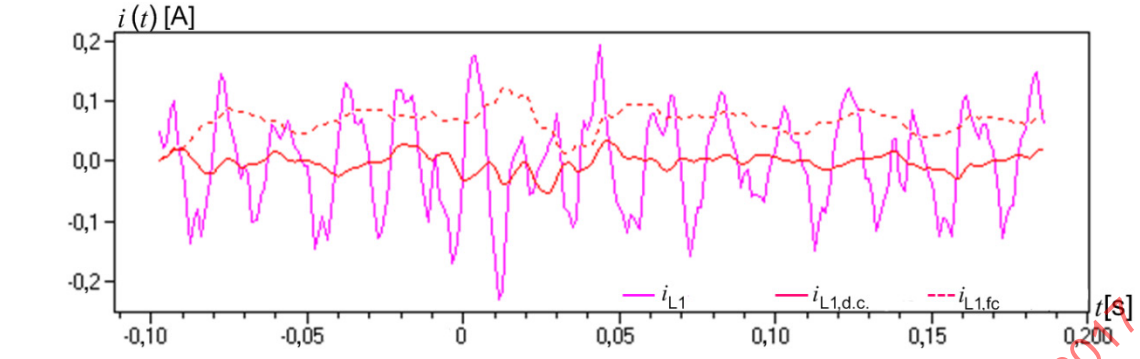

a) **Phase L1**

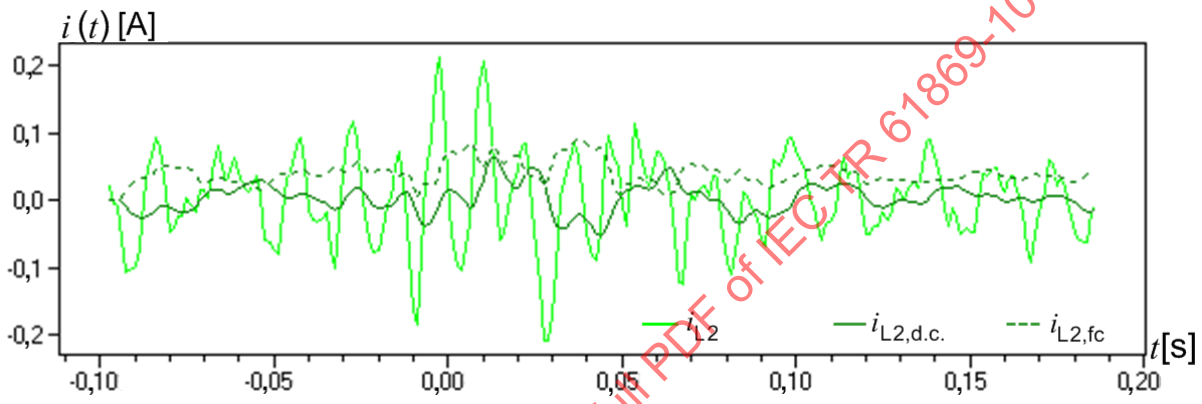

b) **Phase L2**

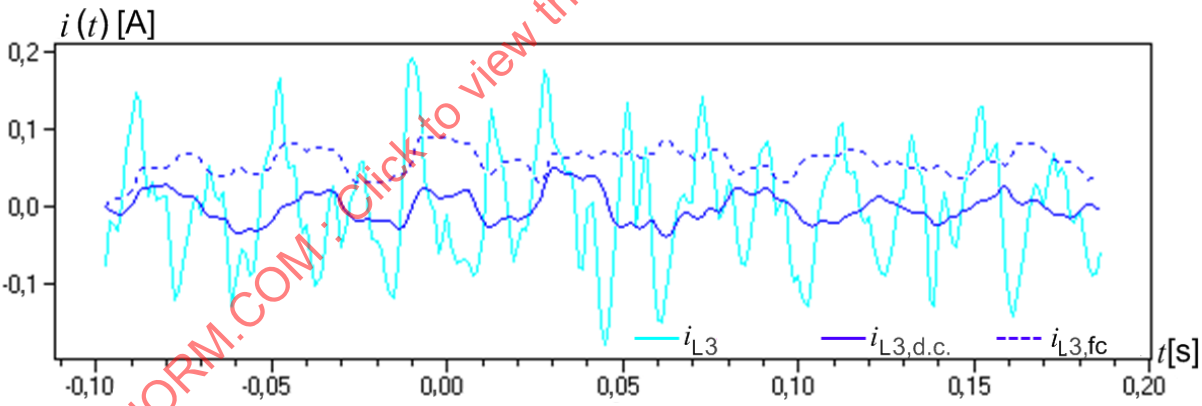

c) **Phase L3**

Key

$i_{L1,}$	$i_{L2,}$	i_{L3}	instantaneous current
$i_{L1,d.c.,}$	$i_{L2,d.c.,}$	$i_{L2,d.c.}$	filtered DC component of i
$i_{L1,fc,}$	$i_{L2,fc,}$	$i_{L3,fc}$	filtered fundamental component of $i_{L1,}$ $i_{L2,}$ i_{L3}
t			time

Figure 54 – CT secondary currents as fault records of arc furnace transformer

b) From the CT secondary side, when working with DC currents (e.g. when using batteries):

- carrying out polarity tests with DC pulses;
- testing of secondary wiring continuity (“beeper”);
- measurement of secondary resistance.
- In the second fault of auto reclosure C-O-C-O duty cycle, a CT core may be in remanence condition, caused by the first duty cycle. This effect can be reproduced by

transient simulations with a magnetic hysteresis model (see traces indicated by “sim” in Figure 56).

- single phase faults and CT secondary currents in a 4-wire cable (Figure 55) connecting the CTs with the protection device:

  Phase L1 saturates earlier than without remanence. The voltage drop across the neutral wire magnetises the CT cores of the healthy phases from the secondary side. As CT core L3 has remanence of K_R = – 95 %, it saturates due to the additional neutral voltage drop and leads to secondary currents through the protection device while no primary current is present. In phase L2, the remanence is much lower; therefore the neutral voltage drop is too low and has no effect.

  It is recommended to apply 6-wire cables (one return wire for each phase) for long distances in order to avoid such coupling effects between the phases.

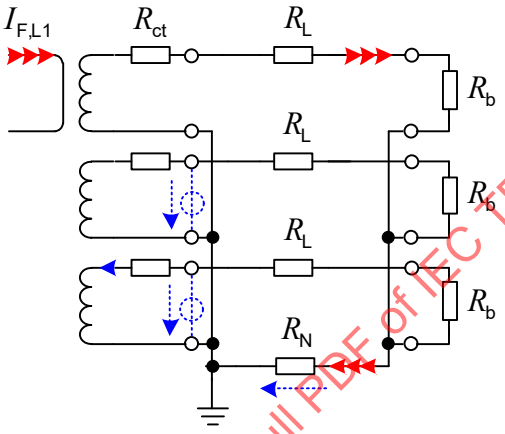

Key

R_{ct}	secondary winding resistance
R_b	resistive burden
R_L	line resistance between secondary terminal and terminal of the protection relay
R_N	resistance of neutral line between secondary terminal and terminal of the protection relay
$I_{F,L1}$	primary fault current in phase L1

Figure 55 – 4-wire connection

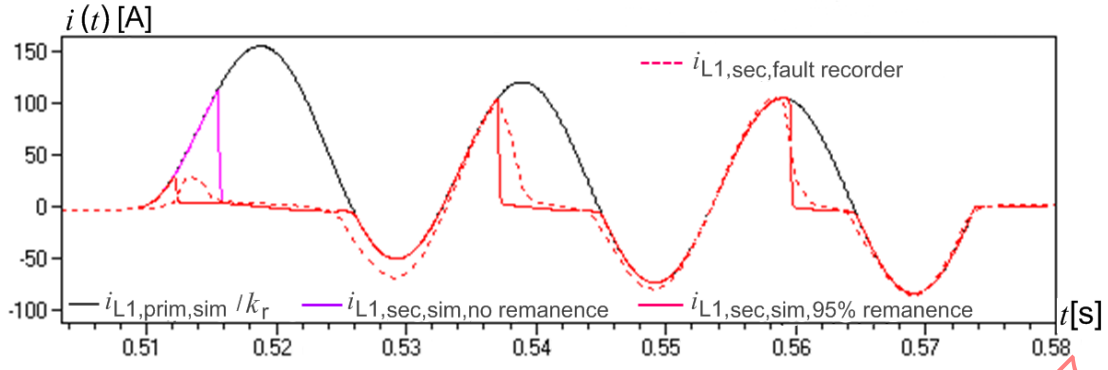

a) Phase L1: fault record and simulation

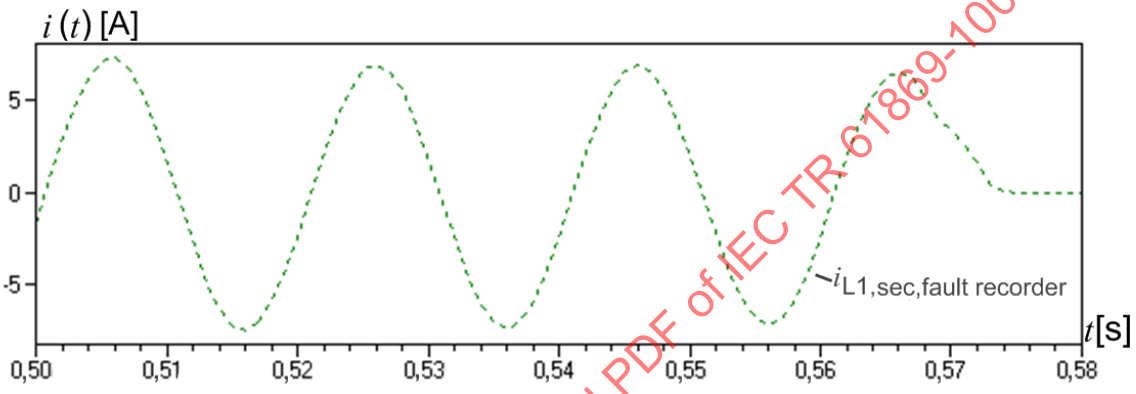

b) Phase L2: fault record and simulation

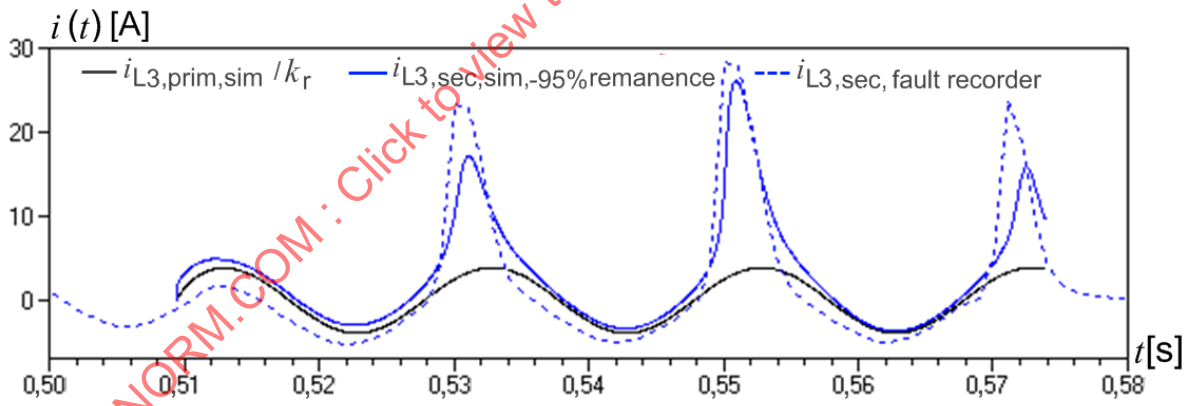

c) Phase L3: fault record and simulation

Key

$I_{L1,prim,sim,}$	$I_{L2,prim,sim,}$	$I_{L3,prim,sim}$	simulated primary current
$I_{L1,sec,sim}$	$I_{L2,sec,sim}$	$I_{L3,sec,sim}$	simulated secondary current (possibly with remanence)
$I_{L1,sec,\ fault\ recorder,}$	$I_{L2,sec,\ fault\ recorder,}$	$I_{L3,sec,\ fault\ recorder}$	measured secondary current
t			time

Figure 56 – CT secondary currents as fault records in the second fault of auto reclosure

9 Practical recommendations

9.1 Accuracy hazard in case various PR class definitions for the same core

Care has to be taken if a PR class is converted to another PR class, for example:

May a current transformer with the class designation	5 VA 5PR 80
be used with the class designation	50 VA 5PR 10 ?

In spite of similar E_{al} values, the errors at rated primary current and at the error accuracy limit condition may no longer meet the specified limits. Table 5 provides a practical example with critical values in red colour.

Table 5 – Various PR class definitions for the same core

I_p A	I_s A	Class	ALF	R_{ct} Ω	S (cosφ 0,8) VA	Z_b Ω	$R_{ct}+Z_b$ Ω	E_{al} V		I_{al} A	Error at rated current %	Min
400	1	5	80	2	5	5	6,71	537	Limits:	4	1	60
									measured:	0,751	–0,49	28
400	1	5	10	2	50	50	51,61	516	Limits:	0,5	1	60
									measured:	0,709	–4,38	187

9.2 Limitation of the phase displacement $\Delta\varphi$ and of the secondary loop time constant T_s by the transient dimensioning factor K_{td} for TPY cores

The following relationship is often used as a basis of the designing of TPY cores. It can easily be shown that for TPY cores, the K_{td} value and the maximum phase displacement $\Delta\varphi$ cannot be chosen independently.

Equation (37) , originally stated in IEC 61869-2:2012, Table 206, and Equation (38), originally stated IEC 61869-2:2012, 7.3.202, can be combined by eliminating T_s, leading to Equation (39).

$$\hat{\varepsilon} = \frac{K_{td}}{\omega[1/s] \cdot T_s[s]} \cdot 100\,\% \tag{37}$$

$$T_s[s] = \frac{3438}{\Delta\varphi[min] \cdot \omega[1/s]} \tag{38}$$

$\Delta\varphi$ is expressed in minutes.

$$\hat{\varepsilon} = \frac{K_{td} \cdot \Delta\varphi[min]}{3\ 438} \cdot 100\ \% \tag{39}$$

With $\hat{\varepsilon} \leq 10\,\%$, we obtain

$$K_{td} \cdot \Delta\varphi\,[min] < 343{,}8$$

Therefore, a higher K_{td} may make it necessary to limit the permissible phase displacement, since:

$$\Delta\varphi[\text{min}] < \frac{343{,}8}{K_{\text{td}}}$$

As a consequence, for K_{td} = 10, for example,

– the maximum allowed phase angle is 34 min,

– and the appropriate minimum allowed value for T_{s} at 50 Hz is 322 ms.

10 Relations between the various types of classes

10.1 Overview

Three different approaches are available for the definition of protective current transformers. In practice, each of the three definitions may result in the same physical implementation (see Table 204 of IEC 61869-2:2012).

10.2 Calculation of e.m.f. at limiting conditions

Although the definitions of the three approaches are quite different, an e.m.f. at limiting conditions related to rated frequency is defined for all of them (Table 6), and they can be compared with each other (Table 7).

Table 6 – e.m.f. definitions

P, PR	$E_{\text{ALF}} = ALF \cdot I_{\text{sr}} \cdot (R_{\text{ct}} + Z_{\text{b}})$
PX, PXR	$E_{\text{k}} = K_{\text{X}} \cdot I_{\text{sr}} \cdot (R_{\text{ct}} + R_{\text{b}})$
TPX, TPY, TPZ	$E_{\text{al}} = K_{\text{SSC}} \cdot K_{\text{td}} \cdot I_{\text{sr}} \cdot (R_{\text{ct}} + R_{\text{b}})$

Table 7 – Conversion of e.m.f. values

	P, PR	**PX, PXR**	**TPX, TPY, TPZ**
P, PR		$E_{\text{ALF}} \approx F \cdot E_{\text{k}}$	$E_{\text{ALF}} \approx E_{\text{al}}$
PX, PXR	$E_{\text{k}} \approx E_{\text{ALF}} / F$		$E_{\text{k}} \approx E_{\text{al}} / F$
TPX, TPY, TPZ	$E_{\text{al}} \approx E_{\text{ALF}}$	$E_{\text{al}} \approx F \cdot E_{\text{k}}$	

The factor F depends on the properties of the iron core material.

Practical values range from

– between 1,2 and 1,3 for non-gapped cores;

– around 1,1 for gapped cores.

For all classes, a dimensioning factor (ALF, K_{X}, $K_{\text{ssc}} \cdot K_{\text{td}}$) exists which can be understood as the ratio of the e.m.f. at limiting conditions to the e.m.f. at rated burden and rated current. They can be compared with each other as well (Table 8).

Table 8 – Conversion of dimensioning factors

	P, PR	PX, PXR	TPX, TPY, TPZ
P, PR		$ALF \approx K_x \cdot F$	$ALF \approx K_{SSC} \cdot K_{td}$
PX, PXR	$K_x \approx ALF / F$		$K_x \approx K_{SSC} \cdot K_{td} / F$
TPX, TPY, TPZ	$K_{SSC} \cdot K_{td} \approx ALF$	$K_{SSC} \cdot K_{td} \approx K_x \cdot F$	

10.3 Calculation of the exciting (or magnetizing) current at limiting conditions

All three approaches contain a limiting current condition, but they cannot be easily compared as their definitions are quite different (Table 9) and are related to various voltage levels.

Table 9 – Definitions of limiting current

5P, 5PR	$I_0 = I_{sr} \cdot ALF \cdot 5\%$	Composite error
10P, 10PR	$I_0 = I_{sr} \cdot ALF \cdot 10\%$	Composite error
PX, PXR	I_e = specified value	r.m.s. value
TPX, TPY	$\hat{I}_{al} = I_{sr} \cdot \sqrt{2} \cdot K_{ssc} \cdot \varepsilon$	Peak value
TPZ	$\hat{I}_{al\,ac} = I_{sr} \cdot \sqrt{2} \cdot K_{ssc} \cdot \varepsilon_{ac}$	Peak value of AC component

10.4 Examples

Given: Class TPY:

R_b = 5 Ω, TPY 20 × 5,5, R_{ct} ≤ 2,8 Ω, T_s = 900 ms, 1 200/1 A

a) Find: Class PR:

This CT is probably better than 5VA class 10 PR 110

Explanation:

– The burdens are comparable:

5 VA at 1 A means 5 Ω with power factor 0,8.

The vector sum of this burden and of the winding resistance is lower than in the TPY case with the 5 Ω burden at unity power factor.

– ALF is considered to be $K_{SSC} \times K_{td}$

NOTE 10 PR 110 may suggest an extremely high short circuit current of 1 320 kA, for which the current transformer is not built.

b) Find: Class PXR:

$$E_k \approx \frac{I_{sr} \cdot (R_{ct} + R_b) \cdot K_{ssc} \cdot K_{td}}{F} = \frac{1\text{A} \cdot 7{,}8\,\Omega \cdot 20 \cdot 5{,}5}{1{,}1} = 780\ \text{V}$$

$$I_e \approx \frac{E_k}{(R_{ct} + R_b) \cdot \omega \cdot T_S} = \frac{780\ \text{V}}{7{,}8\,\Omega \cdot 314 \cdot 0{,}9\ \text{s}} \approx 0{,}35\ \text{A}$$

NOTE Class PXR may require a higher interturn test voltage, for which the current transformer is not built.

10.5 Minimum requirements for class specification

This subclause describes a summary of the minimum requirements for class specification, based on IEC 61869-2:2012,5.6.202. Table 10 shows the minimum requirements for all protection classes.

Table 10 – Minimum requirements for class specification

Class designation	Required	Example for specification
P	accuracy class with accuracy limit factor (ALF) Rated output (S_r)	5 P 20 10 VA
PR	accuracy class with accuracy limit factor (ALF) Rated output (S_r)	5 PR 20 10 VA
PX, PXR	Rated knee point e.m.f. upper limit of exciting current upper limit of resistance of secondary winding alternatively: dimensioning factor upper limit of exciting current rated burden	E_k = 230 V I_e ≤ 0,2 A R_{ct} ≤ 2,8 Ω K_x = 40 I_e ≤ 0,2 A R_b ≤ 3 Ω
TPX, TPY, TPZ	rated symmetrical short circuit current factor for duty cycle C-O: t'_{al} or for duty cycle C-O-C-O: t'_{al}, t', t_{fr}, t''_{al} specified primary time constant rated resistive burden alternatively: rated symmetrical short circuit current factor Rated value of transient dimensioning factor rated resistive burden for TPY cores only: rated value of secondary loop time constant [a]	K_{SSC} = 20 Cycle 100 ms or Cycle (40-100)-300-40 ms T_P= 100 ms R_b = 2 Ω K_{SSC} = 20 K_{td} = 20 R_b = 2 Ω T_s = 500 ms

[a] Practically, for modern protection that requires relatively short time to saturation , the secondary time constant does hardly affect the K_{td}, value. Even if the required time to saturation should be 20 ms to 40 ms (a relatively long time), the difference of K_{td} between TPX and TPY is small. These are the cases where the relay specialist will define a worst-case value of K_{td}, without defining T_S, and the choice of T_S is left to the CT manufacturer. A limitation of T_S is given in 9.2.

NOTE When defining a TPY core using the alternative definition, IEC 61869-2 requires that, besides K_{td}, the secondary time constant T_S be stated. This is principally necessary, because the required over-dimensioning of the CT is dependent on how quickly the flux will decay due to the secondary time constant.

10.6 Replacing a non-gapped core by a gapped core

In many situations, a non-gapped core could be replaced by an equivalent gapped core (P by PR, PX by PXR, TPX by TPY), provided that the air gap is small enough. An air gap of totally 1/1 000 of the core circumference can be sufficient to reduce the remanence factor to a value below 10 %. In any case, the influence of the magnetizing current in the non-saturated range shall be reconsidered. Table 11 shows the remanence properties and the DC behaviour of all protection classes.

Table 11 – Effect of gapped and non-gapped cores

	Remanence	Anti-remanence	High DC damping
P, PX, TPX	x		
TPY, PR, PXR		x	
TPZ		x	x

11 Protection functions and correct CT specification

11.1 General

In this sublause, a basic overview and general guidelines are given for the choice of CT class and the designing of the CT cores with respect to several protection functions. The description is not intended to be fully comprehensive and the data used in the examples, such as the choice of CT class, consideration of worst case scenarios and calculation of CT designing parameters, are general and only for the purpose of illustrating the examples. The CT requirements for the CT core designing that are used in the examples for the various protection functions. These are arbitrary and independent of concrete brands or products and do not claim to be exhaustive. The main purpose of the examples is to show how the formulae for CT designing can be applied in relation to several typical protection functions.

There are two methods for indicating protection relay functions in common use. One is given in ANSI Standard C37-2 (so-called “ANSI codes”) [2], and uses a numbering system for various functions. The functions are supplemented by letters where amplification of the function is required. The other is given in IEC 60617 [3], and uses graphical symbols. Function descriptions are given in the above mentioned standards. In this subclause and its subclauses, the ANSI codes are stated in brackets.

For more details regarding the proper definition of worst case scenarios in the network and CT designing, further standards of the IEC 60255 series shall be considered [4], [5] to [6].

In specific projects, the CT sizing shall be according to CT requirements described in the protection relay manuals.

As an improvement to the old standard IEC 60044, the correct choice of the transient dimensioning factor K_{td} shall not only be based on mathematical formulae, but shall additionally be subject to relay tests with saturated CT models as described in Clause 5, and Clause 6.

11.2 General application recommendations

11.2.1 Protection functions and appropriate classes

Table 12 shows the minimum requirements for current transformers with reference to their protection function. (ANSI codes for protection functions in parentheses).

Table 12 – Application recommendations

Protection function	Recommended CT class	Remark
Overcurrent, phase/earth – non-directional (50/51/50N/51N) – directional (67/67N)	 10P 10P (eventually 5P)	ALF > maximum current setting of definite stages ALF > 20 (for inverse stage) considering the real fault currents
Distance (21/21N)	5P, PX 5PR, TPY, (TPZ), PXR	 to avoid remanence, TPZ for high T_p
Sensitive earth fault – non-directional - isolated, high-ohmic - compensated – directional	window type CT class: class 3 class 1 class 1	If phase CTs as protection class are applied in residual (Holmgreen) CT connection, sensitive settings may be delayed in order to avoid maltrips due to CT saturation.
Differential – unit transformer (87T) – transmission transformer (87T) – auxiliary or MV transformer (87T) – generator transformer (87G) – bus bar (87B) – line (87L) - ΔI - $\Delta\varphi$ – high impedance	5PR, TPY, (TPZ), PXR 5P PX	TPZ for high T_p normally sufficient
Every low impedance protection function with CTs connected in parallel	same classes and data 5PR, TPY, TPZ	
High-impedance	PX	

In special cases of high impedance differential protection schemes, even low fault currents are desired to be detected with high sensitivity. Therefore anti-remanence core classes such as 5PR, 10PR, TPY or PXR are not suitable for such applications. In other protection schemes applying low impedance protection, there are no drawbacks of using anti-remanence core classes, because they don't have a significant damping or filtering effect to the DC component of the current.

However, when applying class TPZ with desired damping or filtering effect to the DC component, the relay suitability (regarding used algorithms) has to be carefully considered. Actually, only their sensitivity concerning the evaluation of the DC component is important. Typically in modern relays, the fundamental component of the signal is filtered out and evaluated, while the DC component is suppressed anyway. Therefore, in differential protection schemes, different CT core classes within the same protection zone (TPZ and non-gapped cores as extreme case) don't normally show practical drawbacks if the differential protection relay uses Fourier filtering.

The damping effect of class TPZ to the DC component in the CT secondary current has significant consequences in cases when low fault or overcurrents with high primary time constant T_p occur (e.g. low transformer inrush currents, sympathetic transformer inrush, low fault current contribution in power stations). It may lead to CT saturation even at very low current levels.

Such scenarios are very hard to stabilize in differential protection relays. Unwanted trips at external faults related to class TPZ occurred in the past, when unfiltered CT secondary currents were compared dynamically, in digital terms “sample by sample”. If the DC components of different CT secondary currents are suppressed with different degree (e.g. due to different CT classes or core sizes), a differential current appears on the CT secondary side even when no internal fault is present on the primary side. Such scenarios shall be focused by the protection relay manufacturers.

11.2.2 Correct CT designing in the past and today

The equations usually applied for core size dimension according to Table 6 are:

$$E_{al} = K_{td} \cdot K_{ssc} \cdot I_{sr} \cdot (R_{ct} + R_b)$$

or

$$E_{ALF} = ALF \cdot I_{sr} \cdot (R_{ct} + Z_b) \approx 1{,}2 \text{ to } 1{,}3 \cdot E_k$$

(using a practical estimation factor, see Table 7),where some of the input parameters shall be specified by the customer according toTable 10.

For the classes P, PR, TPX, TPY and TPZ, R_{ct} is not specified because this is an internal parameter for construction purposes.

In the past (more than 20 to 40 years ago), the networks had generally lower time constants T_p, and electromechanical protection devices had high burdens (10 VA or more). As electromechanical protection devices needed a mechanical torque for operation, the usual rated current of 5 A was a suitable value. Therefore, the conversion of the burden value as impedance or resistance multiplied by the square of the rated current led to high values, such as 30 VA. The mechanical torque was gained from the input current via an input current transformer using the inductive part of its impedance. Therefore, a specified power factor of $\cos\varphi$ = 0,8 for the burden for classes 5P, 10P and measurement classes resulted. Thus it appears that the power factor 0,8 has a historical background.

Due to the longer operation times, when the DC component has already declined, only the symmetrical AC component of the short circuit current was relevant for pick-up. Core saturation was a known phenomenon but not considered to be an important problem in most cases. If two or three relays were connected in series to the CT core, the total rated burden of 30 VA was sufficient in most cases. As, in most cases, the maximum pick-up setting was not higher than $20 \times I_{pr}$, the typical CT core was a 30 VA 5P20 for many applications. This was the time when classes 5P and 10P were only specified for the AC component of the short circuit current.

Nowadays, higher voltage levels are used, generators are constructed for higher power and the losses are lower due to optimization and cooling. Therefore, primary time constants can be higher and have an important influence on the core saturation. This may disturb the selectivity of modern protection devices. They measure and operate within one cycle or shorter. Depending on the purpose and the protection relay age, the factor K_{td} avoids the saturation due to the DC component for

- the time to accuracy limit t'_{al} with typical K_{td} = 2 to 20 (fast operation and trip);
- the full duration of the short circuit current flow. (no saturation allowed, $t'_{al} = t'$, relay shall be stable for currents flowing for longer time, as tripping is performed by other relays);

  In this case, high factors of K_{td} = 10 to 50 result, also because older protection relays had only simple or no stabilizing functions against saturation.

With such high transient factors K_{td}, the cores became larger, which was practicable in outdoor current transformers. Nowadays, gas insulated equipment (GIS) provides only limited

space for current transformers. For very short t'_{al} values for the protection devices, smaller transient dimensioning factors result, and the CT cores can be built smaller.

As electronic protection devices (next generation after electromechanical ones) measure the CT secondary current only as a signal and no longer need any torque, their burden is much lower and mainly resistive, so the transient performance classes TPX, TPY, TPZ are specified for a resistive burden in [Ω] ($\cos\varphi$ = 1). Without the torque needed, the rated current of 1 A is sufficient and even the value of 0,1 A is now in discussion and is already used in special applications.

A typical requirement for TPX, TPY, TPZ (as examples of modern protection relays) could be

$E_{al} = K_{td} \cdot K_{ssc} \cdot I_{sr} \cdot (R_{ct} + R_b)$ with R_b low, K_{ssc}, K_{td} high (e.g. R_b = 2,5 Ω, K_{td} = 5, K_{ssc} = 20).

Each of these specified parameters is chosen strictly according to the application.

But, as classes 5P, 10P are well known from the past, they are still used in the majority of applications with the traditional model which used the high burdens of electromechanical relays and the overcurrent factor ALF, which only considered the AC component.

In many applications, the high rated burden compensates the low ALF. The resulting physical E_{al} remains more or less the same. Superficially, it seems that this philosophy does not need to be changed, but when using CT cores with high rated burden which are extremely "under-burdened", the accuracy may be worse than in the case of CT cores with an operational burden similar to the rated burden. This may be important when using differential protection, and may be considered when old relays with higher burden are replaced by digital relays.

The difference between the parameter data of the past (high rated burden, no K_{td}) and of today (low burden, K_{td} > 1 or K_{td} < 1) is obvious.

Nowadays, in refurbishment projects, it is still common practice to keep the old CT cores and connect them to new, modern protection devices. In such cases, the compliance of the existing old CTs with the requirements of the new, modern relays shall be checked.

The required TPX, TPY or TPZ core with

$$E_{al} = K_{td} \cdot K_{ssc} \cdot I_{sr} \cdot (R_{ct} + R_b)$$

is then realized by a class 5P or 10P core. Its suitability is verified according to Table 8 by

$$K_{td} \cdot K_{ssc} \approx ALF'$$

From the physical point of view (similar accuracy limiting voltage with similar transient performance), this formula shows the similarity between the classes 5P/10P, and TPX/TPY (classes TPZ and TPY with low T_s need special consideration).

Example:

500/1 A, 5P60, 5 VA, R_{ct} = 2 Ω

is similar to

500/1 A, TPX or TPY, R_b = 5 Ω, R_{ct} = 2 Ω, K_{ssc} = 20, K_{td} = 3.

If the operational burden R'_b is different to the rated burden R_b, the following conversion can be applied in order to calculate the operational accuracy limit factor ALF':

$$E_{al} = ALF \cdot I_{sr} \cdot \left(R_{ct} + R_b\right) = ALF' \cdot I_{sr} \cdot \left(R_{ct} + R'_b\right)$$

$$ALF' = ALF \frac{R_{ct} + R_b}{R_{ct} + R'_b}$$

with R_b high and ALF low (e.g. 30 VA 5P20).

But, in this calculation, the winding resistance R_{ct} is needed. If this parameter is unknown, several estimations can be used but may be wrong.

This practice is not in line with IEC 61869-2, because it may lead to maladapted, wrongly characterized cores with high rated burden, where the class is not fulfilled for very low operational burdens.

The reason why such a conversion is still very often used is a historical one, and it is not recommended that it be used for new substations with new CT cores.

Both definitions (S_b and ALF, as well as K_{td}, K_{ssc} and R_b) are applicable. R_{ct} is not needed for specification, it will be chosen by the manufacturer.

11.3 Overcurrent protection: ANSI code: (50/51/50N/51N/67/67N); IEC symbol: I>

11.3.1 Exposition

Overcurrent (OC) relays are typically used in radial and industrial systems. In their simplest form, OC relays measure the current and compare it with the threshold (pickup) setting of the relay. The relay operates either instantaneously or after a time delay for all currents above the threshold. Selectivity can be achieved by time or current grading or by a combination of both.

A typical application often used in medium and high voltage grids in Central Europe is given in Figure 57 as an example. The single-line diagram shown at the bottom represents a simple network. The lines connecting 4 substations are each protected with an OC relay. Since this is a radial system, there is only one source in substation A. The operating curves for the appropriate OC relays are displayed at the top. The relay at substation C is set at the shortest possible operating time or time delay. The operating time of the relays is gradually increased from C to A. The interval between the operating times of each relay shall be long enough in order to achieve correct co-ordination. This ensures that the breaker near the fault can trip and clear this fault before the upstream (backup) relays can operate. It is necessary to combine a time delay OC (TOC) with an instantaneous OC (IOC) to avoid long fault clearing times. This is the case if the fault is close to the source. The IOC curves are displayed as dotted lines.

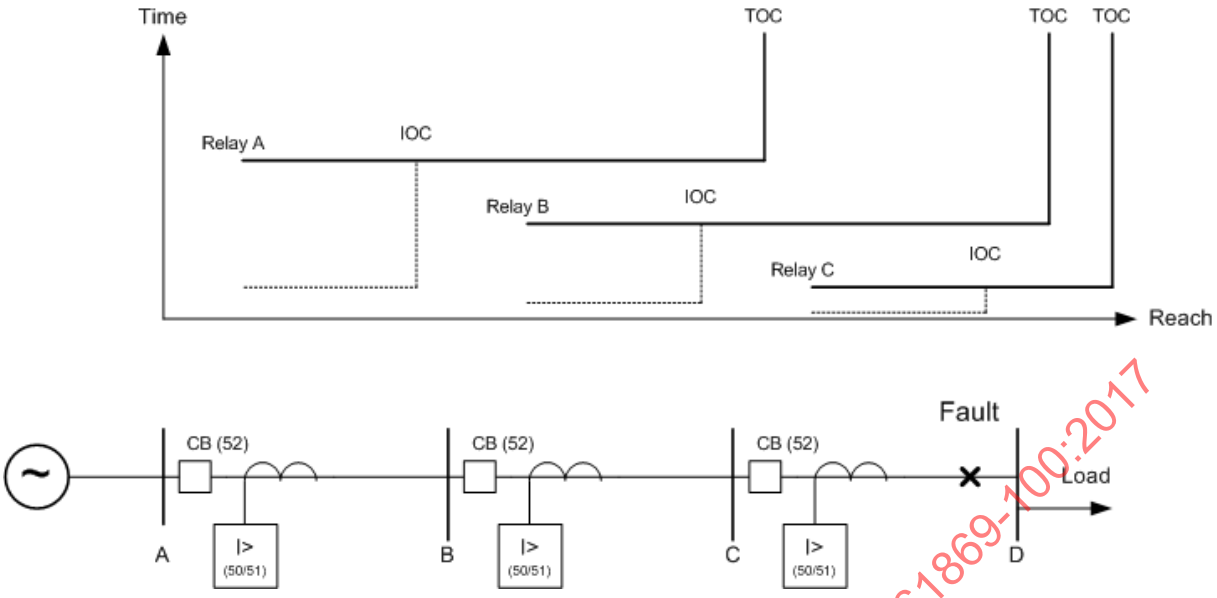

Key

A,B,C,D	substations
IOC	instantaneous overcurrent protection
TOC	time delayed overcurrent protection
CB	circuit breaker
I>	overcurrent protection relay

Figure 57 – Application of instantaneous/time-delay overcurrent relay (ANSI codes 50/51) with definite time characteristic

The (non-dotted) operational curve shown in the above example is defined as the Definite Time Characteristic. Another very common time characteristic is the Inverse Time Characteristic. Both are shown in Figure 58.

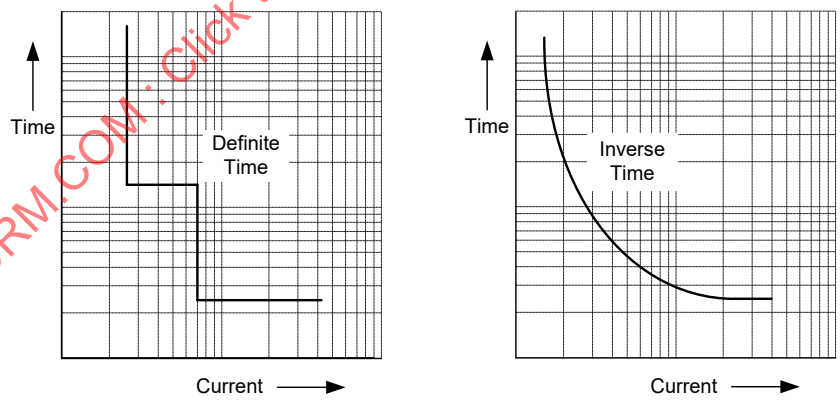

Figure 58 – Time-delay overcurrent relay, time characteristics

The influence of current transformer saturation on OC protection basically depends on the measurement principle used (e.g. r.m.s., peak value, etc.) and the time characteristic chosen. Of course, this influence is also dependent on the relay technology used (electromechanical, static or numerical). In general, CT saturation may cause delayed relay operation. This is easy to see for the inverse curve (see Figure 58). With a high DC component, saturation can temporarily cause secondary currents below the pickup value. If time delay OC or instantaneous OC is used, an extended operation time can be the consequence.

It is well known that CT saturation can cause appreciable errors in both phase and amplitude. The former may lead to wrong directional decisions with the result of unselective tripping in the worst-case.

11.3.2 Recommendation

For overcurrent protection typical ALF or K_{SSC} ≥ 20 can be recommended. This value represents a typical maximum current of an inverse curve, which is often used in time-delayed overcurrent protection. Besides that, ALF or K_{SSC} shall be higher than the maximum prospective and feasible setting used for overcurrent protection (here typically referred to the high current stage protection setting I>>).

11.3.3 Example

500/1 CT; I_{psc} = 40 kA; I>> = 30·I_{pr} = 15 kA; R_b = 3,5 Ω, see Figure 59.

Therefore, a CT with the protection class 5P30 5 VA can be recommended.

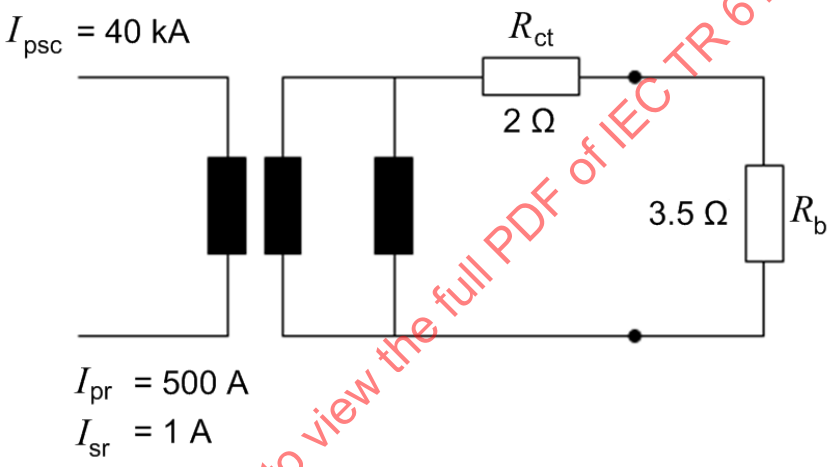

Key

I_{pr}	rated primary current
I_{psc}	rated primary short circuit current
I_{sr}	rated secondary current
R_{ct}	secondary winding resistance
R_b	resistive burden

Figure 59 – CT specification example, time overcurrent

11.4 Distance protection: ANSI codes: 21/21N, IEC code: Z<

11.4.1 Exposition

A distance relay measures voltage and current at the relay location. On the basis of these electrical values, the relay determines the impedance between the relay and the fault location. Since the impedance per kilometre of a transmission line is nearly constant, the measured impedance is proportional to the distance to the fault. The relay compares the apparent impedance determined with the reach point impedance which was defined by the customer. If the determined impedance is less than the reach point impedance, an internal fault is detected and a trip command is issued to the breaker either instantaneously or after a predefined time delay. Due to errors in current and voltage transformers, inaccuracies in line impedance data and errors in relay settings and measurement, Zone 1 shall not cover the entire line. Otherwise, there is a risk of overreaching the protected line, which can by no means be accepted. Therefore, a second, time-delayed Zone 2 is needed to protect the line

between the end of Zone 1 and the remote bus. A third zone can be used for remote backup protection.

Figure 60 illustrates the above-mentioned principle. The simple radial network already used in 11.2.2 is shown. The equipment is protected using distance protection, i.e. a protection system that calculates the impedance (Z) of the faulted loops using the measurement of voltage and current transformers. With this kind of protection, selectivity will be achieved using time-distance grading. This grading can be displayed in a time-distance diagram, as shown at the top. The principle of time-distance grading can be explained by using a fault scenario. For the fault shown on the line between C and D, relay R_C and R_B and possibly R_A would detect the fault. Relay R_C determines that the fault is in its Zone 1 and would instantaneously issue a trip command to its associated circuit breaker. Relay R_B would "see" that the fault is in its time delayed Zone 3. Therefore the fault will be cleared by the distance relay and the breaker in C. The backup relay R_B will be reset before it can trip its breaker.

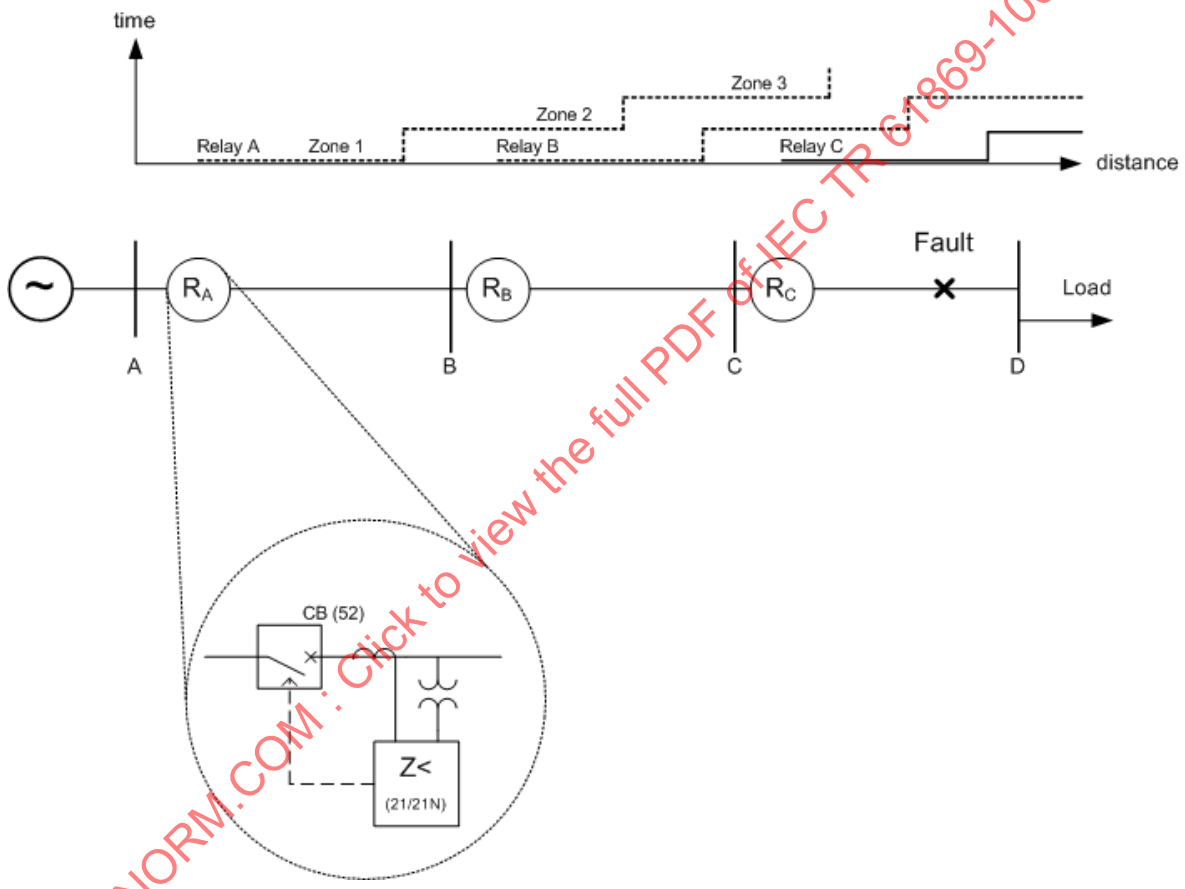

Key

A,B,C,D	substations
CB	circuit breaker
Z<	distance protection relay

Figure 60 – Distance protection, principle (time distance diagram)

It is common practice to use a R/X diagram to visualize the coverage of a distance protection relay. Considering the system above, Figure 61 shows the zones of operation (steps) for the distance relay R_A.

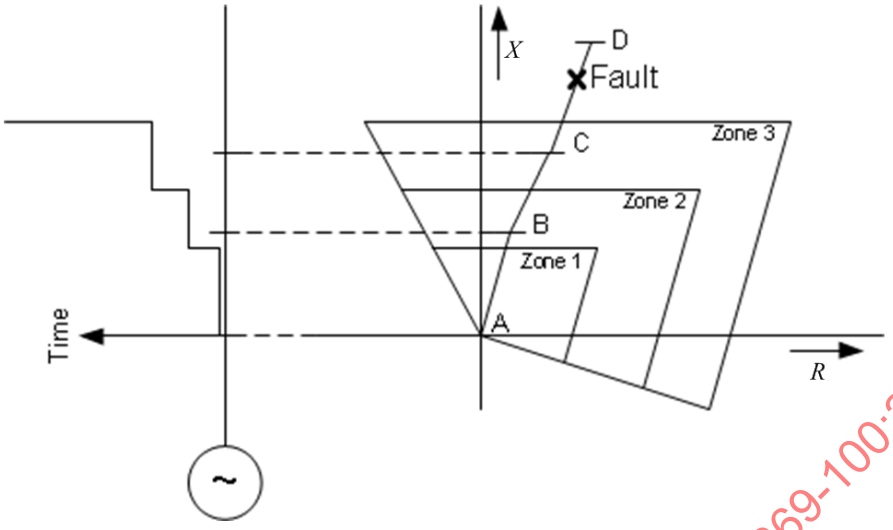

Key

A,B,C,D	substations
R	line resistance
X	line reactance

Figure 61 – Distance protection, principle (R/X diagram)

Depending on the technology, manufacturer and application, the influence of current transformer saturation on distance protection is very complex. Generally the operating characteristic used is an important point; on the other hand, it is a question of the measuring principle implemented, which may depend on the relay technology used. For example, electromechanical relays tend by nature to a reduction of range as the current measured is too low in the case of CT saturation. Solid-state relays behave similarly to electromechanical relays if circle characteristics are applied. The impact on computerized relays is manifold and depends mainly on the impedance measuring algorithm implemented [7],[8]. Without going into details, there is a certain risk of both failure to operate and unwanted operation in cases of severe CT saturation.

Modern relays are equipped with functions that can compensate CT saturation. This may minimise the risk of relay malfunctions.

11.4.2 Recommendations

The protection relay manufacturer defines and provides the CT designing requirements which depend on significant worst-case fault scenarios in the network (fault positions relative to the protected line/set zone boundaries). These requirements may be critical for the relay stability due to CT saturation. (If the voltage transformer is a capacitive type (CVT), an additional special consideration has to be made). Such considerations are proposed in IEC 60255-121 [4], where, for instance, four significant fault scenarios are presented in a very detailed manner and several examples are given. This approach is very interesting, especially from the distance protection point of view. In the following example, only two fault positions are shown and only three-phase faults are considered. This basic example can be easily extended to the more detailed consideration in IEC 60255-121 [4].

11.4.3 Examples

11.4.3.1 Designing example 1

11.4.3.1.1 General

Figure 62 shows a CT designing example for distance protection. It shall be kept in mind that this example shows how to proceed if the time to accuracy limit t'_{al} is used as first assumption

from the protection relay algorithm and as the first input parameter of the whole consideration in order to continue with protection relay tests in a second step. It shows the way rather for authors of relay manuals (who define the CT requirements in general and normalized form) than for project engineers (who apply the general CT requirements from the protection relay manual and specify the CT parameters for a concrete project). The reader/protection engineer shall use the simplified method and results as given by the relay manufacturer in the corresponding manuals (e.g. transient dimensioning factor K_{td}, rated symmetrical short circuit current factor K_{ssc}, recommendations how to handle with remanence, etc.).

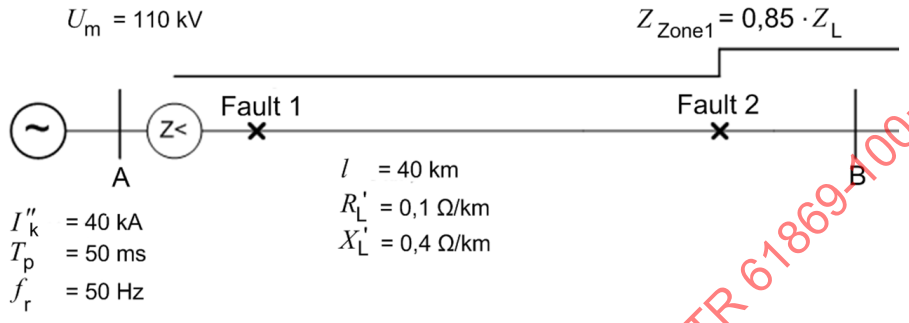

Key

A,B	substations
U_m	highest voltage for equipment
I''_k	Initial symmetrical short circuit current
T_p	primary time constant
f_r	rated frequency
Z_{Zone1}	impedance of zone 1
Z_L	line impedance
l	length of line
R'_L	resistance per length unit
X'_L	inductance per length unit
Z<	distance protection relay

Figure 62 – CT Designing example, distance protection

11.4.3.1.2 Fault 1 (close-in fault)

a) Data from network:

I''_k = 40 kA (initial symmetrical short-circuit current)

f_r = 50 Hz

T_P = 50 ms (primary time constant of source impedance, active at the fault location 1)

b) CT data:

I_{pr} = 500 A (chosen according to the rated current of the protected line)

I_{psc} = I''_k = 40 kA

I_{sr} = 1 A

K_{ssc} = 80 = I_{psc} / I_{pr} = 40 kA / 500 A (symmetrical short circuit current factor)

T_s = 500 ms (class TPY against remanence, assumed value)

t'_{al} = 15 ms (assumed by relay manufacturer for fault location 1)

This is between time range 1 and 2, at the beginning of time range 2 (see also Figure 22).

The start of time range 3 is at $t_{tfp,max}$ = 127,7 ms (from Equation (15)).

For this t'_{al} the worst-case fault inception angle γ, from Equation (23) that leads to the maximum flux and earliest saturation, is

γ = 100° (value from the physical point of view) which is calculated from θ (value used in mathematical formula) with φ = arctan(ωT_p) = arctan(2π × 50 Hz × 0,05 s) = 86,4°.

$\gamma = \theta + \varphi$ = 13,6° + 86,4° = 100°

These values lead to the transient factor K_{tfp}.

K_{tfp} = 5,1 from Equation (12) which could be used either directly as K_{td} = 5,1 for relay tests. Some test results from the relay manufacturer could provide some higher values with safety margins for instance K_{td} = 6 or higher.

In this example, K_{td} = 6 is used and published as CT requirement in the relay manual for further application in the project engineering.

Faster estimation:

As the required t'_{al} = 15 ms is not in time range 1, but very close to it in time range 2, the calculated K_{tf} can also be estimated from Figure 18 or Figure 20 by visual extrapolation.

NOTE The values given above for t'_{al} = 15 ms and 20 ms are on the safe side for a wide range of currents being measured in the relay. For very high short circuit currents, modern protection devices with numerical processors may trip immediately after consideration of only 2 samples when the fault location on the line is very sure and clear. This approach ensures a fast trip and less damage to the equipment.

11.4.3.1.3 Fault 2 (Zone 1 fault)

Data of protected line and protection requirements:

R'_L	= 0,1 Ω/km	(Resistance per length unit)
X'_L	= 0,4 Ω/km	(Inductive reactance per length unit)
l_L	= 40 km	(length)
U_n	= 110 kV	(nominal system voltage)
Z_{zone1}	= 0,85 × Z_L	(K_{lim} = 0,85; protection setting factor)
t'_{al}	= 20 ms	(assumed by relay manufacturer for fault location 2)
c	= 1,1	(security factor for short circuit analysis as per standard IEC 60909-0:2001 [14].

Using the source impedance and the line impedance up to the zone 1 setting, the short circuit current and its DC time constant $T_{p,lim}$ are calculated.

Source impedance:

$$Z_S = \frac{c \cdot U_n}{\sqrt{3} \cdot I''_k} = \frac{1{,}1 \cdot 110\ \text{kV}}{\sqrt{3} \cdot 40\ \text{kA}} = 1{,}746\,\Omega$$

Source resistance:

$$R_S = \frac{Z_S}{\sqrt{1 + (2\pi f_r T_p)^2}} = 0{,}111\ \Omega$$

Source reactance:

$$X_S = \sqrt{Z_S^2 - R_S^2} = 1{,}743\ \Omega$$

Line resistance: $R_L = K_{lim} \cdot l_L \cdot R'_L = 0{,}85 \cdot 40\ \text{km} \cdot 0{,}1\ \Omega/\text{km} = 3{,}4\ \Omega$

Line reactance: $X_L = K_{lim} \cdot l_L \cdot R'_L = 0{,}85 \cdot 40\ \text{km} \cdot 0{,}4\ \Omega/\text{km} = 13{,}6\ \Omega$

Short circuit resistance: $R_{sc} = R_S + R_L = 3{,}511\ \Omega$

Short circuit reactance: $X_{sc} = X_S + X_L = 15{,}343\ \Omega$

Short circuit impedance: $Z_{sc} = \sqrt{R_{sc}^2 + X_{sc}^2} = 15{,}74\ \Omega$

Zone 1 short circuit current: $I_{sc,lim} = \frac{cU_n}{\sqrt{3} \cdot Z_{sc}} = \frac{1{,}1 \cdot 110\ \text{kV}}{\sqrt{3} \cdot 15{,}74\ \Omega} = 4{,}438\ \text{kA}$

Zone 1 primary time constant: $T_{p,lim} = \frac{1}{2\pi f_n} \frac{X_{sc}}{R_{sc}} = 13{,}91\ \text{ms}$

With a short circuit current of $I_{sc,lim} = I_{psc} = 4{,}5$ kA, the symmetrical short circuit current factor is

$$K_{ssc} = I_{psc} / I_{pr} = 4{,}5\text{kA} / 500\,\text{A} = 9$$

With the DC time constant $T_P = 14$ ms (impedance at the fault location source impedance plus line impedance), we find the transient dimensioning factor.

For $t'_{al} = 20$ ms, the worst-case fault inception angle is $\gamma = 93{,}6°$,

which is calculated using

$\varphi = \arctan(\omega T_P) = \arctan(2\pi \cdot 50\text{Hz} \cdot 0{,}014\ \text{s}) = 77{,}2°$

$\gamma = \theta + \varphi = 16{,}4° + 77{,}2° = 93{,}6°$

These data lead to

$K_{tfp} = 4{,}4$

where we may choose $K_{td} = 5$ or some higher value with safety margin as result from relay tests. This result is published as CT requirement in the relay manual for further application in the project engineering.

11.4.3.1.4 Required current transformer

I_{pr} = 500 A

I_{sr} = 1 A

class TPY

T_s = 500 ms (see assumed CT data above)

The values K_{ssc} and K_{td} are both higher for fault location 1, so fault case 1 is decisive:

K_{ssc} = 80

K_{td} = 6 (from above as published CT requirement in the relay manual)

The burden connected via the secondary cable (copper, length, cross section, two conductors)

$$R_b \text{ (CT secondary cable)} = 2\rho_{Cu}(75\,°C)\frac{l_{wire}}{A_{wire}} = 2 \cdot 0{,}02171\frac{\Omega\,mm^2}{m}\frac{200\,m}{4\,mm^2} = 2{,}171\,\Omega$$

and the relay burden of 0,1 VA, (0,1 Ω at I_{sr} = 1 A)

The rated burden is chosen as

R_b = 2,5 Ω.

11.4.3.2 Designing example 2 (TPY, C-O-C-O)

The CT for the protection relay in the preceding example 1 is now dimensioned for auto-reclosure (AR) duty cycle C-O-C-O. The impedance calculation and short-circuit currents are the same as above, also for the second fault, when the AR is not successful.

The required times to accuracy limit for the relay are the same.

Fault location 1:
t'_{al} = 15 ms (assumed by relay manufacturer for calculation of K_{tf} and relay tests)

Fault location 2:
t'_{al} = 20 ms (ditto)

For the chosen CT class TPY with T_s = 500 ms, only the transient dimensioning factor needs to be calculated in addition to the preceding example 1.

The AR duty cycle C-O-C-O can be assumed for calculation of K_{tf} and relay tests as follows:

t'_1 = 55 ms, which contains t'_{al} = 15 ms and delay time of circuit breaker.

t'_{fr} = 400 ms (auto re-closer dead time).

t''_{al} = 15 ms.

The primary current is shown in Figure 63.

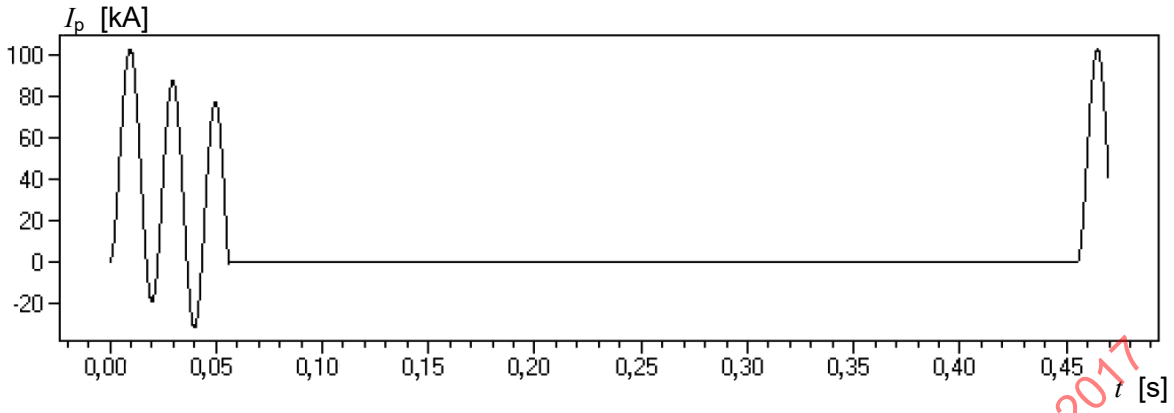

Key

t	time
I_p	primary current

Figure 63 – Primary current with C-O-C-O duty cycle

In the following, the K_{tf} value is determined.

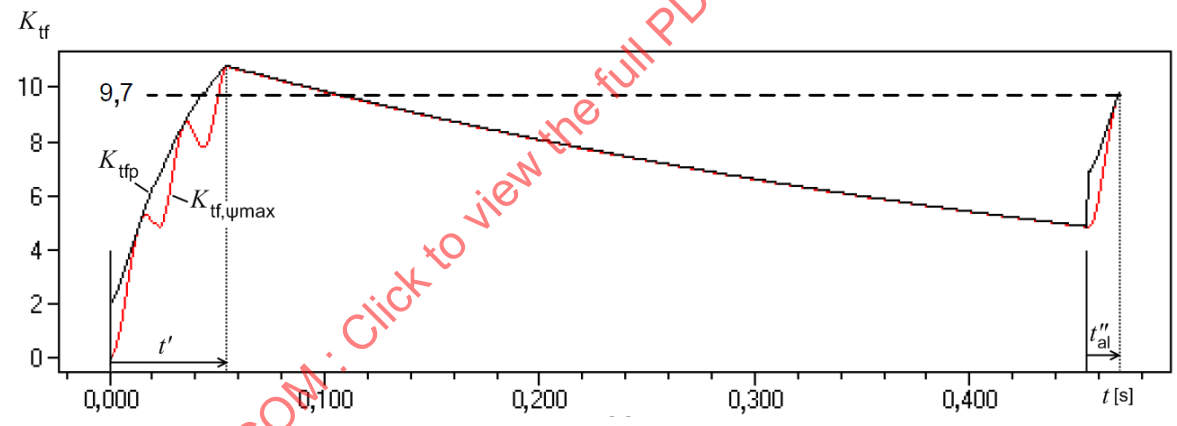

Key

K_{tf}	transient factor
K_{tfp}	envelope of the curve $K_{tf,\psi max}(t)$
$K_{tf,\psi max}$	overall transient factor
t	time
t'	duration of the first fault
t''_{al}	specified time to accuracy limit in the second fault

Figure 64 – Transient factor K_{tf} with its envelope curve K_{tfp}

In Figure 64, the maximum transient factor K_{tf} at the end of the first fault is 10,7.

At the end of the second fault, K_{tf} is 9,7 (This results directly from Equation (26)).

If the CT is dimensioned to the lower value of 9,7, it will saturate during the first fault.

As the required time to accuracy limit t'_{al} = 15 ms is shorter than t' = 55 ms, saturation during the first fault is allowed. Therefore the transient factor can be reduced down to the saturated

value K_{tf} = 9, since saturation does not occur during the second fault until t''_{al} = 15 ms (see Figure 65 and Figure 41). In this case, the required K_{tf} is identical in both faults.

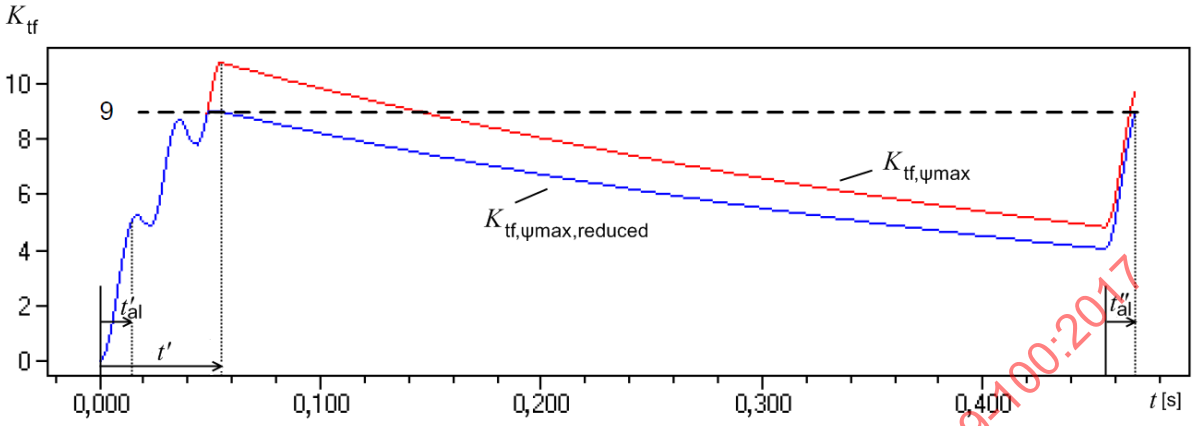

Key

K_{tf}	transient factor
$K_{tf,\psi max}$	overall transient factor
$K_{tf,\psi max,reduced}$	overall transient factor, considering allowed saturation during the first fault
t	time
t'	duration of the first fault
t'_{al}	specified time to accuracy limit in the first fault
t''_{al}	specified time to accuracy limit in the second fault

Figure 65 – Transient factor K_{tf} for CT class TPY with saturation in the first fault

If the transient factor is too high due to slow flux decay during the AR fault repetition time, CT class TPZ can be used with T_s = 61 ms (Figure 66). The K_{tf} is 7,4 at the end of the first fault and 4,7 at the end of the second fault. It can therefore be reduced to K_{tf} = 4,7, allowing saturation during the first fault.

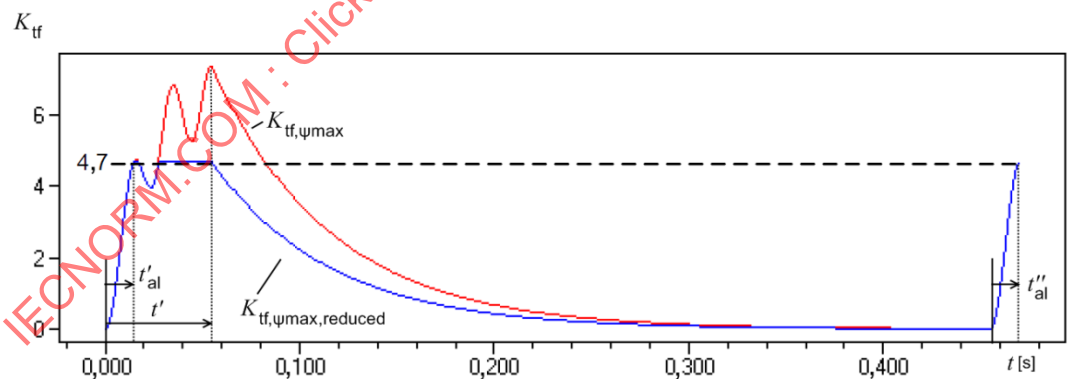

Key

K_{tf}	transient factor
$K_{tf,\psi max}$	overall transient factor
$K_{tf,\psi max,reduced}$	overall transient factor, considering allowed saturation during the first fault
t	time
t'	duration of the first fault
t'_{al}	specified time to accuracy limit in the first fault
t''_{al}	specified time to accuracy limit in the second fault

Figure 66 – Transient factor K_{tf} for CT class TPZ with saturation in the first fault

If CT class TPX with T_s = 10 s is used, the transient factor is much higher, because it does not have a considerable flux decay during the fault repetition time due to remanence, so Equation (25) is applied and no reduction is possible (Figure 67). The required transient factor K_{tf} at the end of the second fault is K_{tf} = 16,5.

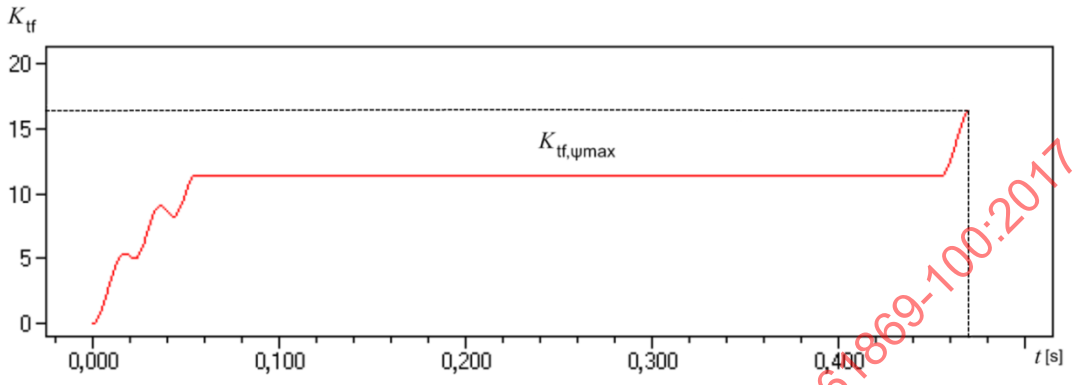

Key

K_{tf}	transient factor
$K_{tf,\psi max}$	overall transient factor
t	time

Figure 67 – Transient factor K_{tf} for CT class TPX

A possible remanence (magnetized TPX core) at the beginning of the first fault is not considered here and could lead to much earlier saturation. For such cases, gapped cores are recommended, especially for new projects, and not only for auto-reclosure.

NOTE However, for existing plants, non-gapped cores can be utilized if tests show their suitability.

11.4.3.3 Summary

With these calculated values of the transient factor K_{tf}, a good theoretical basis is found for verifying tests with protection relays, which may lead to a higher safety margin or even to lower values of the transient dimensioning factor K_{td} (if saturation is uncritical).

It is not of much use to indicate only a single duty cycle C – O in the specification, it is better to cover mixed cases with one or a few global factors of K_{td}. The transient dimensioning factor K_{td} can also be a discrete set of such factors or a smooth curve for several significant worst cases in the network and for different CT classes with additional recommendations. Such data are published in the relay manual. During project engineering these simpler CT requirements are applied for concrete networks and scenarios.

11.5 Differential protection

11.5.1 Exposition

According to the Kirchhoff law, differential protection compares all inflowing and outflowing currents in the protected zone. Under normal or through-fault conditions, the vector sum of all currents entering should be ideally zero. In practice, certain phenomena cause a substantial (false) differential current so the sum is not near zero in healthy conditions. In the case of an internal fault, the current sum is almost equal to the short circuit current at the fault point. In this case, a differential relay uses the apparent differential current as a definite indication of an internal fault. Figure 68 illustrates this principle. The arrows show the current direction.

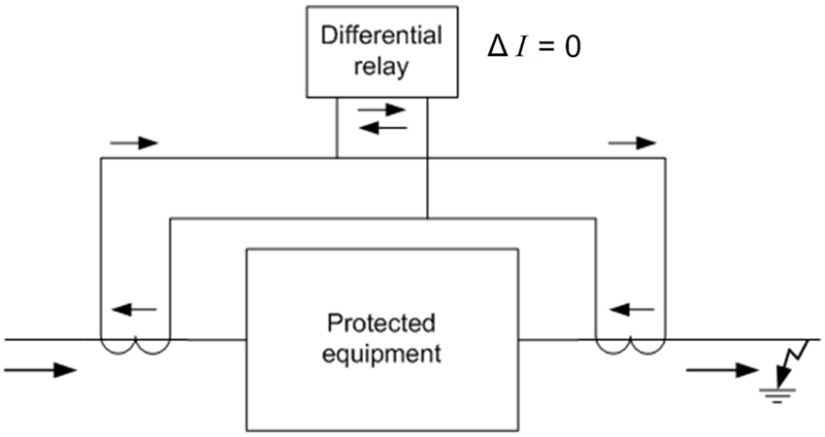

a) Normal or through-fault condition (external fault)

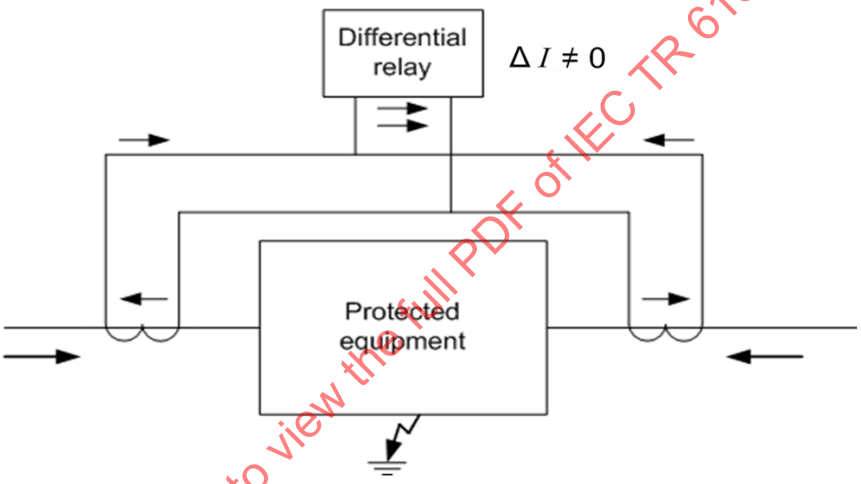

b) Internal fault

Key

ΔI difference between the secondary currents of the two current transformers

Figure 68 – Differential protection, principle

The behaviour of the current transformers plays a major role in differential protection. Normally, internal faults should be recognized by all kind of differential relays. The main issue here is rather to remain stable in the case of external faults with high through-fault currents.

11.5.2 General recommendations

- Both internal and external faults have to be considered.
- Typically, the external fault is the most critical fault for this kind of protection.

11.5.3 Transformer differential protection (87T)

11.5.3.1 Exposition

The basic principle of differential protection has already been described above. It is well known that CT saturation can cause significantly incorrect differential currents in the case of faults. In this application, both internal and external faults have to be considered. As described above, stability against unwanted operation of the protection shall be ensured for all kinds of external faults, in particular for long fault-clearing times.

Of course, internal CT faults can also cause saturation in the worst-case. The most critical situation (Figure 69) is a fault on the high-voltage side between the CT and the transformer. For low source impedances, short circuit currents can be very high. On the other hand, the rated primary current I_{pr} of the CT is relatively low, as its value has to be adapted to the nominal current of the transformer.

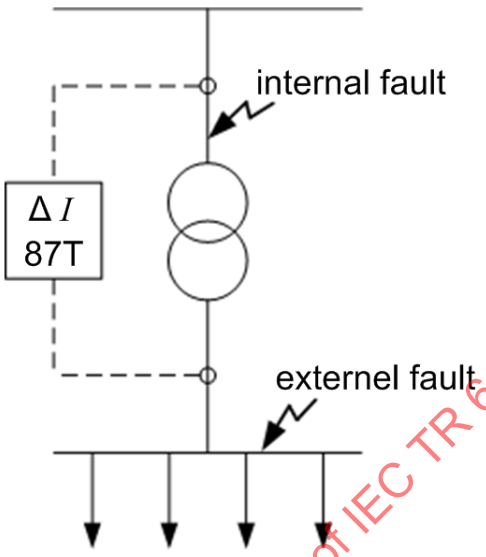

Key

ΔI differential protection relay

Figure 69 – Transformer differential protection, faults

Numerical relays provide specific algorithms which detect saturation and thus help prevent maloperation. Many modern relays need a time to accuracy limit (t'_{al}) equal to or less than a quarter cycle (5 ms at 50 Hz system frequency).

11.5.3.2 Recommendations

- Correct designing of CT cores considering all aspects of fault occurrencies;
- CT ratios have to be adapted to the nominal current of the power transformer;
- Anti-remanence CT type/class: 5PR, TPY, TPZ , PXR (possibly with K_x definition).

11.5.3.3 Example

11.5.3.3.1 General

Figure 70 shows the circuit diagram of a transformer with differential protection between the phase CTs on both voltage sides (87T), and restricted earth fault protection (87N) connected to the phase CTs and neutral CT on the LV side. Protection (87N) is applied in order to compensate the sensitivity loss of (87T) due to vector group adoption where faults very close to the star-point can be detected with higher sensitivity.

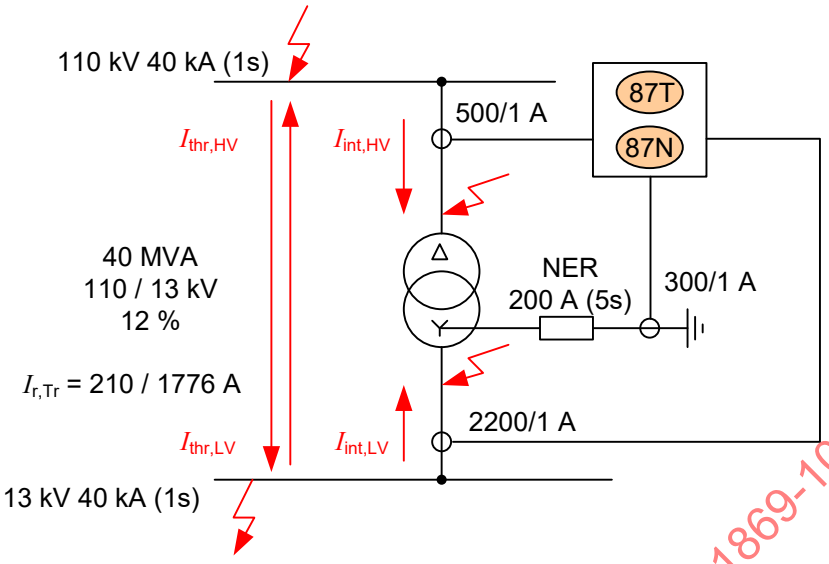

Key

$I_{r,Tr}$	rated transformer current
$I_{thr,LV}$	maximum through fault current on low voltage (LV) side for external faults
$I_{thr,HV}$	maximum through fault current (through the transformer, limited by transformer impedance u_k) on high voltage (HV) side, for external faults on high or low voltage side (maximum current of both cases)
$I_{int,HV}$	maximum internal fault current on high voltage (HV) side, fed by infeeds and feeders on HV side
$I_{int,LV}$	maximum internal fault current on low voltage (LV) side, fed by infeeds and feeders on LV side
NER	neutral earthing resistor

Figure 70 – Transformer differential protection

11.5.3.3.2 Relay CT requirements

Operating current range of the relay:	80 A
K_{td} for internal faults:	$K_{td,int}$ ≥ 0,5 (given in the relay manual)
K_{td} for external faults:	$K_{td,thr}$ ≥ 3 (given in the relay manual)
Max. mismatch factor:	$1/7 \leq I_{pr,CT} / I_{r,Tr,} \leq 7$, where $I_{pr,CT}$ is the rated primary current of the appropriate CT.

11.5.3.3.3 CT primary currents

The rated primary currents of the phase CTs on the HV and LV sides of the transformer are chosen to be at least 120 % of the rated transformer currents of 210 A and 1 776 A respectively because transformer overload currents can occur. If not otherwise specified, CTs cannot be overloaded.

The relay current inputs can be overloaded by up to 80 A (1s) when short circuit currents occur on the CT primary side. If the CT primary current on the transformer HV side is only 120 % × 210 A = 252 A, the maximum short circuit current on the CT secondary side will be 40 kA/252 = 159 A, what is too high. So the minimum CT ratio is $k_{r,min}$ = 40 kA/80 A = 500. Therefore these CTs are chosen as 500/1 A.

On the transformer low voltage side, this problem is not relevant, because the CT primary current is 120 % × 1 776 A = 2131 A; so we choose 2 200 A.

Earth fault currents on the transformer LV side are limited to 200 A by a neutral earthing resistor (NER). Here, the neutral CT 200/1 A could be an option. As required by the relay, the maximum mismatch factor of the CT primary rated current to the transformer rated current is 7 or 1/7.

$I_{pr,min}$ > 1 776 A / 7 = 254 A, therefore 300/1 A is chosen.

The maximum mismatch factor for the phase CTs is not exceeded.

11.5.3.3.4 CT overcurrents at internal faults

Internal faults (faults within the selective zone) shall be tripped correctly and fast, therefore the transient dimensioning factor $K_{td,int}$ should be higher than 0,5 as shown in relay tests and given in the relay manual.

The symmetrical short circuit current factor K_{ssc} should be higher than I_{psc} / I_{pr} (requirement given in the relay manual) for HV and LV side.

K_{ssc} for internal fault on HV side: $K_{ssc,int}$ >= 40 kA/500 A = 80

K_{ssc} for internal fault on LV side: $K_{ssc,int}$ >= 40 kA/2 200 A = 18,2

11.5.3.3.5 External faults

External faults outside the selective zone shall not be tripped at least until the fault is cleared by other protection relays. The required transient dimensioning factor K_{td} should be greater than 3, as defined by relay tests and given in the relay manual. In general, differential protection relays are more unstable on external faults than on internal faults.

The maximum through-fault current flowing through the transformer during an external fault $I_{sc,thr}$ is limited by its short circuit impedance u_{sc} of 12 %. This is on the safe side as the internal impedance of the network source is neglected.

$$I_{sc,thr} = I_{r,Tr} / u_{sc}$$

Through-fault current on HV side: $I_{sc,thr}$ = 210 A / 12 % = 1 750 A

K_{ssc} for external fault on HV side: $K_{ssc,thr}$ >= $I_{sc,thr}$ / $I_{pr,CT}$ = 1 750 A / 500 A = 3,5

Through-fault current on LV side: $I_{sc,thr}$ = 1 776 A / 12 % = 14,8 kA

K_{ssc} for external fault on LV side: $K_{ssc,thr}$ >= $I_{sc,thr}$ / $I_{pr,CT}$ = 14,8 kA / 2 200 A = 6,8

It is clear that the lower through-currents need a higher K_{td} factor. On the other hand, higher internal fault currents need a lower K_{td}.

The results are summarized in (Table 13):

Table 13 – Calculation results of the overdimensioning of a TPY core

	Internal fault		External fault
HV	K_{ssc} = 80 K_{td} = 0,5 $K_{td} \times K_{ssc}$= 40 *	↔	K_{ssc} = 3,5 K_{td} = 3 $K_{td} \times K_{ssc}$= 10,5
LV	K_{ssc} = 18,2 K_{td} = 0,5 $K_{td} \times K_{ssc}$= 9,1	↔	K_{ssc} = 6,8 K_{td} = 3 $K_{td} \times K_{ssc}$= 20,4 *
The relevant scenarios (fault scenarios in the network) for CT core sizing on the HV and LV side are marked with an asterisk.			

To comply with the requirements of internal and external faults as well, it is impossible to find a common solution without overdimensioning the CTs.

If on both HV and LV side, the highest values of K_{ssc} and K_{td} are combined, the following overdimensioning is obtained:

HV side: $K_{ssc} \times K_{td}$ = 80 × 3 = 240

LV side: $K_{ssc} \times K_{td}$ = 18,2 × 3 = 54,6

This approach may lead to huge unfeasible CT cores.

The solution is to multiply $K_{td} \times K_{ssc}$ for HV and LV scenarios separately and take the maximum result among these products. In Table 13, the relevant scenarios (fault scenarios in the network) for CT core sizing on the HV and LV side are marked with an asterisk.

HV side: K_{ssc} = 80, K_{td} = 0,5

LV side: K_{ssc} = 6,8 K_{td} = 3

It shall be considered that actually for classes TPY or TPZ, the K_{ssc} and K_{td} values can be chosen arbitrarily.

In some applications, the class PX is used for low impedance differential applications. In the following, the dimensioning of class PX CTs is described.

Firstly, the factor K_x for class PX is calculated in Table 14, considering the factor F taken exemplarily as 1,25 (see Table 7):

Table 14 – Calculation results of overdimensioning as PX core

	Internal fault $K_{x,int} = K_{td,int} \times K_{ssc,int} / F$	External fault $K_{x,ext} = K_{td,ext} \times K_{ssc,ext} / F$
HV side: K_x = max($K_{x,int}$; $K_{x,thr}$) = max(32;8,5) = 32	= 0,5 × 80 / 1,25 = 32	= 3 × 3,5 / 1,25 = 8,5
LV side: K_x = max(7,28; 16,32) = 16,32 choose 17	= 0,5 × 18,2 / 1,25 = 7,28	= 3 × 6,8 / 1,25 = 16,32

The winding resistances of the CT are assumed to be:

HV side: R_{ct} = 2 Ω

LV side: R_{ct} = 8,8 Ω

If the total connected burden is 2,1 Ω (for example), the overcurrent factor K_x and the burden of the CT can be specified as follows:

HV side: 500/1A class PXR, R_b = 2,5 Ω, K_x = 32

LV side: 2 200/1A class PXR, R_b = 2,5 Ω, K_x = 17

The knee point voltage and the winding resistance are assumed in this example to be:

HV side: R_{ct} = 2 Ω; $E_k \geq K_x \times I_{sr} \times (R_{ct} + R_b)$ = 32 × 1A × (2 + 2,5) Ω = 144 V

LV side: R_{ct} = 8,8 Ω; $E_k \geq K_x \times I_{sr} \times (R_{ct} + R_b)$ = 17 × 1A × (8,8 + 2,5) Ω = 192,1 V

As remanence leads to earlier saturation which can be critical for differential protection relays in general, an anti-remanence class is recommended, e.g. PXR, 5PR, TPY. If DC components are expected to be high, class TPZ is recommended.

If a 5PR class is chosen, the ALF value is calculated as K_x × 1,25, and the nominal burden is 2,5 VA.

11.5.4 Busbar protection: Ansi codes (87B)

11.5.4.1 Exposition

In the majority of cases, this application has to cope with extreme saturation. On the one hand, short circuit currents are typically high. On the other hand, ratio and type of CT can differ significantly. The example shown below shall not be understood as recommendation for the design of protection scheme. It shall only highlight the possible and exemplary difficulties, and show how they could be handled. One of the most critical cases for busbar protection is shown in Figure 71. In this example, the high short circuit current (I''_{sc}) unfortunately occurs in the feeder with the current transformer having the lowest ratio (low primary rated current I_{pr}). Nevertheless, the busbar protection shall remain stable for such external faults.

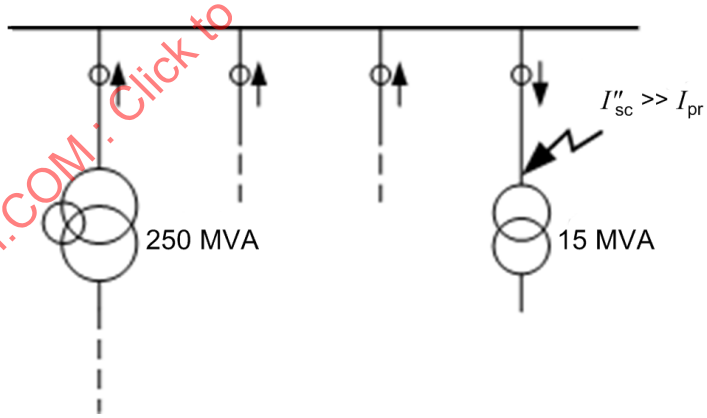

Key

I_{pr} rated primary current

I''_{sc} rated primary current

Figure 71 – Busbar protection, external fault

With modern busbar protection, time to accuracy limits (t'_{al}) less than 4 ms are normally sufficient to decide whether an internal or external fault is present. In the case of an internal fault, fast tripping will be executed. Several methods and algorithms (e.g. saturation detection) ensure stable operation in the case of external faults with high through-fault currents and extreme CT saturation.

Short time to accuracy limits (e.g. t'_{al} = 4 ms) lead to low transient factors below 1 and to relatively low CT requirements.

11.5.4.2 Recommendations

For CT designing:

- Consider internal and external faults
- CT type 5PR is recommended

NOTE However, for existing plants, non-gapped cores can be utilized if tests show their suitability.

Most of modern numerical busbar protection devices are able to handle different CT ratios, because each ratio is a flexible parameter which scales the measured CT secondary current to a particular busbar object current. Therefore, each CT ratio (and primary rated current) can be adapted to the rated current of its feeder. Current limitations, e.g. of the measurement range, may influence the maximum secondary current, i.e. the minimum current ratio. This is one of the main differences compared with the high-impedance principle of differential protection, which is described later.

11.5.4.3 Example

One feeder of a 110 kV substation is a 12 MVA transformer with a rated current of I_{Tr} = 63 A, therefore a CT ratio of 100/1 is chosen. The applied burden shall be the rated burden.

The rated short circuit current of the busbar I''_k = 40 kA; so the maximum possible CT secondary current without saturation is

$$I_s = \frac{I_{psc}}{k_r} = \frac{40\,\text{kA}}{100/1} = 400\,\text{A}$$

The operating range of current $I_{s,max}$ of the protection device is, however, limited to 80 A. Therefore, the CT ratio is calculated using

$$k_r = \frac{I_{psc}}{I_{s,max}} = \frac{40\,\text{kA}}{80\,\text{A}} = 500/1\text{A}$$

The protection device may operate with a real-time algorithm where every feeder current $i(t)$ at each time step is processed for the stabilizing and differential quantity. The required time to accuracy limit t''_{al} may be typically 3 ms (assumed value during relay development). This value is in time range 1 in the calculation process for the instantaneous dimensioning factor K_{tf} (see Figure 14).

A recommended anti-remanence class, such as TPY or 5PR, is chosen.

From Equations (9),(20) , (22) (or directly from c)), for a high secondary time constant T_s, and for t''_{al} = 3 ms as well as for a wide range of T_p = 5 ms to 250 ms, the transient factor K_{tf} is 0,43 or, rounded, 0,5.

Protection relay tests with this K_{tf} value and saturated CT currents may confirm the choice and lead directly to the same transient dimensioning factor K_{td} = 0,5 which is then published in relay manual as CT requirement and which shall be used in project engineering.

This result can also be obtained by different input parameters and assumptions regarding the considered worst case conditions.

The maximum current to be considered for protection stability is the maximum short circuit current of the busbar. This current is the internal and external fault current for the selectivity zones of the differential protection.

With K_{td} = 0,5, Equation (3) shows that the steady-state short circuit current (index $_{stst}$) is transformed by the CT only at half of the r.m.s. value due to saturation:

For TPY: $K_{ssc,stst} = K_{td}K_{ssc} = 0{,}5 \cdot K_{ssc}$

For 5PR: $ALF = K_{td}K_{ssc} = 0{,}5 \cdot K_{ssc}$

For the real-time algorithm, it is sufficient to measure only the highest peak of the primary current.

The simulation (Figure 72) of an example with

CT 500/1A, I_{psc}= 40 kA,I T_p = 70 ms, $\gamma_{\psi max}$ = 162°, K_{ssc}= 80

shows

- the first saturation after t'_{al} = 3,2 ms;
- saturation at the peaks after every half cycle during steady state operation.

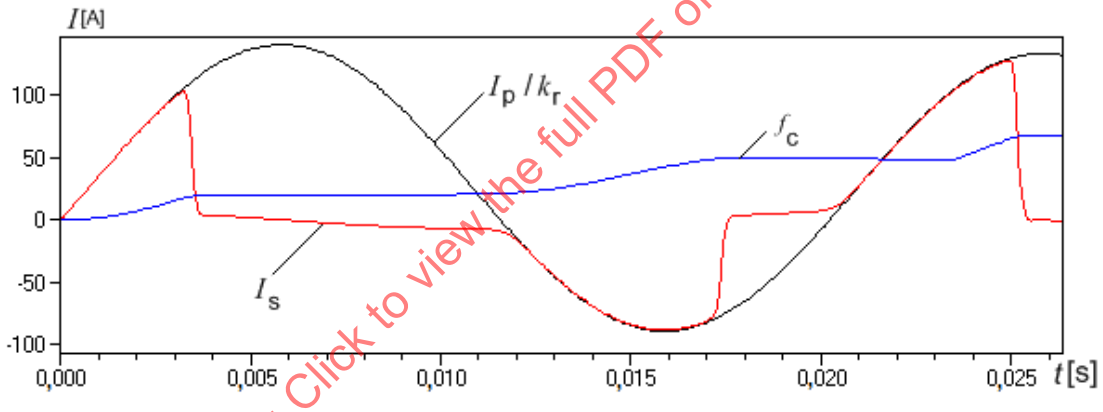

a) Time range 0 ms to 27 ms

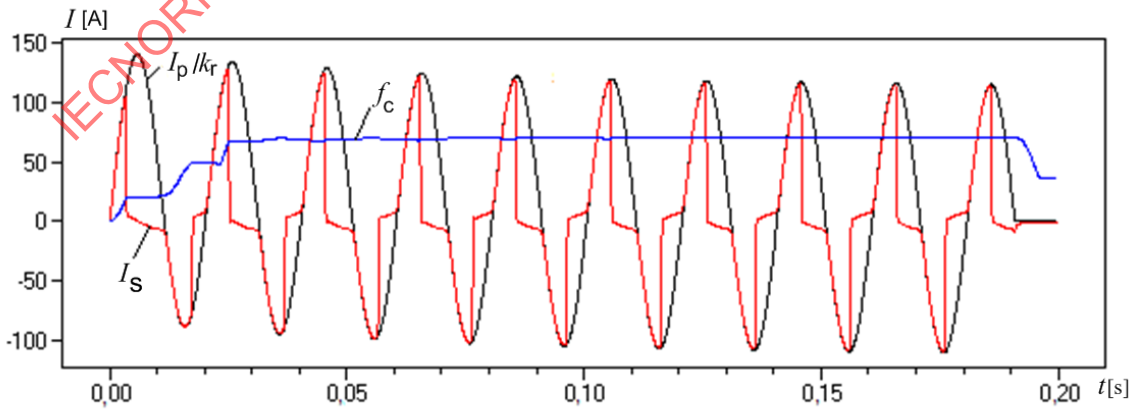

b) Time range 0 ms to 200 ms

Key

f_c moving average of the fundamental component of I_s considering the last cycle

I current

I_p primary current

I_s secondary current

k_r rated transformation ratio

t time

Figure 72 – Simulated currents of a current transformer for bus bar differential protection

11.5.5 Line differential protection: ANSI codes (87L) (Low impedance)

11.5.5.1 Exposition

This application basically can be classified into two categories:

- current differential protection,
- phase comparison protection.

The basic principle of current differential protection has already been described in 11.5.1.

Line differential relays using the phase comparison principle compare the phase angle between the currents at both ends of a line. In healthy or through-fault conditions, the primary currents are theoretically in phase. In the case of an internal fault, the two currents are in phase opposition (antiphase). Under healthy conditions, charging currents also lead to a phase shift in the currents. Furthermore CT saturation leads to shifted current zero-crossings in the secondary current. The influence of saturation on phase comparison protection is therefore high. Some special measures in the protection algorithms may lead to more stability against unwanted operation.

11.5.5.2 Recommendations

Basic recommendations for CT designing:

- same CT type on each end of the line,
- anti-remanence CT type is recommended.

NOTE However, for existing plants, non-gapped cores can be utilized if tests show their suitability.

11.5.5.3 Example

In Figure 73, the CT designing for a simple line with two ends is shown for a system frequency of 50 Hz. Protection schemes also exist for up to six ends (e.g. for tapped lines).

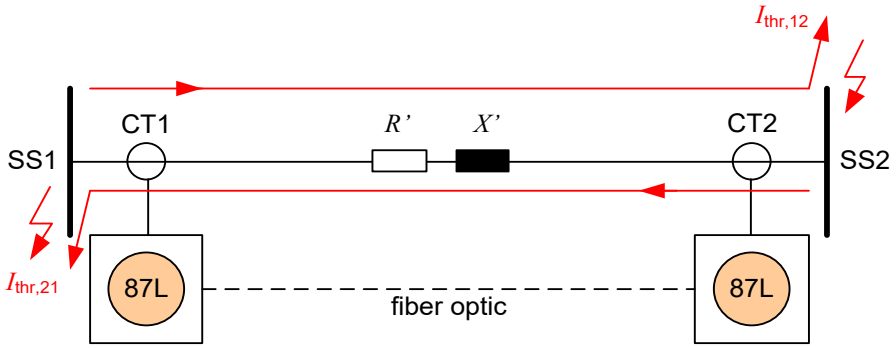

Key

$I_{thr,12}$ through fault current for external faults in station SS2 fed from station SS1

$I_{thr,21}$ through fault current (through the selective zone of protected object: overhead line or cable) for external faults in station SS1 fed from station SS2

R' line resistance per length unit

X' line inductance per length unit

SS1, SS2 substation 1, substation 2

Figure 73 – CT designing for a simple line with two ends

The following data for a typical overhead line is assumed (the Thevenin equivalent impedance as the worst case is neglected):

U_n = 380 kV

Length = 50 km

R_{line} =27 mΩ/km × 50 km = 1,35 Ω

X_{line} = 255 mΩ/km × 50 km = 12,75 Ω

$T_p = X_{line} / R_{line} / 2\pi f_r$ = 30 ms

$S_{th,max}$ = 1 800 MVA, what is equivalent with $I_{th,max}$ = 2 735 A

The rated primary currents I_{pr} of the CTs are chosen according to the rated current(s) of the line. For two ends, they are usually the same, but, for more than two ends, the rated currents can be different. In this example, a rated line current of 2 750 A is chosen. At one end, the CT ratio is, accordingly, 3 000/1 A, but, at the opposite end, an old CT has a ratio of 4 000/1 A. As the line may be overloaded by 150 %, the continuous thermal current is chosen accordingly.

The maximum short circuit current of the substation SS1 is I''_k = 40 kA, that of SS2 is 31,5 kA. The protection relay requires the CT to transform the full through-fault current for external faults with t'_{al} = 8 ms and inner fault currents with t'_{al} = 3 ms (both time values assumed during relay development). In general, an anti-remanence CT class is recommended for differential protection. Both t'_{al} = 3 ms and 8 ms are in time range 1 for a wide range of T_p (see Equations (9), (19),(20)) and Figure 20 c) and lead to transient factors K_{tf} or transient dimensioning factors K_{td} of 0,5 and 2,5 respectively (rounded up from slightly lower K_{tf} values from analytical calculation to the final K_{td} during protection relay tests). Such final K_{td} factors are published in the relay manual for CT sizing during the project engineering.

In addition, for each CT the maximum mismatch factor is

$$\frac{I_{pr}}{I_{obj}} = \frac{I_{pr}}{I_{line}} \leq 2$$

with

I_{obj} = object current;

I_{line} = line current;

and for all CTs

$$\frac{I_{pr,max}}{I_{pr,min}} \leq 6$$

with

$I_{pr,max}$ = maximum rated primary current of all involved CTs;

$I_{pr,min}$ = minimum rated primary current of all involved CTs.

Table 15 shows the appropriate calculation scheme.

Table 15 – Calculation scheme for line differential protection

	CT1	CT2
I_{pr}	3 000 A	4 000 A
$I_{psc} = I''_k$	40 kA	31,5 kA
Z_1, Z_2: Source impedances R_1, R_2: Source resistances X_1, X_2: Source reactances	Z_1 = 1,1 × 380 kV/(√3•40 kA) = 6 Ω R_1 = 0,381 Ω X_1 = 5,988 Ω	Z_2 = 1,1 × 380 kV /(√3• 31,5) kA = 4,82 Ω R_2 = 0,255 Ω X_2 = 4,813 Ω
T_p	50 ms	60 ms
Inner fault:		
$K_{ssc} = I_{psc} / I_{pr}$	13,33; rounded up to 14	7,875; rounded up to 8
t'_{al} = 3 ms, leading to K_{td} = 0,5 (1)		
$K_{td} \times K_{ssc}$	7	4
External fault:		
Z_{tot}: total impedance R_{tot}: total resistance X_{tot}: total reactance	$R_{tot} = R_2 + R_{line} = 1{,}605\ \Omega$ $X_{tot} = X_2 + X_{line} = 17{,}563\ \Omega$ $Z_{tot} = \sqrt{R_{tot}^2 + X_{tot}^2} = 17{,}63\ \Omega$ $I_{thr,21} = \frac{U_n}{\sqrt{3} \cdot Z_{tot}} = 12{,}5\ \text{kA}$ $T_p = \frac{X_{tot}}{\omega R_{tot}} = 35\ \text{ms}$	$R_{tot} = R_1 + R_{line} = 1{,}731\ \Omega$ $X_{tot} = X_1 + X_{line} = 18{,}738\ \Omega$ $Z_{tot} = \sqrt{R_{tot}^2 + X_{tot}^2} = 18{,}81\ \Omega$ $I_{thr,12} = \frac{U_n}{\sqrt{3} \cdot Z_{tot}} = 11{,}7\ \text{kA}$ $T_p = \frac{X_{tot}}{\omega R_{tot}} = 35\ \text{ms}$
$I_{thr,max}$: maximum through fault current	$I_{thr,max} = \max\{I_{thr,21}; I_{thr,12}\} = 12{,}5\ \text{kA}$	
$K_{ssc} = I_{thr,max} / I_{pr}$	4,16, rounded up to 5	3,125 rounded up to 4
t'_{al} = 8 ms, leading to K_{td} = 2,5 [a]		
$K_{td} \times K_{ssc}$	12,5	10
Mismatch factors:		
$\frac{I_{pr}}{I_{obj}} = \frac{I_{pr}}{I_{line}} \leq 2$	1,097	1,463
$\frac{I_{pr,max}}{I_{pr,min}} \leq 6$	4 000 / 3 000 = 1,33	

[a] The requirement of t'_{al} = 8 ms which results in K_{td} = 2,5 does not consider remanence as far as antiremance classes (gapped cores) are applied, which is a general recommendation for differential protection in new substations. However, for existing plants, non-gapped cores can be utilized if tests show their suitability (see 11.5.5.2). In such a case, an additional overdimensioning factor for remanence K_h has to be considered (see 8.2).

11.5.6 High impedance differential protection

11.5.6.1 Exposition

11.5.6.1.1 General

The protection principles previously described evaluate CT secondary currents which may be saturated by their high burden and/or high secondary currents. For differential protection principles, multiple CT currents are evaluated where each CT saturates independently from

the others, i.e. the CTs do not influence each other in their performance. If the protection relays are stabilized against maloperation due to CT saturation and distorted current signals, they can only evaluate the signals in an unprocessed state. Therefore, manufacturers of protection devices apply several different stabilizing measures and algorithms for better stability and selectivity. Dependent on the protection function, the maximum burden and a worst-case short circuit current are, when possible, considered for CT designing in order to avoid CT saturation.

In the past, the first differential protection relay was a simple electromechanical relay without any stabilizing measure installed in the differential path of all CTs connected in parallel. Such an example is shown in Figure 74 for busbar protection. For simplification, Figure 74 shows five feeders only and is presented as a single-line diagram. The compromise between sensitivity to internal fault currents and stability over and against external fault currents can only be influenced by the current threshold setting I_{set} of the relay. If one of the CTs saturates during an external fault (in many cases it is the CT of the faulty feeder through which the sum of all fault currents flows), the differential current is relatively high and the relay may trip.

In order to avoid such maltrips, one of the stabilizing methods is to calculate a stabilizing current I_{stab} from the sum of the absolute values of each feeder current. This is done for low-impedance differential protection. Nowadays the calculation of differential and stabilizing current is performed numerically from each individually sampled current as described in the sections above.

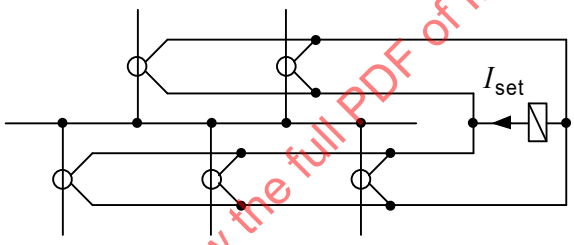

Key

I_{set} setting of pick up current of the relay

Figure 74 – Differential protection realized with a simple electromechanical relay

Another stabilizing method is to connect a relatively high stabilizing resistor R_{stab} in series to this simple overcurrent relay in the differential branch. Normally, all impedances in the CT secondary circuit should be as low as possible or as low as feasible in practice. Therefore, the relatively high impedance value leads to the name of this wanted stabilizing principle: 'high-impedance differential protection'. This is described in the following.

11.5.6.1.2 High impedance protection principle – physical explanation

The prerequisite for this principle of galvanic parallel connection of all CTs to the differential branch is that all CT ratios shall be equal.

Figure 75 shows an example in a single-line diagram for busbar protection with two feeders. The same diagram applies for all three phases.